Proteoglycan characterization in COG7-deficient cells

Tomasz Konopka

Master Thesis

Department of Biosciences
The faculty of Mathematics and Natural Sciences

UNIVERSITETET I OSLO

June 2014

Acknowledgements

The work presented in this thesis was carried out at the Department of Biosciences in University of Oslo, under the supervision of Dr scient. Kristian Prydz and Dr Gunnar Dick.

I would like to thank my supervisors for their continuous support and guidance. Thank you for answering my questions and giving me much needed encouragement. Without you none of this would be possible.

I would like to thank the rest of the PG-group for their kindness and technical assistance during experimental and writing stages

Thanks to all my laboratory friends: Flavia, Ignacio, Margrete, and Markus. The time I spent with you was special and thank you for all the banter and support you showed me when I needed it the most.

Thanks to my family for their kind support and encouragement.

Oslo, May 2014

Tomasz Konopka

Abstract

COG is a protein complex (units 1 -8) involved in retrograde transport of the resident Golgi proteins in intra-Golgi retrograde transport. Mutation in cog7 gene leads to congenital disorder of glycosylation (CDG-COG7) which causes severe mental retardation and, in some cases,death. There is significant amount of literature that describes glycosylation disorder in COG7 patients, but there is no data describing PGs from CDG-COG7.

Metabollic labelling with WB and MS was performed.

COG7 cells secrete high M_w PG with extensive sulfation level. The main modification of the PG in secreted fraction is CS -95% ,and HS comprises of 5 %. Cellular proteolgycans show reduced synthesis of HS 65% compared with healthy 85%.

Secreted proteolgycans from COG7 showed reduced PG variation and the presence of serglycin was detected. Intracellular decorin was detected in COG7 cells with possible formation of complexes with collagen type I or type II. Aggrecan PG was detected intracellularly as well as in a secreted form.

Distorted recycling mechanism of uptaken proteins was discovered with long delay in release of uptaken protein.

List of contents

Contents

List of abbreviations

cABC	Chondroitinase A, B, C
CDG	Congenital disorder of glycosylation
CL	Cell lysate fraction
CMM	Cisternal maturation model
COG	Conserved oligomeric Golgi
COG4	COG4-deficient
COG7	COG7-deficient
COG8	COG8-deficient
COP I	Coat protein I
COP II	Coat protein II
CS	Chondroitin sulfate
CTR	Control
Da	Dalton
DMEM	Dulbecco's modified Eagle's medium
DMSO	Dimethylsulfoxide
ER	Endoplasmic reticulum
ERGIC	ER-Golgi intermediate compartment
GAG	Glycosaminoglycan
Gal	Galactose
GalNAc	N-acetylgalactosamine
Glc	Glucose
GlcA	Glucuronic acid
GlcNAc	N-acetylglucosamine
Hep	Heparinase I, II, III
HS	Heparan sulfate
LLO	lipid-linked oligosaccharide
M	Medium fraction
Man	Mannose
Met	Methionine
min	Minute
MS	Mass spectrometry
M_w	Molecular weight
PBS	Phosphate buffer saline
PG	Proteoglycans
RPM	Rapid partitioning model
UDP	Uridine diphosphate
V_0	Void Volume
VSV-G	Vesicular stomatitis virus glycoprotein
V_t	Terminal Volume
VTM	Vesicular transport model
WB	Western blotting
Xyl	Xylose
$^{35}S\text{-}SO_4^{2-}$	Radioactive ^{35}S – sulfate ion

Aim

Congenital disorders of glycosylation (CDGs) are a group of genetic syndromes affecting many patients. Most of the syndromes have severe consequences leading to multiple adverse conditions (e.g. mental retardation, failure to thrive) and, in some cases, death. CDGs affect glycosylation pathways in the cell and have global effects. Recently, the incidence of CDGs is low due to high misdiagnosis. It is proposed that there are approximately 1 million people diagnosed with CDGs in the world, although the real incidence number is, presumably, much higher.

Conserved oligomeric Golgi (COG) complex is an important eight-subunit protein complex that functions in Golgi organelle and it is implicated in retrograde transport within Golgi and between Golgi and ER. COG7 is one of the COG's subunits and patients with mutated cog7 gene have shown affected glycosylation pattern. Mutation in cog7 gene leads to reduced level of COG7 protein and the N-glycosylation and O-glycosylation pattern is, in turn, affected, according to current literature. However, there is no data that describes PG O-GAG glycosylation in COG7 patients. It is possible that this glycosylation pathway is affected in the same manner as N-glycosylation and O-glycosylation. On the other hand, it is entirely possible that O-glycosylation is not affected in COG7 patients.

Proteoglycans (PGs) are glycans where the biological and chemical characteristics are determined by the attached sugar nature, rather than protein. The most abundant modification carried out on PG is glycosaminoglycan chain(s) (GAG(s)) attachment on serine residue. GAGs are long polysaccharide chain (essentially a polymer), up to a hundred residues, that are essential for determination of PG characteristics. Different GAG types (chondroitin, heparan, keratan) are present on PGs and are instrumental in the glycan's function (ligand binding, water binding). PGs are synthesized in ER and modified in Golgi, where biosynthesis of GAG chains occurs.

If COG7 patients have aberrant N-glycosylation, is it possible that the PG synthesis is also aberrant? How does it relate to COG complex function? There is no data that answers this question.

In this project, we tried to establish the nature of secreted and cellular PGs from fibroblasts of COG7 patient. Are they different than healthy fibroblast's PGs? If it is so, to what extent are

they different? Moreover, how does the change of PGs synthesis relates to COG complex functionality, especially in the light of the retrograde transport function?

Overall aim of this project was to establish ground work for future project involving COG-mutants and PG synthesis. In this way, one can learn more about GAG synthesis and protein transport within the Golgi apparatus.

1Introduction

1.1 The Golgi apparatus

1.1.1 The Golgi apparatus origins and structure

The Golgi apparatus is a crucial organelle in the cell responsible for sorting and processing of various cargo proteins, both soluble and transmembrane. Its origin goes as far as to the common eukaryotic ancestor. Its structure varies between species. In most organisms the Golgi apparatus is organized in a stack-like fashion with flattened membrane structures (known as *cisternae*) acting as basic building blocks to form a polarized (*cis, medial* and *trans*- orientation) moiety. The *cis* side of the Golgi organelle system faces the nuclear side, while *medial cisternae* are stacked between *cis* and *trans-cisternae* that face towards cell periphery.

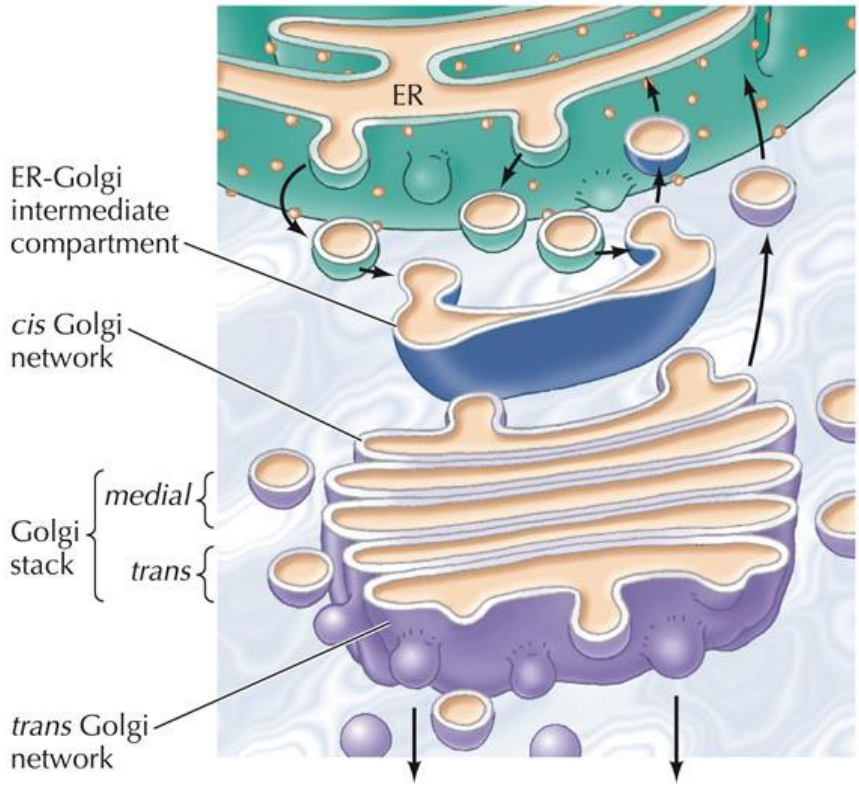

Figure 1. Schematic representation of the Golgi apparatus; adopted form THE CELL(Bruce Alberts, Alexander Johnson, Julian Lewis, Martin Raff, Keith Roberts 2002).

Although the Golgi apparatus shares similarities in general structure, the actual appearance of it can change. In mammals, it forms a ribbon like membrane structure via lateral connection,

while in plants and invertebrates the Golgi apparatus exist as separate bodies disposed throughout the cytosol. Moreover, in yeast, different Golgi cisternae are present as separate compartments within the cell(Wilson et al. 2011). However, there is a group of organisms that lack visible Golgi stacks into which we can include parasites (e.g. Giardia intestinalis) microsporidia, heterolobosea and numerous apicomplexans (Babesia, Theileria)(Mowbrey & Dacks 2009). Although it is well known that the Golgi apparatus functions as a sorting centre for transmembrane and soluble proteins, it is also regarded as a glycan factory and it also possesses a number of different functions which include proteolytic processing (Stamnes 2004) and lipid homeostasis(Wilson et al. 2011).

1.1.2 Protein transport to Golgi apparatus

Newly synthesized cargo proteins arriving to the Golgi apparatus are coming from ER exit sites via vesicular bodies covered with COP II (coatemer protein II) proteins. This system regulates secretory cargo concentration in anterograde transport (from ER to Golgi). Cargo that needs to be returned back to the ER is transported in COP I type vesicles via vesicular transport mechanism that regulates recycling of cargo back into ER.(Lee et al. 2004) The fusion between COP II vesicles and the Golgi apparatus occurs, in mammalian cells, at the ERGIC (ER-Golgi intermediate compartment) site. There is evidence suggesting that ERGIC is the primal sorting site for the cargo that is destined to be recycled to the ER from cargo targeted for the *cis* -Golgi. This primal sorting is achieved by recognition of amino-acid motifs in the recycled proteins that determine their subsequent faith. Even though there is evidence showing presence of the ERGIC, in several cell types the stability and dynamics of this "organelle" are still elusive(Wilson et al. 2011).

1.1.3 Protein transport through the Golgi apparatus

When cargo molecules reach the *cis*-Golgi, they must pass through the *cisternae* within the stacks to be completely modified and sorted to their appropriate destination. In today's scientific community, several different models have been proposed to explain how cargo can traverse the Golgi's *cisternae*. Three independent models are:

1. The cisternal maturation model (CMM)
2. The vesicular transport model (VTM)
3. The rapid partitioning model (RPM)

1.1.4 The cisternal maturation model

This model projects that cisternae are formed on the cis-side of the Golgi apparatus and then progress through the Golgi stack while carrying secretory cargo molecules in order to form exit vesicles at the trans-side of the Golgi. It is believed that Golgi-resident proteins recycle between "old" and "new" cisternae via retrograde vesicular transport using COP I-type vesicles that interact with the COG (conserved oligomeric Golgi) complex (Suvorova et al. 2002). There is much supporting evidence towards the cisternal maturation model and it is a prevailing model accepted by the majority of researchers(Emr et al. 2009). Obtained morphological data fit well with the CMM, due to the fact that cisternae constituted at the cis-side and disintegrate (or "peel off") at the trans-side. This model also explains how large cargo molecules (i.e. bigger than transport vesicle) could be secreted (e.g. procollagen in mammalian fibroblasts) and the model also incorporates COP I vesicles and the fusion machinery components in its mechanism. In this model, COP I vesicles act as retrograde carriers of resident Golgi proteins and therefore one can explain why given Golgi resident proteins are present in a number of different Golgi compartments as well as why Golgi resident proteins move rapidly within and between different Golgi cisternae (Emr et al. 2009). Similarly, the CMM could project clear predictions with respect to: cargo speed through Golgi cisternae, composition of resident proteins in maturing Golgi cisternae that should vary over time and that cisternal maturation should require COP I vesicles. There is clear evidence that procollagen and the VSV-G transmembrane glycoprotein move through Golgi stack at the same rate. The cisternal composition of resident proteins is dynamic and was visualized by live-cell fluorescence microscopy, and the rate of the cisternal maturation was similar to the transit speed of secretory cargo, suggesting that cisternal maturation fits, with observation of anterograde transport in the Golgi apparatus. Moreover, COP I deficient yeast cells had slower maturation of cisternae compared with the wild type (Emr et al. 2009).

1.1.5 The vesicular transport model

In this model, also known as the stable compartment model, each Golgi stack is a stable structure and cargo molecules are transported into *cisternae* via specialized transport vesicles. It was first suggested by Rothman and Wieland in 1996 (Rothman & Wieland 1996). In this model resident Golgi proteins are retained in *cisternae* while secretory cargo molecules are moved, from one *cisterna* to the next, by anterograde COP I- coated vesicles (Emr et al. 2009).This model has a number of advantages: it explains the polarity of the Golgi stack and gives reason for the abundance of COP I vesicles in proximity to the Golgi. The polarity of Golgi is achieved due to the notion that each *cisterna* has a distinctive set of resident proteins therefore it could be viewed as a distinctive organelle. Abundance of COP I vesicles around the Golgi membranes could be explained by their formation and fusion at the *cisternal* rims. However, this model has encountered a number of conflicting evidence (Bonfanti et al. 1998) which raises doubts about its validity. The most prevalent evidence is that the Golgi can transport and secrete cargo molecules that are larger than what a secretory vesicle can accommodate (e.g. procollagen in mammalian fibroblasts and scales in algae). This could be explained by the existence of mega-vesicles, but no putative mega-vesicles are seen in algae and procollagen seems to remain in the Golgi *cisterna*. (Bonfanti et al. 1998)

1.1.6 The rapid partitioning system

In this model, proposed by Patterson et al. in 2008 (Patterson et al. 2008), cargo is predicted to exit the Golgi apparatus with exponential kinetics rather than showing a distinctive lag phase which would be observed if the cargo would follow the cisternal maturation model. Secondly, this model shows that upon entry, transmembrane cargo quickly distributes itself throughout Golgi membranes and subsequently divides itself into two diverse membrane environments. Patterson et al proposed that there are two distinctive membrane regions: a processing domain and a secretory domain. In the processing domain one can find a large number of cargo-processing enzymes, while secretory domains are capable of forming transport intermediates. The different domains in the Golgi membranes possibly arise due to different composition of membrane lipids. In this model, the secretory domain is modelled to be enriched in cholesterol and glycosphingolipids, whereas the processing domain is mainly composed of glycerol phospholipids (Patterson et al. 2008).

1.1.7 The Golgi apparatus - a glycan factory

The Golgi apparatus can be named a glycan factory, as almost all pathways for glycosylated proteins and lipids pass through this organelle.

After initial processing, glycoconjugates leave the ER and travel towards the Golgi stacks. Almost all glycoproteins are exposed to trimming and extension as they pass through a Golgi stack. In the case of N-glycosylation (most common glycosylation mechanism for proteins), the glycoprotein already possesses an oligosaccharide which is then trimmed and/or extended by actions of enzymes that are present in the Golgi lumen (Reynders et al. 2011).

PGs acquire their GAG chains in the Golgi apparatus ,thus Golgi acts as a glycan synthesis centre for PGs as well as for other O-linked glycoproteins (Prydz & Dalen 2000).

The Golgi apparatus is not only a harbour of glycosyltransferase enzymes but provides substrates for glycan biosynthesis. UDP-sugar, GDP-sugar and PAPS (3`-phospho-adenosine-5`-phospho-sulfate) specific transporters translocate UDP-sugars, GDP-sugars and PAPS (substrates) from the cytoplasm into the Golgi lumen; this translocation process is energy-dependent. Saccharides are supplied via dietary routes and converted into UDP-sugars in cytoplasm(Caffaro & Hirschberg 2006).

1.1.8 Proteoglycans (PGs) synthesis

PGs are protein structures with one or more GAG chains attached via O-glycosylation of serine residues with neighboring glycines in the peptide backbone. In contrast to glycoproteins, where the scientific focus is mostly on the protein part, it is the glycan nature that gives the PG its subsequent characteristics.

1.1.9 Types of proteoglycans

Small leucine rich PGs (SLRP) contain a protein core with leucine rich repeats with N-terminal cysteine cluster, “ear repeats” and at least one GAG chain. Those PGs form a family with sub-classes- traditionally defined classes I-III and non-canonical classes IV and V. SLRP are important in a number of biological functions: binding to collagen, inhibition of cell growth or modulation of bone morphogenic protein (Schaefer & Schaefer 2010). Decorin

is a prototype member of SLRP, consisted of 359 amino acids with M_w of 39 kDa. There are five isoforms of decorin and canonical isoform possesses one O-glycosylation site (GAG) and three N-glycosylation sites. It is mostly secreted from cell and localized in the extracellular matrix (Uniprot n.d.).Decorin is able to bind transforming growth factor-β (Hildebrand et al. 1994). Biglycan is another member of SLRP family. It is a PG with 368 amino acids constituting 41 kDa of M_w. Biglycan is mostly secreted from cells and is found in the extracellular matrix. It has four possible O-glycosylation sites (GAG) and two N-glycosylation. There is only one isoform of biglycan and it is capable of binding, as well as decorin, to transcription growth factor β (Uniprot n.d.; Hildebrand et al. 1994)

Serglycin is a PG expressed mostly in hematopoietic and endothelial cells. It plays a vital role in formation of mast cells secretory granules and is required for storage of some proteases in connective tissue. It has a 158 amino acids protein core and its M_w is 17 kDa. It possesses eight O-glycosylation sites (GAG) with two sites experimentally proven and six potential sites; no know isoforms are reported. The GAGs attached to serglycin are of CS and HS nature (Uniprot n.d.; Kolset & Tveit 2008).

Aggrecan family of PGs consists of four PGs: aggrecan, versican, brevican and neurocan. All of those PG have hyaluronic acid binding domain at N-terminal, central region binding CS GAGs and C –terminal contain C-type lectin domain. Out of aggrecan family PGs, the best studied is aggrecan(Esko et al. 2014).

Aggrecan is a 250 kDa PG with 2415 amino acid protein core. There are three isoforms and two known O-glycosylation sites (both probable) and nine known N-glycosylation sites (eight are potential). (Uniprot n.d.) It is reported that aggrecan have more than100 CS chains and 20-30 keratan sulfate chains (Kjellen & Lindahl 1991) It is a major component of extracellular matrix in cartilage tissue and its function is to resist the compression of the cartilage. It is tissue specific and exists solely in a secreted form (Uniprot n.d.).

1.1.10 The linkage region formation

The synthesis of PGs begins at the ribosomes, in the ER, where the protein core of the future PG is being translated from mRNA. O-glycosylation on serine residues in the early secretory pathway with a single xylose sugar starts the synthesis of GAG chain. The xylose sugar is attached to a serine next to a glycine by a xylosyltransferase enzyme- either XYLT1 or

XYLT2. Subsequently two galactose sugars are attached, in sequence, by the action of two galactosyltransferase enzymes: GalT-1 and GalT-2. The addition of a glucuronic acid (GlcA) moiety by GlcAT-1 transferase concludes the formation of the linkage or linker region (Kreuger & Kjellén 2012a).

There are two types of modifications that can affect the linker region: phosphorylation of xylose sugar and sulfation of galactose sugars. It has been shown that these modifications can affect downstream enzymatic polymerization process. The result of intense modification of xylose and/or galactoses can be restriction or even inhibition of enzymes involved in synthesis of the linkage region. It is stipulated that 4-O-sulfation of the second galactose residue can be driving CS formation (Kreuger & Kjellén 2012a). In this respect, addition of the fifth sugar, the first N-acetylhexosamine is critical for selective assembly of CS or HS chains (Mikami & Kitagawa 2013).

1.1.11 Synthesis of heparan sulfate (HS)

Addition of the fifth moiety, the first sugar subsequent to the linker region is the deciding point in selection between heparan (N-acetylglucosamine) and chondroitin (N-acetylgalactosamine) sulfate synthesis. The exact mechanism that rules this choice is still elusive. The "gagosome" model suggests a competition between different enzymes involved in GAG polymerization would result in either CS synthesis or HS synthesis (Dick et al. 2012).

HS polymerization is initiated by enzymes from the EXTL family of glycosyltransferases. Those enzymes attach N-acetylglucosamine (GlcNAc) to a non-reducing end of the 4^{th} moiety on the linker. Enzymes EXTL -1, -2 and -3 have been shown to possess ability to transfer N-acetylglucosamine; therefore each one of them can be involved in HS-chain polymerization. EXTL-3 seems to be the enzyme most involved in initiation of HS biosynthesis, but EXTL-2 and -1 are also necessary for proper HS biosynthesis. The increased level of EXTL-3 results in increased HS chain length which suggests a complex regulation of HS biosynthesis (Kreuger & Kjellén 2012a). EXTL-2 exhibits dual transferase activity. It can attach either GlcNAc or GalNAc to the tetrasaccharide linker region. Addition of GlcNAc will initiate HS biosynthesis whereas addition of GalNAc (by EXTL-2) is suggested to inhibit CS biosynthesis, as GalNAc does not serve as an acceptor for successive CS polymerization (Kreuger & Kjellén 2012a).

Following EXTL-mediated initiation, the HS chain is polymerized by a functional HS polymerase complex which is composed of EXT-1 and EXT-2. This complex transfers GlcA and GlcNAc sugars in alternative fashion onto growing chain. The interaction between EXT-2 and N-deacetylase/N-sulfotransferase 1 enzymes is implied in regulation of the HS chain length (Kreuger & Kjellén 2012a).

1.1.12 Synthesis of Chondroitin sulfate (CS)

The linker region synthesis is a common pathway for HS and CS, while the elongation and modification of HS and CS GAG chains is carried out by different sets of enzymes, which also generally seem to be localized to different sub-regions of the Golgi apparatus (Prydz & Dalen 2000).

The elongation of CS chains is mediated by an action of two distinct transferases that extend the GAG chain with alternating Glucuronic acid (GlcA) (by GlcA Transferase II) and N-acetylgalactosamine (GalNAc) (by GalNAc Transferase II) residues, where the GalNAc is the first to be added to the linker region (Mikami & Kitagawa 2013).

In recent years, six homologous glycosyltransferases that are indicated in CS synthesis have been cloned and characterized *in vitro*. Based on their enzymatic activity they have been termed chondroitin synthase -1 (ChSy-1), chondroitin synthase -2 (ChSy-1), chondroitin synthase-3 (ChSy-3), chondroitin polymerizing factor (ChPF), chondroitin GalNAc transferase-1 (ChGn-1) and chondroitin GalNAc transferase-2 (ChGn-2). ChSy-1, ChSy-2 and ChSy-3 enzymes have dual glycosyltransferase activity (GlcAT-II and GalNAcT-II), but are incapable of synthesizing CS on their own. However, the co-expression of any two out of four proteins (ChSy-1, ChSy-2, ChSy-3 and ChPF) results in significant increase of GlcAT-II and GalNAcT-II activity. (2) This leads to CS chain elongation where the chain length is dependent on the composition of synthesizing enzymes. In conclusion, CS polymerization can be achieved by enzyme complexes (chondroitin polymerases) that consist of multiple combinations of the four enzymes: ChSy-1, ChSy-2, ChSy-3 and ChPF (Mikami & Kitagawa 2013).

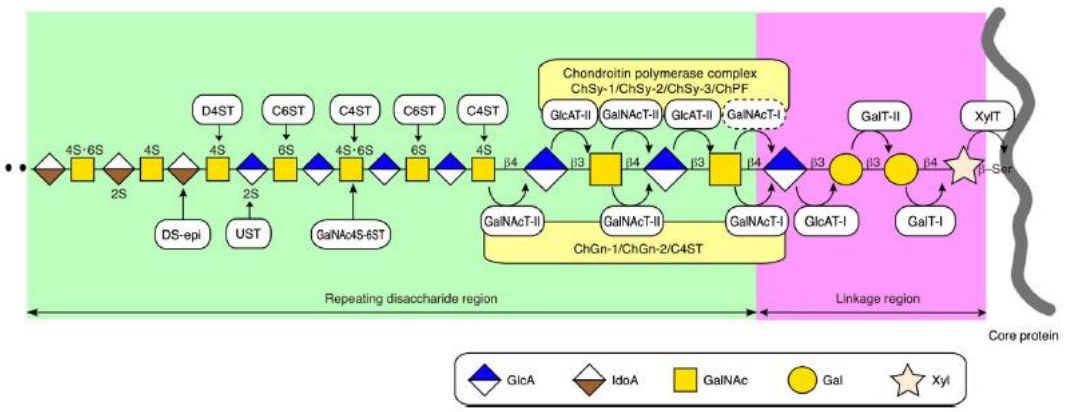

Figure 2. Schematic representation of CS GAG; names of glycosyltransferases are given in white boxes (Mikami & Kitagawa 2013).

The ChGn-2 and ChGn-2 enzymes have both GalNAcT-I and GalNAcT-II activities and thus are believed to be involved in CS chain backbone initiation and elongation steps. They are also needed for CS chain length regulation and/or regulation of the GAG numbers (Prydz & Dalen 2000).

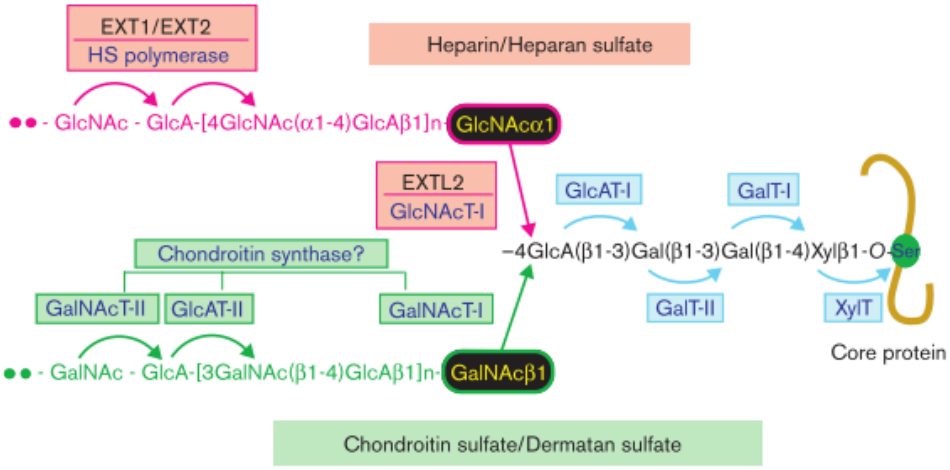

Figure 3 Overview of CS and HS biosynthesis(Sugahara & Kitagawa 2000).

1.1.13 HS and CS synthesizing enzymes localize to the Golgi apparatus

Enzymes needed for completion of HS PG synthesis are localized in *cis* -, and *medial*- Golgi *cisternae*. On the other hand, enzymes needed in biosynthesis of CS PG are localized to the *trans*-region of the Golgi apparatus(Prydz & Dalen 2000).

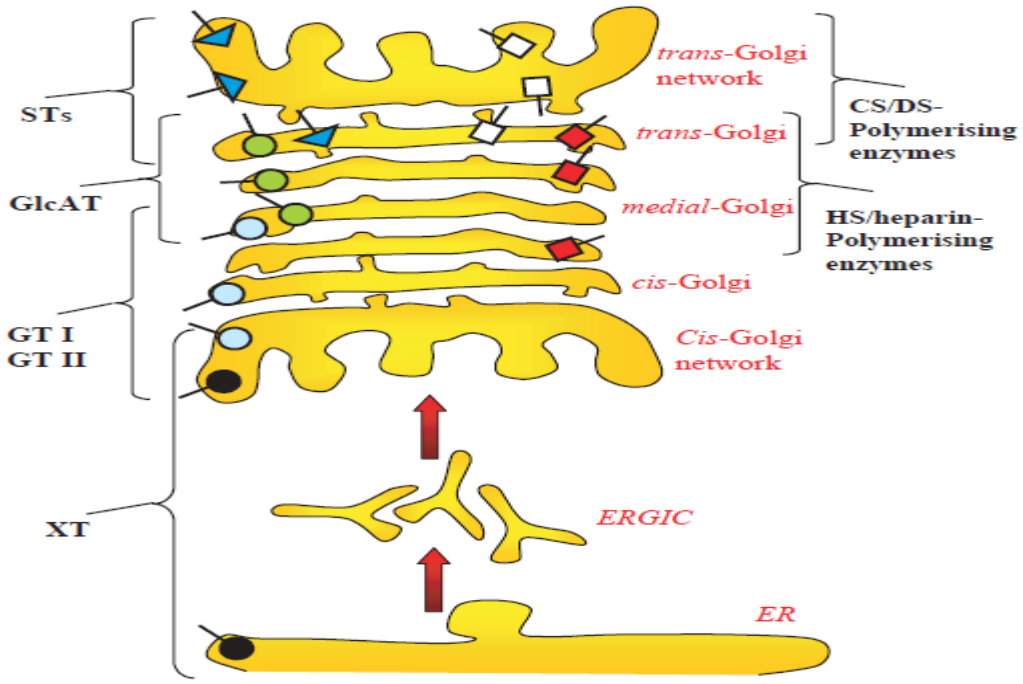

Figure 4. Localization of PG polymerizing enzymes in the Golgi apparatus; STs- sulfotransferases, GlcAT- glucuronic acid transferases, GT- galactosyltransferases, XT- xylosyltransferase (Prydz & Dalen 2000).

1.2 N-glycosylation

N-glycosylation is present in all domains of life: bacteria, archea and eukaryotes. It involves a process in which an oligosaccharide is attached via an N-glycosidic linkage to a side chain of an asparagine residue of a protein core. The attachment site is specified by a consensus sequence of N-X-S/T (Aebi 2013).

A lipid-linked oligosaccharide (LLO) is first biosynthesized on dolichol (an isprenoid lipid), which acts as a carrier molecule. The building blocks of LLOs are: mannose (Man), GalNAc and glucose (Glc). These are delivered as nucleotide-activated sugars to the site of synthesis. The biosynthesis of LLO is carried out by a group of glycosyltransferases that act in a sequential manner. The LLO biosynthesis starts at the cytoplasmic side of the ER membrane with addition of GlcNAc-P to Dol-P and formation of Dol-PP-GlcNAc. Subsequent reactions result in formation of $Man_5GlcNAc_2$ before the LLO is "flipped" to the lumenal side of the ER. The exact molecular mechanism and protein involved in LLO-flipping are still poorly understood (Aebi 2013).

1.3 The COG complex

1.3.1 COG structure

COG- is an acronym for conserved oligomeric Golgi-complex which was initially described by Daniel Ungar and his team in 2002 (Ungar et al. 2002), while working with yeast and mammalian cell lines on the low density lipoprotein receptor. This complex is a heteromer composed of 8 subunits (labelled 1-8), where units 1 to 4 compose lobe A and units 5 to 8 compose lobe B (Ungar et al. 2002). It localizes peripherally to Golgi membranes. It was shown that COG subunits 2-4, 1/8 and 5-7 form stable entities which indicated that the COG complex is composed by two lobes with a bridge in form of COG1-COG8 structure (Ungar et al. 2006).

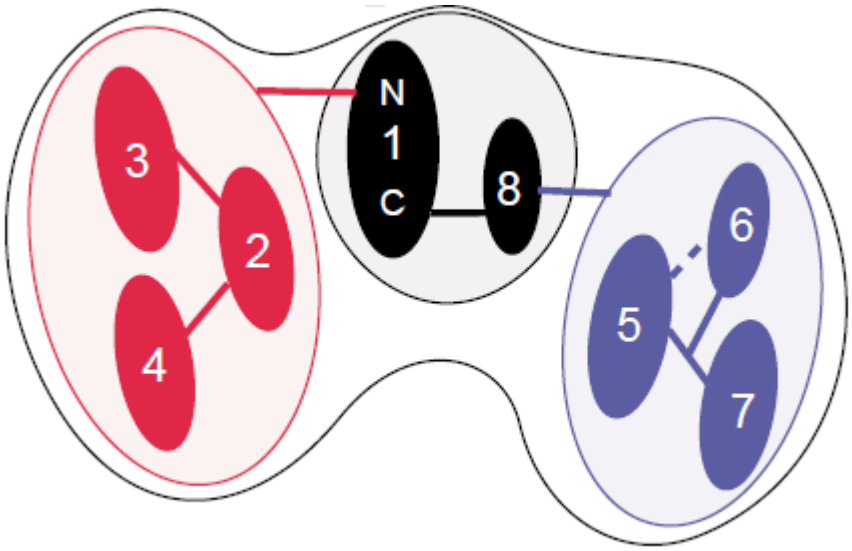

Figure 5. Schematic diagram of the COG complex (Ungar et al. 2006).

1.4 COG complex function.

The best documented example of COG function is its indirect involvement in glycosylation processes where defects in COG lead to severe glycosylation-linked syndromes. According to Ungar et al, 2006, the majority of published data suggests that the COG complex is involved in retrograde trafficking within the Golgi apparatus and in endosome to Golgi transport.

In order to understand a protein's function, it is vital to establish its interactive partners. The COG complex is shown to have a number of those. SNAREs, proteins involved in membrane fusion, are shown to interact extensively with COG complex subunits. Secondly, small GTPases- Rabs, which localize to the Golgi apparatus and are thought to take part in trafficking, are indicated in the COG interaction scheme (Willett et al. 2013). Moreover, COP I proteins are shown to strongly interact with the COG complex. With the abovementioned three classes of proteins: SNAREs, Rabs and COP I, that are pivotal to protein transport in the Golgi apparatus, the COG complex shows strong indication of involvement in protein intra-Golgi trafficking (Ungar et al. 2006). Furthermore, interaction with COP I proteins suggest that the COG complex is involved in retrograde transport, rather than anterograde.

Subsequent studies of the COG complex revealed that its involvement in retrograde transport is more than a suggestion. A study by Oka, T. et al. (2004) (Oka et al. 2004) indicated the presence of type II integral Golgi membrane proteins with reduced steady-state levels in CHO cells that lacked the COG 1 and COG 2 subunits. Those proteins were termed GEARs and are comprised of the following family members:

GEAR	Function
CASP	Elongated coiled coil protein of the golgin family. Proposed function is vesicle tethering
Giantin	Elongated coiled coil protein of the golgin family. Proposed function is vesicle tethering
Golgin-84	Elongated coiled coil protein of the golgin family. Proposed function is vesicle tethering
GOS-28	SNARE protein, functions in vesicle fusion
GPP130	Heavily glycosylated Golgi protein of unknown function
GS15	SNARE protein, functions in vesicle fusion
Mannosidase II	Glycosidase enzyme

Figure 6. List of GEAR-proteins (Ungar et al. 2006).

The function of mannosidase II (an enzyme involved in glycosylation) as GEAR could explain the global glycosylation defects in COG1 and COG2 deficient cell lines.

Zolov and Lupashin showed in 2005 that cells with silenced COG3 gene, accumulated vesicles that carried a number of Golgi proteins: v-SNAREs, GS15, GS28 and *cis*-Golgi glycoprotein GPP130 (Zolov & Lupashin 2005). Those vesicles were labelled COG-complex depended vesicles (CCD vesicles) and showed to incorporate at least three GEARs on their membranes. CCD vesicles showed retrograde transport activity (Ungar, 2006). Up to date,

experimental data shows that the COG complex is most likely involved in retrograde Golgi transport. However, the exact mode of action is still not fully understood.

Other tethering factors, that are present in the Golgi proximity and involved in vesicle tethering (i.e. TRAPP, GARP/VFT), share some similarity with the COG complex. All of them, including COG, seem to react with Rab and SNARE proteins. It is possible that the COG complex could be, in fact, a Rab effector protein (Ungar et al. 2006).

The COG complex is also implied in a number of activities surrounding vesicle trafficking. The COG complex, at least in some cases, is shown to recruit and activate Rab GTPases. Moreover, COG is implemented in possible remodeling of actin near the plasma membrane, and, in formation of membrane-bridging SNARE complexes (Ungar et al. 2006).

1.5 Congenital disorders of glycosylation (CDGs)

Glycosylation is a crucial process in a eukaryotic cell, but like all processes, it can malfunction. Because of its complicated nature and involvement of many steps there are many steps that can become aberrant.

Congenital disorders of glycosylation are a group of syndromes that affect glycosylation process in humans. The moieties that are affected by CDGs are mainly glycosylated proteins, but lipids can also be affected, in which case the glycosylation of protein or lipid is defective or reduced.

The two main types of glycosylation: N- and O- linked glycosylation differ in many aspects. N-glycosylation is two –step (trimming and extension) that occurs at three different sites (the cytoplasm, the ER lumen, and the Golgi lumen), while O-linked glycosylation has most of its assembly in the Golgi lumen. The spatial arrangement of N-glycosylation in which oligosaccharides is transferred from a lipid-linked state in the ER lumen onto a protein gives CDG numeral nomenclature that divides this group into two sub-groups: CDG I and CDG II type.

CDG I –type syndromes affect the oligosaccharide synthesis on dolichol (Dol) oligosaccharide carrier, before it is transported onto a protein, while CDG II-type in modern

nomenclature concerns all other glycosylation defects affecting N-glycosylation after proteins have been initially decorated with pre-synthesized glycan and all other defects affecting the synthesis of O-glycans and glycolipids.

Until recently, glycosylation diseases were named using the CDG acronym followed by a sub-group number and a letter assigned alphabetically following a chronological order of the subsequent discovery. Currently, it is recommended to use genomic nomenclature in order to specify which gene(s) is the causative effect. Therefore it is recommended to put a mutated gene abbreviation along with the CDG acronym.

However, even though nomenclature of glycosylation disorders has changed, two systems are still used.

Within the CDG's linked to N-glycosylation pattern, there are 15 identified defects- 12 from CDG I and 3 from CDG II sub-groups (Jaeken 2013).

In the O-glycosylation pathway, defects have been found in the following biosynthesis pathways: O-xylosylglycans, O-N-aceltylgalactosaminoglycans, O-N acetylglucosaminoglycans, O-fucosylglycans and O-mannsylglycans. The glycosphingolipid and GPI glycosylation pathways have two syndromes described up to date: SIAT9-CDG and PIGM-CDG. There are numbers of glycosylation syndromes that affect multiple glycosylation and other pathways and in this group COG4-CDG, COG8-CDG and COG7-CDG are described (among others) (Jaeken 2013).

	COG1	COG4	COG7	COG8
Clinical phenotype	Failure to thrive Hypotonia	Mild psychomotor retardation	Lethal Growth retardation	Encephalopathy Neurological and psychomotor regression
	Mild psychomotor retardation	Mild dysmorphia	Dysmorphia	Hypotonia
	Growth retardation	Epilepsia	Hyperthermia	Mild mental retardation
Mutation(s)	c.2659-2660insC p.P888fsX900	c.2185C>T p.R729W submicroscopical deletion 16q22	c.IVS1+4A>C altered splicing leading to frame shift and stop codon	c.1611C>G p.Y537X
Origin	Portuguese	Portuguese	Moroccan	Spanish
Publication	Foulquier *et al.* (15)	This publication	Wopereis *et al.* (17)	Foulquier *et al.* (12)
BFA defect (% cells with Golgi remnants)	74.6 ± 2.5	22 ± 3.5	88.8 ± 2.33	34.4 ± 7.9
Glycosylation defects	Sialylation Galactosylation Demannosylation	Sialylation (Galactosylation)	Sialylation Galactosylation Demannosylation	Sialylation Galactosylation
Golgi morphology	Typical Golgi stacks (as in WT)	Typical Golgi stacks (as in WT)	Many undulated Golgi stacks with many swollen cisternae	Some undulated Golgi stacks
	Some undulated Golgi stacks	Some undulated Golgi stacks, less rigid	Less rigid Golgi stacks	Fragmented Golgi
	Few fragmented/ disrupted Golgi.	Few fragmented/disrupted Golgi		Many tubular and vesicular profiles

Figure 7 Comparison of different COG-CDGs. Glycosylation defects apply to N-glycosylation. (Reynders et al. 2009)

Patient with COG4-CDG displayed seizures, dysmorphic facial features, mild ataxia and psychomotor development delay (Reynders et al. 2009).

Patient with COG8-CDG showed seizures, failure to thrive, dysmorphism (small feet and hands), ataxia and neurological regression (Foulquier et al. 2007).

1.5.1 COG7 mutation and COG7-CDG

COG7-CDG was firstly described by Wu et al in 2004 (Wu et al. 2004), when two siblings (P1 and P2) with Mediterranean background were diagnosed with several severe clinical symptoms. Their parents were consanguineous, but otherwise healthy. Siblings displayed dysmorphia, mental retardation, general hypotonia and failure to thrive. Their lysosomal enzymes were elevated in their circulation and abnormal glycosylation of transferrin was observed. Moreover, significant reduction of sialic acid levels in serum led to a final diagnosis of a glycosylation defect - a CDG. Further diagnosis revealed that P1 had decreased sialylation, while P2 did not deviate from the normal pattern in this regard. Furthermore P1 has shown defects in O-linked oligosaccharide synthesis that seemed to be a result of decreased activity of nucleotide sugar transporters as well as glycosyltransferases; cells from P2 did not show the same changes (Wu et al. 2004).

These particular patterns in glycosylation defects lead the team to a discovery that P1 had mutation in its COG complex. The result was a homozygous intronic mutation (for both P1 and P2) IVS+4 A →C. This allowed cryptic, conserved alternative splicing site near the 1st intron/exon boundary that resulted in 19-base deletion of COG7 mDNA. The COG7 protein level was reduced in both patients, due to reduced splicing efficiency, a premature termination codon or both. P1 and P2 had the COG7 protein levels reduced by 95% and 85 %, respectively, and COG7 mRNA reduction also followed those values. Introduction of wt-cog7 DNA via molecular cloning could rescue glycosylation and trafficking properties in COG7 cells. Wu et al were the first to show a new class of CDG in which the affected gene is not directly involved in synthesis of complex glycans or synthesis or transport of sugar donors, but rather coding a protein involved in trafficking of the glycosylation machinery (Wu et al. 2004)

..

2 Materials and Methods

2.1 Cell tissue culture

Cells used in this project were made available by Dr Erik Eklund, Lund University. COG7, E42, and E12 were the names of the cell lines. E42and E12 were fibroblasts harvested from lower arm skin of healthy individuals and COG7 were fibroblasts harvested form neonatal patient that showed COG7-deficiency.

All culture work was carried out using standard aseptic techniques, unless otherwise specified.

1. Used complete medium and trypsin were always heated to 37°C before being applied to cell cultures, unless otherwise specified.

2. Throughout most of the project E42 cells were used as control, or "healthy" cells. Unless otherwise specified, it should be assumed that E42 cells were used as a control.

3. COG7 cells showed satisfactory cell growth initially, but after few months their growth rate deteriorated and cells stopped dividing. This resulted in limited amount of data obtained in the project. It is worth notifying that the patient form which the cells were obtained, deceased at age of 2 months.

Standard incubation conditions: air-flow incubator; 5 % CO_2 and 37°C

2.1.1 Culturing cells from frozen samples

The cells were obtained in medium from the University of Lund, multiplied by continuous culture and frozen down as ampules for later use. Upon thawing, the cells were grown in the cell lab according to the following procedure:

1. Ampules were thawed in water bath at 37°C.

2. Thawed cell suspension was transferred aseptically into 20 ml of DMEM (complete medium), supplemented with 10 % fetal bovine serum (FBS) and 1 % Penicillin/Streptomycin in 75 cm^2 cell culture flasks.

3. Cells were cultured in an air incubator under 5 % CO_2 and 37°C for 3 days.

4. After 3 days, the growth progress was examined under the light microscope and if confluence was satisfactory, cells were passaged. If the confluence wasn't satisfactory, the medium was changed and replaced with a new 20 ml and the cells were grown for another 3 days with daily checking of confluence.

2.1.2 Cell passage

Cell passage was performed in order to increase number of proliferating cells and increase their living space. Cell passage was only performed on fully confluent cell culture flasks. The procedure was carried out as follows:

1. Old medium was removed from culture flask and cells were washed briefly with 5 ml of trypsin at 37°C, for 1-2 min.

2. 5 ml trypsin was removed from the culture flasks and replaced with fresh 1.5 ml of trypsin. Cells were then incubated, with trypsin, for 30 min in an incubator at 37°C and 5 % CO_2..

3. After incubation, cells were checked to ensure full release from the culture flask.

4. Trypsin was then quenched with 20 ml of complete medium and the total volume was spun down at 1500 rpm for 7 min.

5. The supernatant was discarded and the pellet war re-suspended in 5 ml of complete medium. 2.5 ml of the cell suspension was transferred into fresh 20 ml complete medium in a new culture flask. This was repeated for the remaining 2.5 ml of the cell suspension.

6. Two new flasks were then incubated in an air-incubator under 5 % CO_2 and 37°C for 3 days and the cell growth was investigated.

2.1.3 Cell transfer to well plates (6 x 2 ml)

In order to carry out metabolic labelling [section 2.2], cells were split and transferred into cell culture plates. The procedure was carried out as follows:

1. Cells were trypsinated as per 2.1.2, points 1 to 3.
2. Trypsin was quenched with 5 ml of complete medium and the solution was centrifuged for 7 min at 1500 rpm.
3. The supernatant was discarded and the pellet was resuspended in a suitable volume of complete medium (2.0 ml per well, i.e. for 4 wells- 8.0 ml of complete medium).
4. 2.0 ml of the cell suspension was transferred into each new well in a 6-well cell culture plate and incubated for 3 days at standard conditions.

After 3 days, cells were observed under the light microscope to ensure proper adhesion and cell density.

2.1.4 Cell tissue maintenance

If the cells were not used in experiments, their complete medium was changed every 3 to 4 days. Old medium was discarded and replaced with an equal amount of fresh complete medium. If the cells were completely confluent, the cells were passaged as per section 2.1.2.

2.1.5 Freezing of cells

Unused cells were frozen in order to increase their viability and create a working bank for later cell culture.

The cell freezing procedure was carried out as follows:

1. Cells were removed from cell culture flasks using trypsination [section 2.1.2, points 1-3].
2. 5.0 ml of complete medium was added to the cell suspension in trypsin before centrifugation for 7 min at 1500 rpm.

3. The supernatant was discarded and the pellet was dissolved in 1.2 ml of freezing medium (Complete medium with 10 % dimethyl sulfoxide (DMSO)).

4. The cells suspended in freezing medium were transferred to a cryoampule and labelled accordingly.

The ampule was placed ASAP in -80 °C freezer for 24 hr. After 24 hr, the ampule was transferred to liquid nitrogen for long term storage.

2.1.6 Harvest of non-radioactively labelled fractions (M and CL)

Non-radioactively labelled medium (M) and cell lysate (CL) fractions were used for WB analysis [section 2.8] and protein concentration [section 2.12] for subsequent analysis. The harvesting procedure was carried out only with cell culture flasks that showed full confluence. Collected medium was serum-free, in order to exclude any proteins from sources other than the analysed cells.

Harvest of non-radioactively labelled medium

The harvest of M was carried out as follows:

1. Old medium was removed from cell culture flask followed by two washings steps, each with 20 ml of DMEM without supplements. Used DMEM was discarded.

2. New 20 ml of DMEM was added to culture flask and the cells were incubated for 30 min in an incubator at 37°C, 5 % CO_2. The medium was discarded and the cells were washed briefly once more in DMEM.

3. The washing medium was replaced with 20 ml of fresh DMEM and incubated for 24 hr under the same conditions (1^{st} incubation period).

4. Medium was harvested, and replaced with 20 ml of another fresh DMEM for further 24 hr (2^{nd} incubation period). The harvested Ms was labelled accordingly and frozen at -80 °C.

After the 2^{nd} incubation period, the medium was collected again, labelled accordingly and frozen at -80°C.

Harvest of non-radioactively labelled CL

1. Harvest of CLs was carried out immediately after the final medium harvest to achieve paired data sets.

2. The harvest of CL was carried out as follows:

3. After harvesting medium [section 2.1.4.1], cells were briefly washed three times with 10 ml of ice-cold, sterile, 1x PBS (phosphate buffered saline). Washings were discarded.

4. 5 ml of ice cold, sterile 1x PBS was added to the culture flask and the cells were scraped off from the bottom of the culture flasks, using a rubber policeman. The culture flasks were then inspected under the light microscope to ensure complete removal of attached cells.

5. 5 ml of ice cold, sterile 1x PBS was added and additional cells were poured off and all cells removed were centrifuged for 7 min at 1500 rpm. The supernatant was discarded.

6. The cell pellet was labelled accordingly and frozen at – 80 °C.

When it was necessary to use CL fraction, frozen pellet was removed from freezer, thawed and lysed in 1.0 ml of lysing buffer for 20-30 min at room temperature.

2.2 Metabolic labelling

2.2.1 Substrate supply

Metabolic labelling was carried out in order to provide cells with radioactive $^{35}S\text{-}SO_4^{2-}$. These sulfate ions would in turn be incorporated in sulfated GAG chains on PGs. When working with live cells, the aseptic procedure was put into place. Procedure for metabolic labelling was as follows:

1. From 2.1.3, old complete medium was removed from each well in a 6-well cell culture plate and replaced with 1.5 ml of $^{35}S\text{-}SO_4^{2-}$ (0.2 mCi/ml) in RPMI-1640 without sulfate. The medium also contained 2 % FBS.

2. Cells were incubated for 24 hr in an incubator at 5 % CO_2 and 37°C.

3. After 24 hr, the media and cell fractions were harvested

2.2.2 Radioactively labelled CL and M harvest

1.0 ml of harvested medium from radioactively labelled cells was applied to 4 ml G-50 fine Sephadex column and labelled macromolecules were eluted using 1.5 ml of dH_2O.

1. The elutes were collected, labelled accordingly (cell line name plus M) and frozen.

2. Cell fractions remaining in wells were washed twice using ice cold PBS (2 x 2.0 ml) for 20 min, in order to prevent cross contamination from medium macromolecules.

3. Washed cells were lysed by addition of 1.0 ml of ice cold lysis buffer and incubation for 40 min with shaking, on ice.

4. CLs were collected and added to G-50 fine Sephadex columns and macromolecules were eluted following the same procedure as for the Ms.

5. Elute was labelled accordingly (cell line name plus CL) and frozen at -20°C

2.3 Scintillation counting

Scintillation counting is a method used to determine radioactivity in a given sample. Radioactivity is measured by applying scintillation liquid to the samples to be measured. The scintillation liquid, upon exposure to radioactivity will emit light. This light emission is then measured by the scintillation counter and converted into counts per min (CPM).

Scintillation counting was performed as follows:

1. Appropriate sample volume was added to in scintillation count vials.

2. Into each vial, 3.0 ml of scintillation fluid was added and the mixture was thoroughly mixed by inverting 5-10 times.

3. Vials were placed in the scintillation counter racks and the appropriate measuring program was set up and executed, using manufacturer’s software.

4. Read out was collected in printed form and the data was transferred into an excel file.

5. Used vials were discarded following the appropriate procedure.

For analysing crude samples (CL and M), 40 µl of sample volume was used. For Gel size-exclusion chromatography [section 2.7] 1.0 ml of sample volume was used.

2.4 SDS-PAGE

SDS-PAGE (sodium dodecyl sulfate polyacrylamide gel electrophoresis) is a method used for separation of protein molecules based on their molecular mass (M_w). Each molecule possesses more or less intrinsic electrostatic charge, which makes it attracted to the opposite charge and thus may move through a medium through which an electric current is applied. In SDS-PAGE, SDS is a detergent that gives uniform charge for all protein molecules after incubation at high temperature so each protein will ideally have the same mass-charge ratio, but not the same mass. The mass will determine the speed by which a protein would travel through the gel (polyacrylamide). The lighter proteins travel faster through the gel and the heavy proteins travel more slowly. Over fixed time period, the proteins will separate themselves on the basis of M_w.

This procedure describes the SDS-PAGE analysis with gel drying, that subsequently lead to radiographic imaging.

Into each gel a molecular marker was loaded (1-3 µl/well).SDS-PAGE analysis used for WB and silver stain imaging is described in section [section 2.8]

The SDS-PAGE analysis was carried out as follows:

1. Appropriate volume of sample (calculated beforehand) was dried in a freeze dryer in order to concentrate it.

2. Concentrated samples were re-suspended with a calculated volume of a previously created master mix.

3. Samples were heated for 3 min at 97°C, to allow proper denaturation of proteins.

4. Samples (maximum total volume of 40 μl) were loaded into the wells of a Criterion XT Precast Gel Bis-Tris 4-12 % along with molecular marker (1-3 μl).

5. Gel was run for 80 min at 180 V, 180 mA. In some cases , increased time was applied in order to bring the protein front closer to the gel's end, thus achieving better separation.

6. The gel was removed from SDS-PAGE running buffer, washed twice with dH_2O, and put into t fix solution overnight, with rocking (minimal time needed for fixation is 1 hour, recommended overnight).

7. After fixation, fix solution was discarded following the standard procedure. Gel was washed twice with dH_2O and amplified with Amplify solution (GE Healthcare) for 30 min.

8. Following amplification, gels were washed twice with dH_2O and placed on a slob gel dryer at 80°C until dry. Filter paper was placed under the gel to prevent contamination and plastic foil was placed on top for protection.

9. Dry gels were then removed and processed for radiographic imaging

2.5 Radiographic imaging

Radioactive atoms emit energy as radiation, eitherα-particles or β- or γ- rays. The exact energy and nature of radiation is specific for each radioactive element. In this project, the radioactive sulfur isotope, ^{35}S, was used in the form of sulfate ions $^{35}S\text{-}SO_4^{2-}$. Radioactively labelled PGs [section 2.2] incorporate radioactive sulfate during synthesis and may be visualised after separation on SDS-PAGE gels.

The radiographic imaging was carried out in a PhosphoImager as follows:

1. Previously dried gels [section 2.4] are placed in an exposure cassette for overnight exposure. One must take care to make sure that the gel is properly dried; any traces of water would damage the cassette and distort the results.

2. Exposure screen was placed on a Typhoon PhosphoImager for gel imaging. The Typhoon Reader should be turned on at least 30 min before taking the image for better results.

3. Using software (Typhoon scanner control 3.0), a gel image was taken at 200 pixels/micron resolution. The file was saved on external memory for further analysis.

4. Used exposure cassette was erased using image eraser equipment.

2.6 Enzymatic digestion of GAGs

Enzymes that can digest HS or CS were used to determine the characteristics of PGs present in the sample. Hep digests HS, leaving CS and other GAGs, while chondroitinase ABC (cABC) digests chondroitin and dermatan sulfate, leaving HS and other GAGs undigested.

2.6.1 cABC digestion

cABC, E.C. 4.2.2.4, is an enzyme that catalyses the eliminative cleavage of N-acetylhexosaminide linkages in CS A, CS B, CS C, chondroitin, dermatan sulfate and hyaluronic acid yielding mainly disaccharides (Amsbio n.d.). The yielded disaccharides will travel through an SDS-PAGE gel and will not be seen as a band on a radiographic gel image of ^{35}S-labelled macromolecules. The remaining bands would mostly represent HS PGs and to some extent other sulfated molecules.

The digestion with cABC enzyme was carried out as follows:

1. An appropriate volume of samples (8-40 µl) was transferred into 1.5 ml Eppendorf tubes and dried in the freeze dryer.

2. Fully dried samples were re-suspended in 15 µl of 1x cABC buffer.

3. 30 mU of cABC enzyme was added to each re-suspended sample and incubated for 1hour at 37°C in a heating block. For control samples, 5 µl of 1x cABC buffer was added instead of cABC enzyme.

4. Digestion was stopped after 1 hour with 2 min of heating at 97 °C. The samples were then either applied to SDS-PAGE gel analysis [section 2.4] with radiographic imaging [section 2.5], or in the size-exclusion gel column chromatography [section 2.7].

2.6.2 Heparinase I, II, III (Hep) enzymatic digestion

Heparinase I, II, III, (Hep) E.C. 4.2.2.8, is an enzyme mix that cleaves selectively, via an elimination mechanism, sulfated polysaccharide chains containing 1-4 linkages between hexosamines and glucuronic acid residues. It cleaves HS solely and does not cleave fractioned heparin or low M_w heparin (IBEX Pharmaceuticals 2011). The saccharide that is yielded in the reaction would, similarly to cABC digestion, travel through gel and the bands remaining will be CS PGs and other sulfated molecules.

The digestion with Hep was carried out as follows:

1. An appropriate sample volume (8-40 µl) was dried using a freeze dryer.

2. Dried pellet was re-suspended in 15 µl of 1x Hep buffer.

3. 0.1 mU of Hep enzyme was added to the re-suspended sample.

4. The sample was mixed and incubated for 16 hr at 28°C on a heating block.

Digestion was stopped after 16 hr with 2 min incubation at 97 °C. The samples were either subjected to SDS-PAGE gel analysis [section 2.4] with radiographic imaging [section 2.5] or to gel filtration chromatography [section 2.7].

2.7 Size exclusion gel chromatography

Size exclusion gel chromatography separates molecules based on their M_w. In size exclusion chromatography, the columns are filled with beads that contain pores of a defined size. Molecules larger than the pore will be excluded from entering the beads and travel fast through the column and elute in V_0 (void volume), while molecules that fit in the pore will also travel through the beads and will elute later, at V_t (total volume) if the molecules have full access to the internal volume of the bead material. In this project, radioactively labelled PGs were analysed by size-exclusion gel chromatography. In theory, PGs with full GAG chain modification would elute in V_0, and small molecules (i.e. disaccharides) would elute in V_t.

Gel material used was CL6-B Sepharose ™; plastic column was 1x40 cm, gel volume was 40 ml. Samples for column chromatography were previously metabolically labelled [section 2.2] and enzymatically digested [section 2.6].

The size exclusion gel chromatography was carried out with the following steps

1. Obtained sample was supplemented with 150 µl of blue dextran/potassium dichromate solution or more to avoid too much dilution. This solution provided molecular size markers for V_0 (blue dextran- blue colour) and V_t (potassium dichromate-yellow colour).

2. Columns were purged with running buffer at 0.14 ml/min flow rate for 30 min. Columns were then equilibrated with running buffer at a flow rate of 0.14 ml/min.

3. Sample was applied dropwise onto the column, allowed to sink into the column material and overlayered with running buffer.

4. Fractions were collected at 7 min/fraction. Collection started when the blue marker had approached the end of the column. For each run, 40 fractions were collected directly into scintillation vials.

5. After collection was completed, each fraction was supplemented with 3.0 ml of scintillation liquid. Fractions with strong blue and yellow colour were marked as V_0

and V_t. Subsequently, the radioactivity in each fraction was determined in a scintillation counter and the data was recorded in an excel file. V_0 and V_t fractions were marked accordingly.

2.8 Western blotting (WB)

In WB, proteins that have been separated on SDS-PAGE gels are transferred to a membrane. This allows for subsequent incubation with antibodies that will detect the presence of specific proteins. WB is used to detect and quantify proteins of interest, although the quantitation may be regarded as semi-quantitative.

The WB was performed in this project using NuPAGE 4-12 % Bis-Tris gels, in contrast to SDS-PAGE gels used in radioactive imaging (Criterion XT).

Through this project only the wet transfer method was used.

The WB was carried out as follows:

1. An appropriate, calculated, volume of each sample (2-16 µl) was mixed with NuPAGE master mix, in order to achieve a satisfactory dilution level.
2. Samples were heated at 70°C for 10 min on a heating block.
3. Gel was run, following the manufacturer's suggestion, at 120 V for 120 min.
4. Transfer of the proteins to a PVDF membrane was carried out using the manufacturer's manual, at 30 V and 180 mA for 1 hour.
5. The membrane was then blocked with 2 % ECL Blocking agent in 1x TTBS at 4°C, overnight.
6. After blocking, the membrane was blotted with the primary antibody (1^{st} Ab) solution at 4°C for overnight. The recommended dilution of each antibody was obtained from the supplier's records (between 1:2000 and1:5000).
7. After primary antibody incubation, the membrane was washed 5 times for 10 min, each time with fresh 1x TTBS.
8. After washing steps, membrane was blotted with a secondary antibody (2^{nd} Ab) solution for 1 hour at room temperature. The dilution used was 1:50 000.
9. The membrane was then washed 5 times for 10 min, each time with fresh 1 x TTBS

10. The membrane was then incubated with ECL™ Detection reagent using Amersham ECL ™ Select WB Detection reagent manufacturer's manual. For each membrane 1.0 ml to 1.5 ml of the final development solution was used.

2.8.1 WB imaging

Imaging of WB membranes was carried out on a Kodak Image Station 400R Pro using luminescence settings and the exposure time was 1-5 min. Files were saved on an external drive. Methods for taking images followed the manufacturer's manual.

2.9 Dialysis and concentration of Ms

Ms from E42 and COG7 were dialysed and concentrated to achieve a high protein concentration required for WB analysis. This was carried out due to the fact that PGs are expressed at low levels in cells when compared with more abundant proteins.

Dialysis was only performed on non-radioactively labelled harvested Ms [section 2.1.6] from E42 and COG7 cells.

The dialysis of Ms was carried out as follows:

1. 5.0 ml of harvested medium was placed in a dialysis cassette.
2. The cassette was placed in 3 litres of dH_2O with stirring overnight at 4°C.
3. Dialysed medium was removed from the cassette and placed in a centrifugal filter tube for concentration.
4. The tube was centrifuged at maximum rpm (in Alexa X-22 centrifuge) for 40 min or until the un-filtrated medium reached 1.0 ml in volume
5. Un-filtrated liquid was transferred into 5 Eppendorf's tube, 200 µl in each. The tubes were labelled and placed in freeze dryer and dried.
6. The tubes were dried until there was no liquid present and/or a precipitate formed. Then the tubes were removed from the freeze dryer and either the precipitate was frozen at -20°C for future work or it was re-suspended with 20 µl of appropriate solvent (dH_2O or buffer).

2.10 Ion-exchange chromatography

Ion-exchange chromatography separates molecules on the basis of their affinity to ligand on the column, which is either positively or negatively charged. In theory, all PGs, since they have negatively charged GAGs chains, should bind to a positively charged column and would not elute until displaced by ions with higher affinity. In this project 2 x 5 cm plastic columns were used with a DEAE-sephacel gel volume of 1.0 ml.

All steps were carried out in the cold room at 4-8°C.

The ion-exchange chromatography was carried out as follows:

1. A 2 x 5 cm plastic column was filled with 1.0 ml of DEAE-sephacel column material and was equilibrated with 6.0 ml of buffer A. Flow rate was established at 3-5 seconds/drop.

2. Sample was applied (5.0 ml of dialysed, but not concentrated medium) at 5-10 seconds/drop. The flow-through was collected and labelled Elute 1.

3. The column was washed with buffer A twice with 5.0 ml each time at elution rate of 3-5 seconds/drop. Elute was collected as “Elute 1.2” and “Elute 1.3”.

4. 5.0 ml of buffer B was applied to the column and the elute was collected as “Elute 2” with rate of 5-10 seconds/drop.

5. 5.0 ml of buffer B was applied to the column and the elute was collected as “Elute 3” with rate of 5-10 seconds/drop.

6. The column was washed with 2 x 5.0 ml of buffer A, capped and stored at 4°C.

Elutes 1.2 and 1.3 were eventually discarded as these low-salt washes do not contain any PGs of interest. Elutes 1and 2 were analysed by mass spectrometry to establish the presence of PGs. Elutes 1 and 2 were also analysed by SDS-PAGE followed by silver staining to visualize proteins.

2.11Mass Spectrometry (MS)

Mass spectrometry is a powerful tool used to identify proteins and protein modifications based on their mass to charge ratio (m/z ratio). In this project, MS was used to identify potential PGs and their modifications from COG7 and E42 M samples.

Procedure:

The samples submitted for analysis were derived from Elute 1 and 2 obtained during ion – exchange chromatography.

All MS analysis was carried out by Anders Moen, the Head Engineer in mass spectroscopy facility at Department of Biosciences, University of Oslo. Peptide search and identification was carried out by Anders Moen.

2.12Protein measurement- BCA™ Assay

This method is based on reduction of copper ions (from Cu^{2+} to Cu^{+}) by protein in an alkaline solution. Highly sensitive and selective colorimetric detection is connected to the reduction reaction by a unique reagent based on bicinchoninc acid. The detection is carried out at 562 nm and may be read in the spectrophotometer.

The procedure was carried out according to manufacturer's manual (BCA™ Protein Assay Kit, 23225, 23227, Pierce, Rockford, IL) with minor deviations, listed below:

1. BSA standards were prepared using DMEM instead of dH_2O for measuring protein concentration in the medium.
2. BSA standards were prepared using lysis buffer instead of dH_2O for measuring protein concentration in CLs.
3. The sample working dilution was 1:20 at all times.
4. Incubation took place in an air incubator.
5. Before each read in spectrophotometric plate reader, the plate was shaken for 5 seconds and left to settle for 10 seconds
6. Readouts were printed and transferred into an excel file.

2.13 Silver staining

Silver staining is a sensitive method to detect proteins in an SDS-PAGE gel. It utilizes silver nitrate which binds to selective amino acids in proteins at neutral or weakly alkaline pH. The protein bound silver ions are reduced by formaldehyde at alkaline pH to form metallic silver in the gel. The proteins are visualized as dark bands in the gel.

Procedure:

Silver staining was carried out according to manufacturer's manual (Sigma, ProteoSilver™ Plus Silver Stain Kit, Product code: PROT-SIL2) with a development time of 4.5 min.

2.14 Radiographic gel quantification

Bands obtained from radiographic imaging were quantified and analyzed using ImageQuant ™ software using the software manufacturer's procedure. Mathematical analysis was carried out in Microsoft Excel 2010 using data obtained from ImageQuant™ steps. This data should be treated with caution, as only a limited number of samples were analyzed and thus statistical analysis could not be performed.

3 Results

3.1 Overview of the work

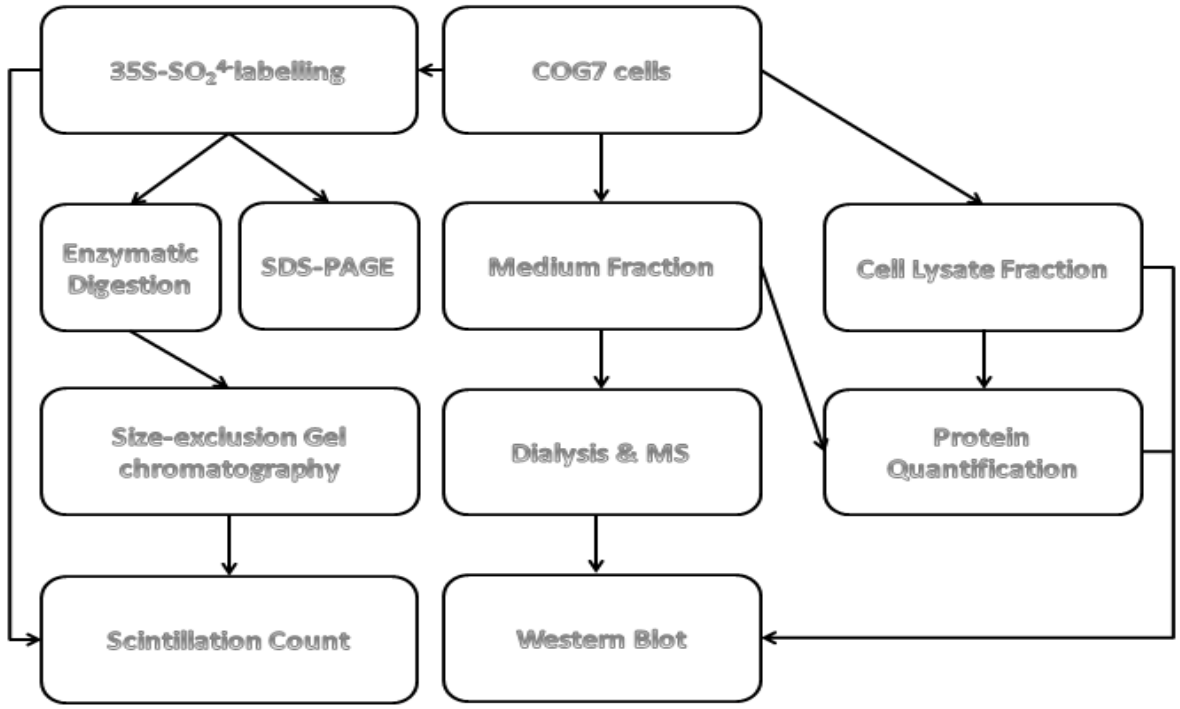

Figure 8. Overview of the work carried out

Aim of this project was to characterize PGs synthesized by COG7 deficient (throughout this document referred as COG7) cells. As of May 2014, scientific literature did not cover this area of research. The initial hypothesis was that PG synthesis is altered in COG7 cells.

Throughout the project two control cell lines were available, entitled: E42 and E12. These cell lines were dermal fibroblasts collected from the lower arm of two healthy human individuals and should, in theory, provide representative sample of wild-type PG expression. However, some heterogeneity was observed during the initial experimental stage, and from that moment on E42 cell line was used as a control, but some data came from E12 cells were also generated. Within this document control refers to the E42 cell line, unless otherwise stated.

One can divide proteins into two major fractions according to their localization: cellular and secreted. In this project, samples of PGs have been divided accordingly into these two fractions: cell lysate (CL) and medium (M). The medium in which the cells have grown and

to witch proteins and PGs are secreted is labelled medium, M, and cell lysate is labelled CL. Control (CTR) refers to two instances:

1. A “normal” cell line (E42) and

2. Non-enzymatically treated sample.

3.2 Metabolic labelling

3.2.1 Introduction

In order to determine if in fact PG synthesis is aberrant in COG7 cells, metabolic labelling with radioactive sulfate was initially performed. This means that radioactively labelled ^{35}S-SO_4^{2-} sulfate is fed to cells and gets incorporated during sulfation modification in the GAG chains of PGs. Since most of the sulfate is used in GAG chain modification (a smaller fraction of the sulfate is used in other ways), one can assume that this radioactive sulfate will label mainly PGs. However, when it comes to quantitative description of sulfate –labelled PGs, one has to take into account that the sulfate-labelling level does not correspond directly to the sulfation density on the GAG chain. Increased amounts of sulfate could also relate to longer GAGs, increased number of GAGs and, of course, to increased expression of PG protein cores.

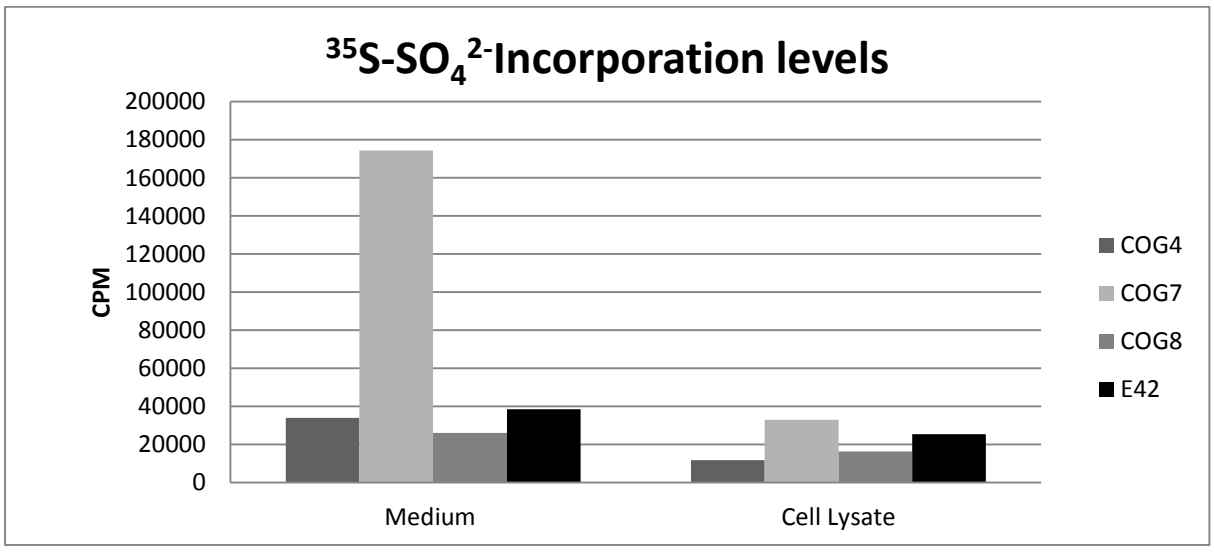

Figure 9 ^{35}S-SO_4^{2-} incorporation levels for COG4, COG7, COG8 and E42 cell lines. Cells were radioactively labelled for 24 hr. M and CL fractions were collected as per section 2.2.2and the unincorporated ^{35}S-SO_4^{2} ions

were removed by G-50 fine columns and the samples were measured via scintillation counting. Each sample contains equal volume (30 µl) of M and CLfraction

It is clear that COG7 cells incorporate significantly more $^{35}S\text{-}SO_4^{2}$ in the secreted PGs than E42, COG4 or COG7 cells. The interesting feature in COG7 cells is increased incorporation when compared to other COG-mutants (COG4 and COG8) suggesting that increased sulfation of secreted PGs is a COG mutation specific. The difference in sulfation level was only observed in secreted COG7 PGs, where the COG7 CL fraction did not differ significantly from E42 and other COG mutants (COG4 and COG8)

3.2.2 Metabolic labelling with ^{35}S-sulfate- overview

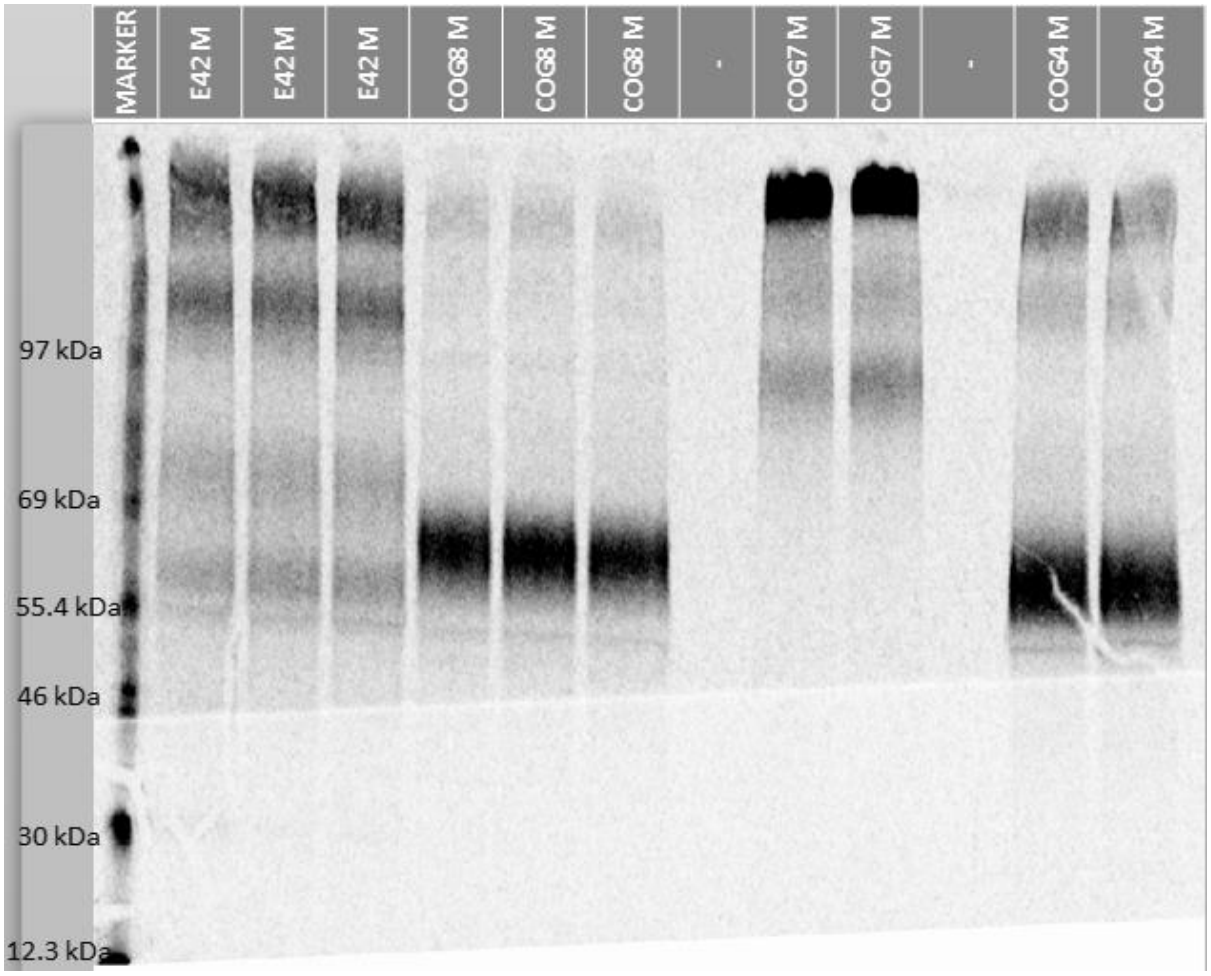

Figure 10. Overview of secreted PGs in E42, COG8, COG7 and COG4 cells. Cells were grown in 2 ml plastic wells with $^{35}S\text{-}SO_4^{2-}$ RPMI 1640 medium with dose of 0.2 mCi/ml for 24 hr. Medium was harvested according to section 2.2.2 and loaded onto SDS-PAGE gel with sample size of 30µl in each of the wells. Gel image was taken using PhosphoImager at 200 pixels per micron.

Figure 10 shows clearly that there is extensive diversity between control and COG7 cell lines with respect to PG synthesis. In addition, also COG8 and COG4 cell lines showed deviation

form wild-type. The control cell line (E42 M) showed heterogeneity in its secreted PGs, while, in contrast, COG7 showed comparative homogeneity. It is clear that the most highlighted feature of COG7's secretion profile is very high M_w PGs. COG4 and COG8 show strong bands at approximately 60-70 kDa. Those bands are also present in E42, but to a lesser intensity and with slightly modified M_w.

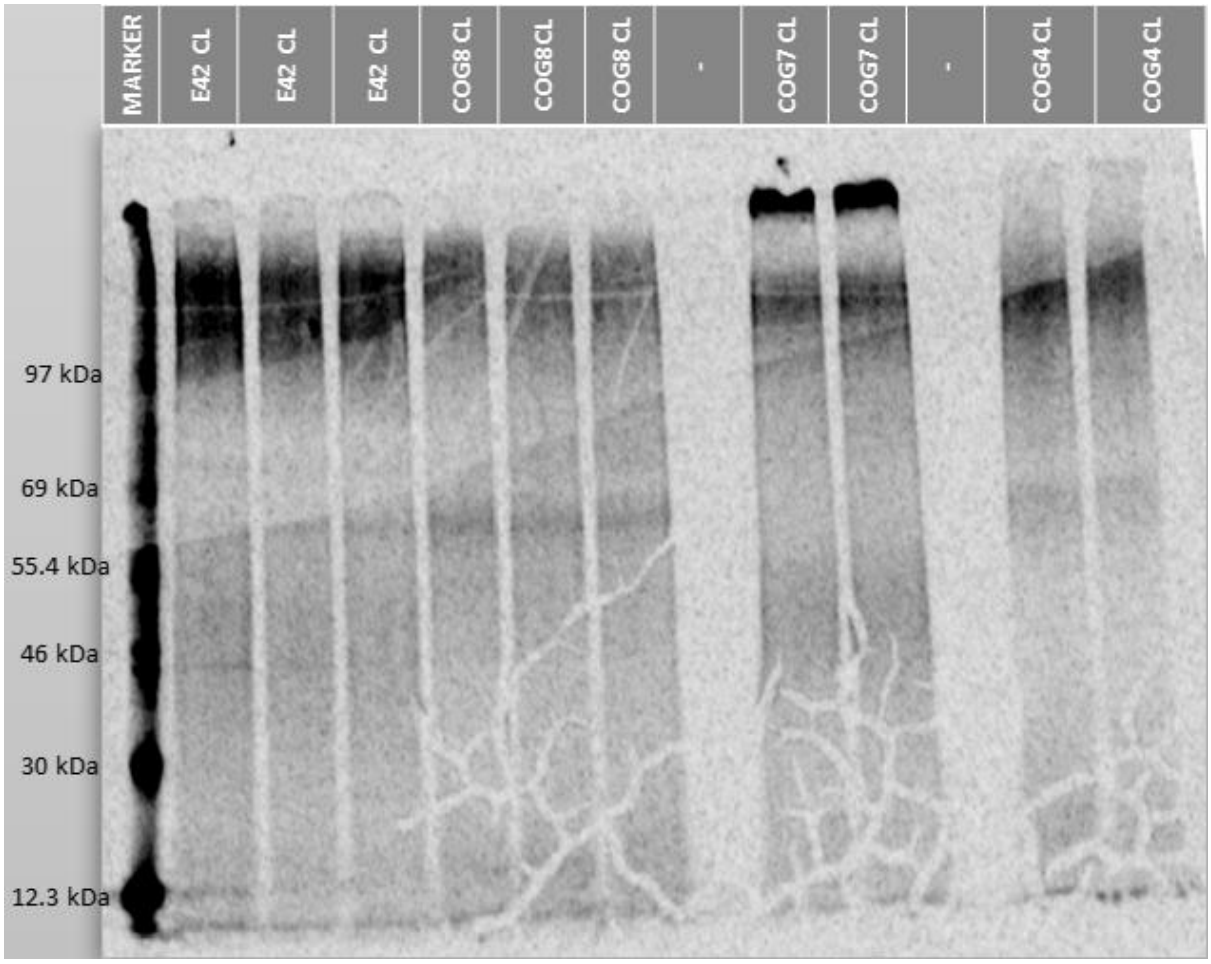

Figure 11. Overview of PGs in CL from E42, COG8, COG7 and COG4. Cells were grown in 2 ml plastic wells with $^{35}S\text{-}SO_4^{2-}$ RPMI 1640 medium with dose of 0.2 mCi/ml for 24 hr. Medium was harvested according to section 2.2.2 and loaded onto SDS-PAGE gel with sample size of 30µl in each of the wells. Gel image was taken using PhosphoImager at 200 pixels per micron. The symbol "-"indicates an empty well.

Figure 11 shows that in CLs, changes in PG synthesis are also present in COG7 cells when compared to control cell lines. It is clear that a predominant feature of COG7 CL PGs is their high M_w. A high molecular mass band of strong intensity does not appear in COG8, COG4 or E42 cell lines and thus appears to be specific to COG7 cells. All cell lines show bands at approximately 100 kDa, albeit with different signal intensities. E42 cells show the highest intensity in this band, whereas COG8 shows the lowest. COG4 and COG7 show similar intensity. COG7 CL lanes are the only ones that do not have bands at approximately 60 kDa,

with E42, COG8 and COG4 showing weak bands at this position. Similar bands are shown in Figure 10.

3.2.3 Enzymatic degradation of GAG chains

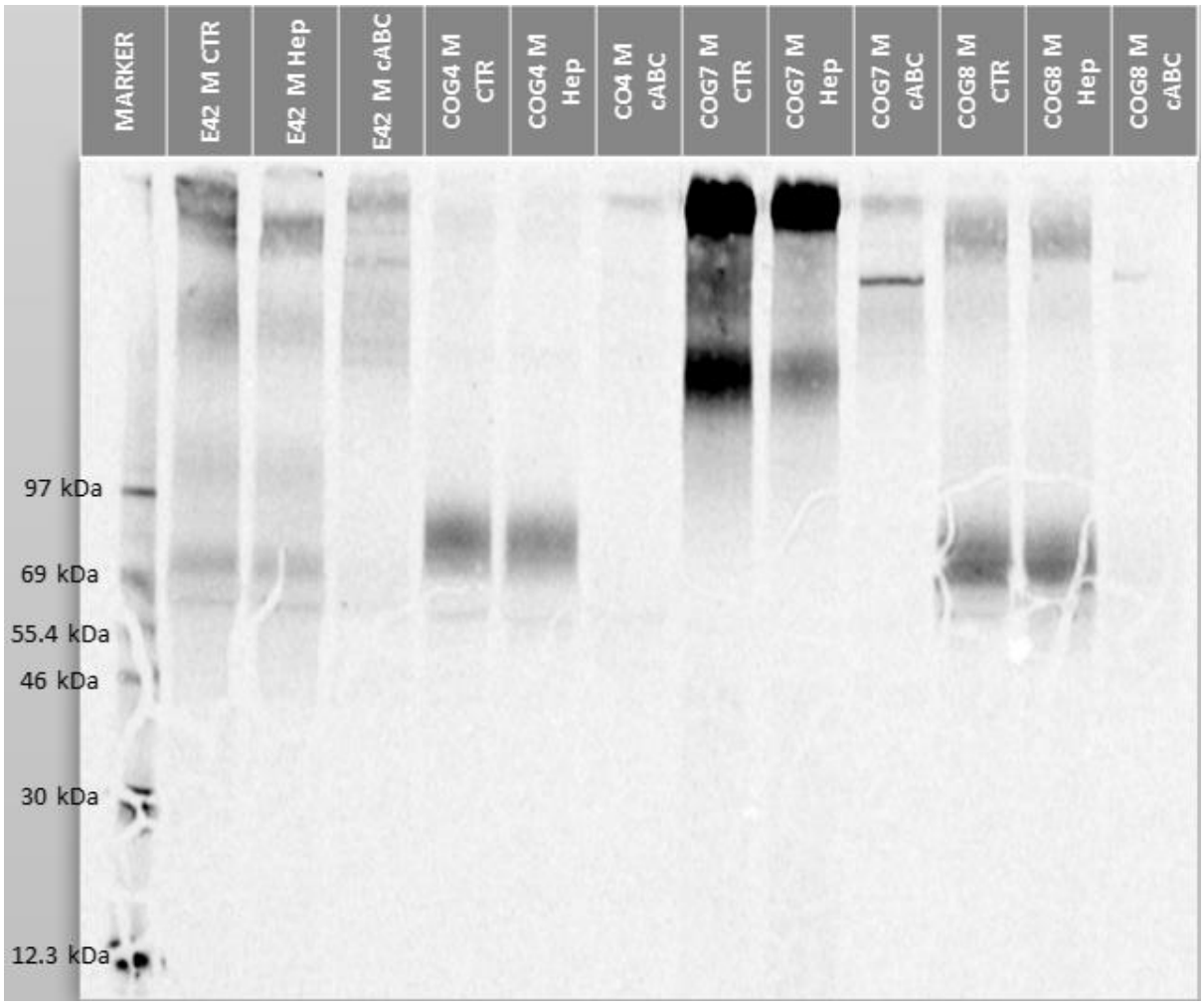

Figure 12. Enzymatic digestion E42, COG4, COG7 and COG8 M with Hep and cABC. Radioactively labelled Ms were digested with Hep and cABC as per section 2.6. CTR is control, where 1x cABC buffer was used instead of cABC. Total sample size of 30 µl was loaded onto each well in the SDS-PAGE gel and the image was taken using PhosphoImager at 200 pixels per micron.

This figure shows a significant difference between wild type cells and COG-deficient cell lines. Although all shown COG-deficient samples showed aberrant digestion, COG7 exhibits an unusual pattern, when compared to COG4 and COG8.

The most prominent feature of this enzymatic digestion is the dominating presence of CS in all of the COG-deficient cell lines. This is characterized by the presence of strong bands in the Hep lanes (COG4 M Hep, COG7 M Hep and COG8 M Hep) and complete disappearance of bands in the cABC lanes (COG4 M cABC, COG7 M cABC and COG8 M cABC).

Moreover, there is weak presence of HS in all of the COG-cells. Weak bands in the cABC lanes show remaining HS left after cABC digestion. Control cell lines showed greater proportion of HS in their secreted PGs. This is visualized by lesser reduction of signals in E42 M Hep and E42 M cABC lanes.

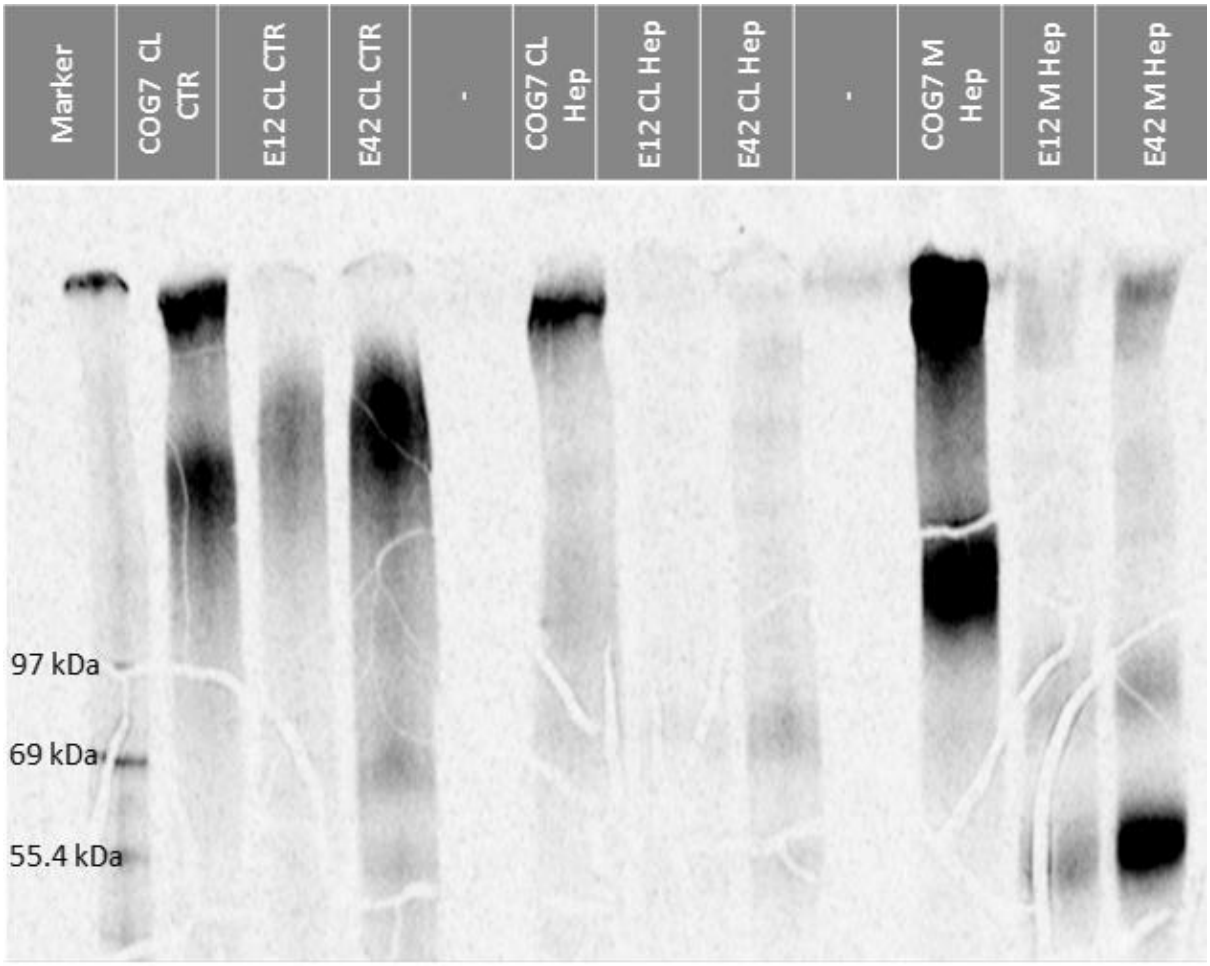

Figure 13. Enzymatic digestion of E12, E42 and COG 7 M & CL with Hep. Radioactively labelled Ms and CLs were digested with Hep as per section 2.6.2. CTR is control, where 1x Hep buffer was used instead of Hep. Total sample size of 30 µl was loaded onto each well in SDS-PAGE gel and the image was taken using PhosphoImager at 200 pixels/micron. The symbol "-"indicates empty well.

It is clear that a significant fraction of cellular PGs from COG7 cells have HS glycosaminoglycan chain modification. Moreover, this HS modified PG has a lower molecular mass than the CS-modified PG that remains as a strong band at the top of the gel. Figure 13 shows also difference between cellular PGs from control cells (E12 CTR, E42 CTR) and COG7 cells (COG7 CL).

PGs from the CL of control cells showed almost complete modifications with HS, as there are only weak bands present in the lanes E12 CL Hep and E42 CL Hep. One could speculate that

there possibly could be the same band in E12 CL lane as in E42 CL Hep lane (approximately 70 kDa) , but lower sulfation or lower PG expression could make the signal in E12 CL Hep undetectable.

3.2.4 Enzymatic digestion quantification from gel images

Gel images were quantified using Image Quant™ software.

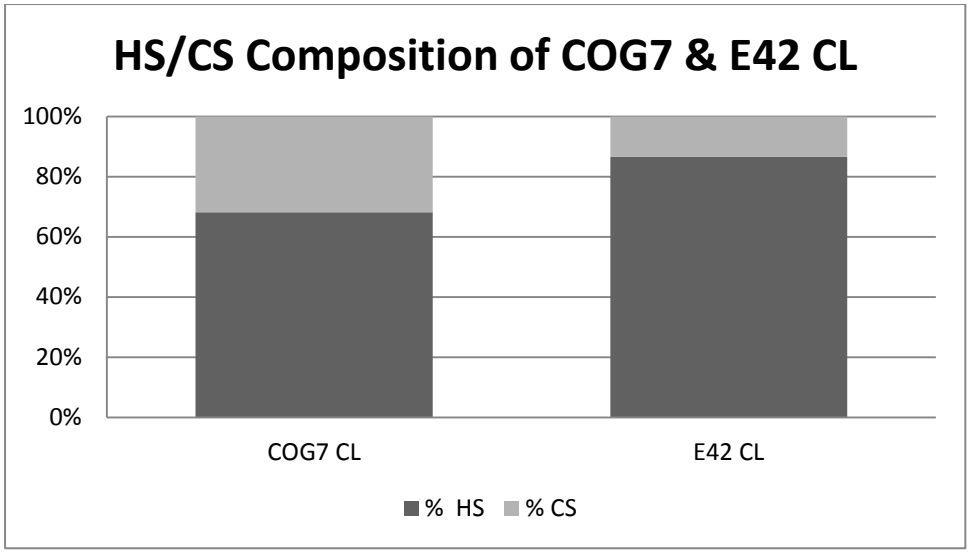

Figure 14. HS and CS composition of CL PGs from E42 and COG7 cells. Figure 13was quantified using ImageQuant™ software and the results were visualized by the above column chart. The difference between total signal value from CTR lane and total signal from Hep digest lane was expressed as a percentage of CS. The difference between total signal value from CTR lane and total signal from cABC digest lane was expressed as a percentage of HS.

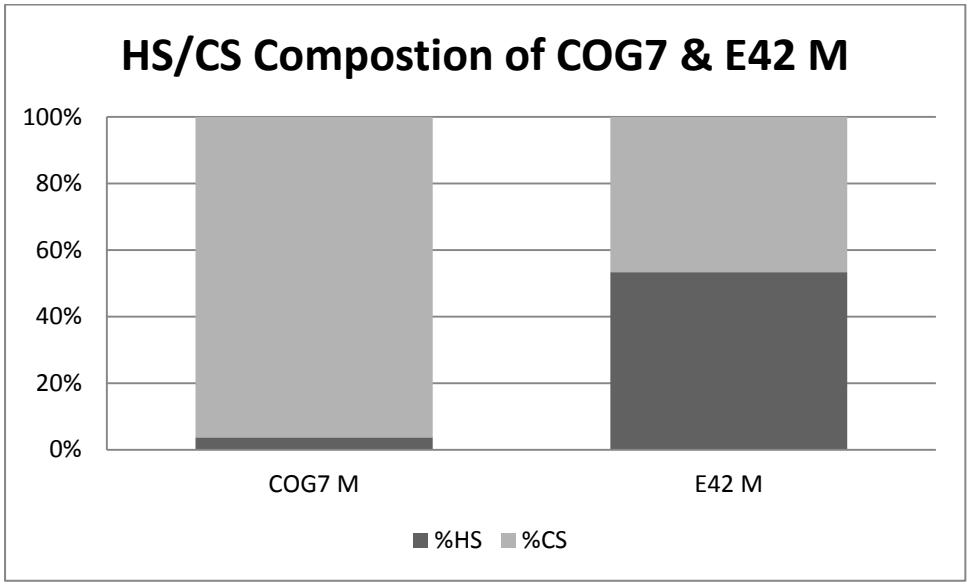

Figure 15. HS and CS composition of M PGs from E42 and COG7 cells. Figure 12 was quantified using ImageQuant™ software and the results were visualized by the above column chart. The difference between total

signal value from CTR lane and total signal from Hep digest lane was expressed as a percentage of CS. The difference between total signal value from CTR lane and total signal from cABC digest lane was expressed as a percentage of HS.

Figure 14 and Figure 15 show the composition of GAGs in the COG7 and E42 M and CL fractions. It is clear that the majority of PG modification in COG7 M is of CS nature. Moreover, the HS composition in the CL varies between COG7 and the control cell lines. From this one may assume that COG7 cells have distorted both cellular and secreted PGs with respect to the HS/CS percentage composition. It is difficult to comment on the absolute level of HS or CS synthesis in COG7 and E42 cells due to significantly higher sulfate incorporation in COG7 cells. It is not clear what the HS synthesis level is in COG7 cells when compared to the E42 cells.

3.3 Size –exclusion gel filtration chromatography

Gel filtration chromatography is a powerful analytical tool used to describe molecular masses of macromolecules in the analyte. In all chromatograms, the x-axis describes the fraction coefficient and y-axis shows the percentage of the strongest (most intensive) peak.

Fraction coefficient is a dimensionless number that is directly related to a fraction number. Fraction coefficient of 0 is equal to elution time of blue dextran (void volume, V_0) and fraction coefficient of 1 is equal to elution time of potassium dichromate ($K_2Cr_2O_2$) which will indicate the terminal volume where all molecules applied have been eluted, V_t.

In theory moieties that are bigger than 200 kDa would elute at V_0, along with blue dextran, which is a saccharide (polymer of anhydroglucose) with blue colour and high molecular mass (>200kDa). When it comes to PG analysis, the molecules eluted in V_0 are high- M_w PGs (e.g. aggrecan core protein – 250 kDa) or medium to low M_w PGs with extensive glycosaminoglycan chain modification. It is important to notice that GAG chains could contribute largely to the overall PG mass, not only by the length of the polymer itself, but also by the sheer number of GAG chains attached to the core protein.

As the harvested samples showed different levels of radioactive sulfate incorporation, the direct measurements of radioactivity deviated significantly. To counteract this, a normalization of peaks was performed in which the data was shown as percentage of the highest observed value. In this case, peaks can be compared with greater ease and conclusive remarks could be drawn. In all cases, the highest peak was present either at V_0 or at V_t.

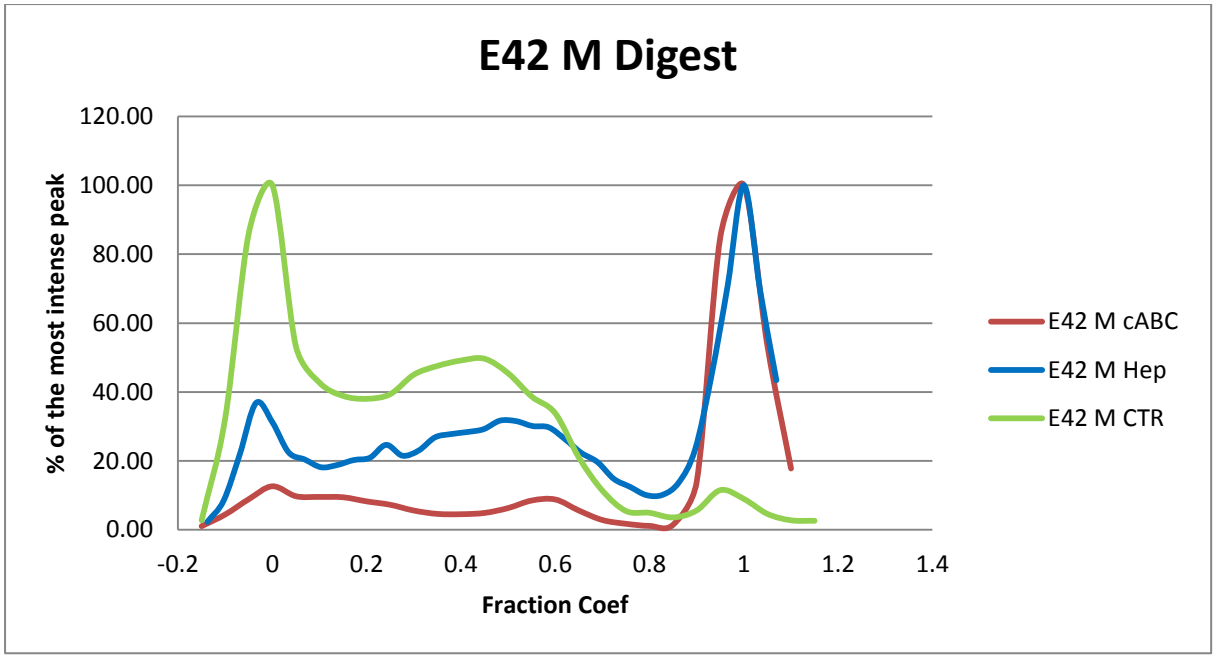

Figure 16. Gel filtration chromatogram of ^{35}S-labelled E42 M with or without digestion with cABC or Hep. Radioactively labelled and harvested M was digested with cABC and Hep as per section 2.6. Sample was eluted in CL-6B column with blue dextran/potassium dichromate markers for V_o and V_t respectively Sample loaded was equal to 30 000 cpm. Elution speed of 0.14 ml/min; collected fraction volume of 1 ml.

Figure 16 shows the natural expression of sulfated PGs in human skin fibroblasts, compared with enzymatically treated samples. Judging the profile of E42 M cABC (red line), one can notice that there is small red peak at V_0- this peak corresponds to undigested HS PG. Similarly, one should take notice on the blue line- E42 M Hep. The blue peak at V_0 represents the undigested CS PG. It is clear, that the majority modification on the secreted PGs in the E42 cells is CS, but the presence of HS is significant.

The two peaks that are present in the control sample, at fraction coefficient 0 and 0.45, describe two different PGs with different molecular masses. It is clear that both of those peaks contain heparan and CS modified PGs. It seems that the larger PGs (peak at fraction coefficient of 0) have been mostly modified with CS and to a smaller extent with HS. The second peak represents PG(s) that are possibly with a higher share of HS GAGs.

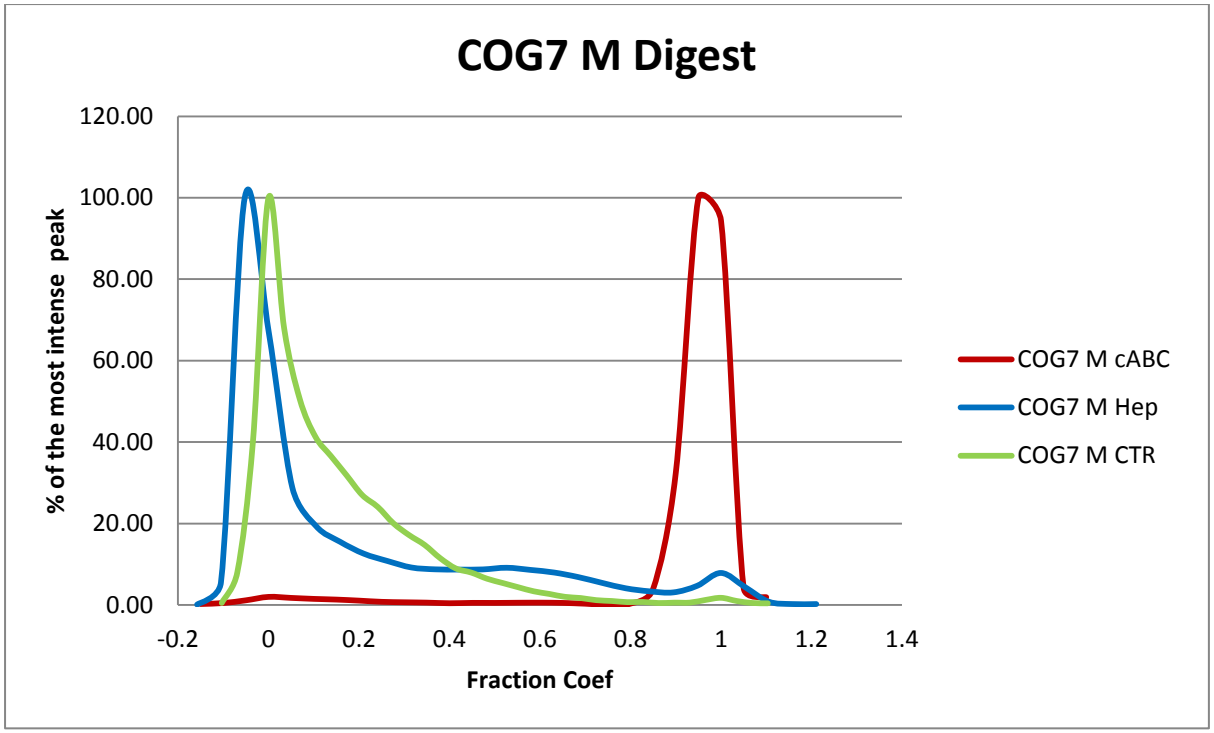

Figure 17. Gel filtration chromatogram of ^{35}S-labelled COG7 M after digestion with cABC or Hep. Radioactively labelled and harvested M was digested with cABC and Hep as per section 2.6. Sample was eluted in CL-6B column with blue dextran/potassium dichromate markers for V_o and V_t respectively Sample loaded was equal to 30µl. Elution speed of 0.14 ml/min; collected fraction volume of 1 ml.

Figure 17 shows the expression of secreted PGs from COG7 cells. It is clear that the majority of the PGs in the M are of CS nature. The unchanged peak profile at V_0 in the COG7 M Hep line suggests a large quantity of CS. Additionally, the high peak at V_t from COG7 M cABC confirms this finding. A minor peak at V_t from COG7 M Hep suggests that there is some HS modification of PGs, but the level is very low.

Both Figure 16 and Figure 17 support the main findings in the SDS-PAGE gel images and their quantification for the M fractions (Figure 15). It is clear that CS is mostly (95%) present on secreted PGs in COG7 cells, while control cells show a more balanced HS/CS composition.

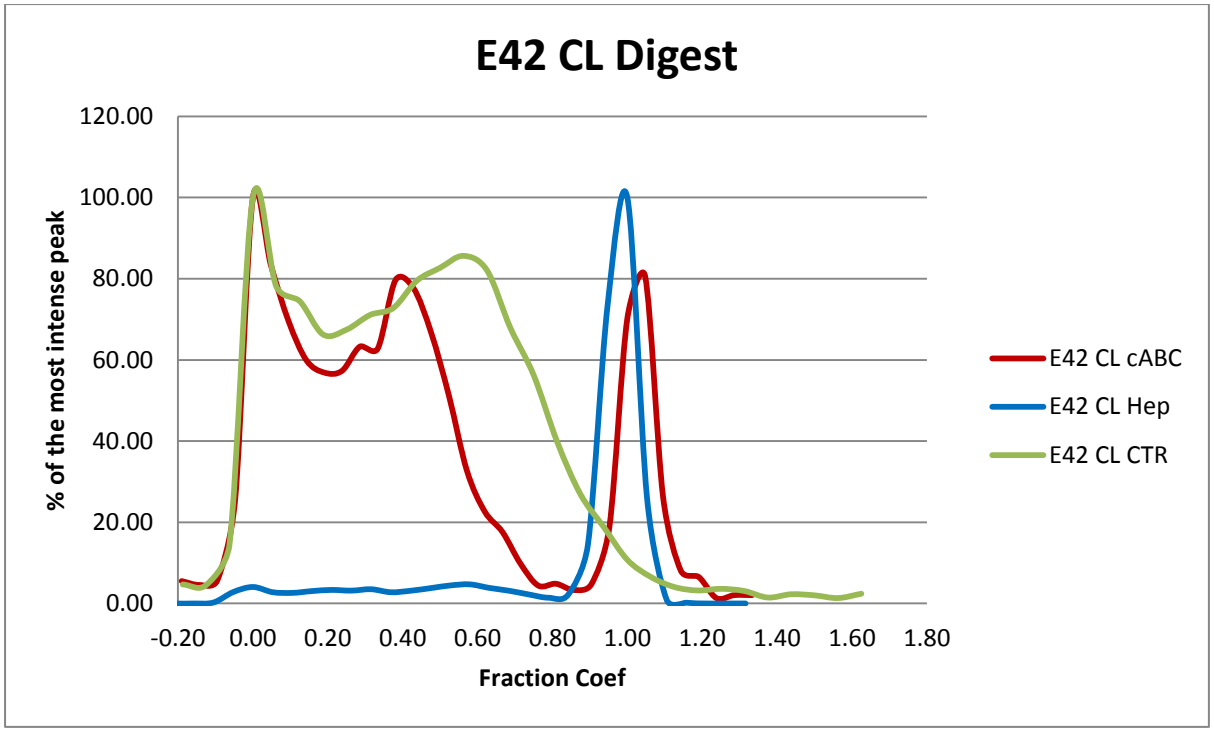

Figure 18. Gel filtration chromatograph of ^{35}S-labelled E42 CL digestion with cABC and Hep Radioactively labelled and harvested CL was digested with cABC and Hep as per section 2.6. Sample was eluted in CL-6B column with blue dextran/potassium dichromate markers for V_o and V_t respectively Sample loaded was equal to 30 000 cpm. Elution speed of 0.14 ml/min; collected fraction volume of 1 ml.

In Figure 18, it is shown that PGs present in E42 CLs possess both types of glycosaminoglycan chains: chondroitin and HS. The CS modification is present, but to a much lesser degree than HS modification. The peak at fraction coefficient of 0.60 is shifted to 0.40 after cABC digest. This suggests that this low M_w PG is modified with CS. However, almost complete digestion with Hep suggests that in fact, HS is the dominating modification.

It is clear that the amount of HS is higher than CS. This data corresponds to Figure 13, in which Hep would degrade almost the entire HS from the sample and to Figure 14 where HS comprises approximately 85% of the GAGs modifications in the E42 CL.

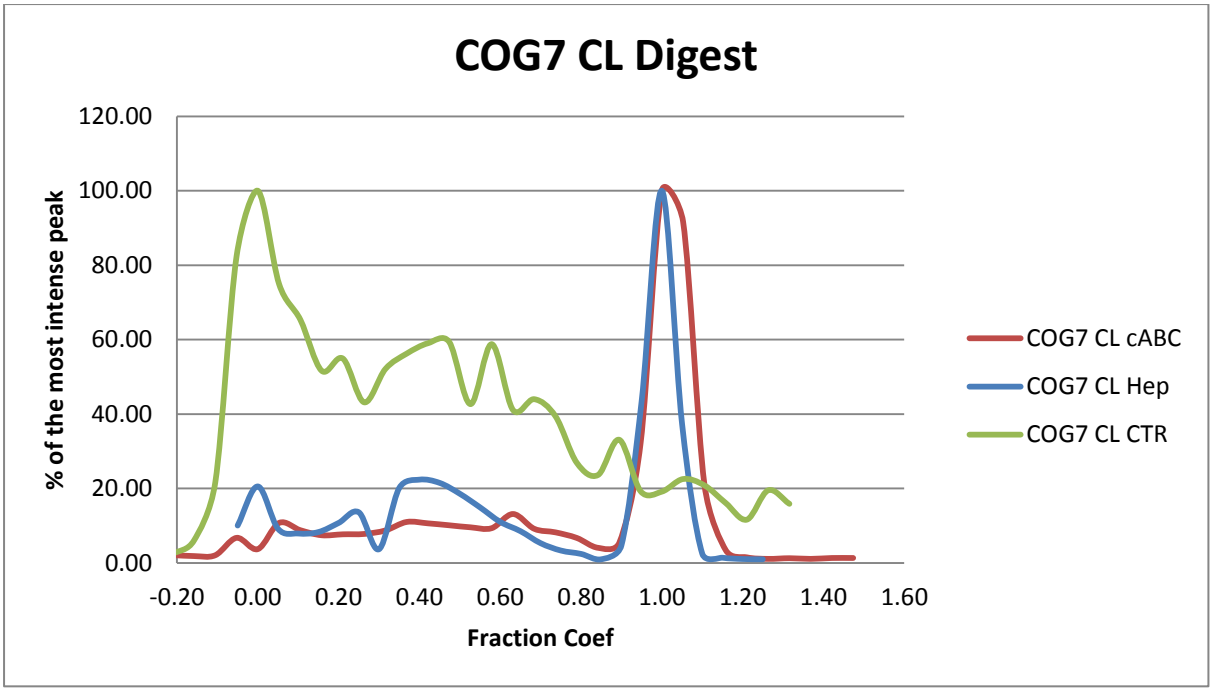

Figure 19. Gel filtration chromatograph of ^{35}S-labelled COG7 CL digestion with cABC and Hep. Radioactively labelled and harvested CL was digested with cABC and Hep as per section 2.6. Sample was eluted in CL-6B column with blue dextran/potassium dichromate markers for V_o and V_t respectively Sample loaded was equal to 30µl. Elution speed of 0.14 ml/min; collected fraction volume of 1 ml

Figure 19 shows the presence of both CS and HS in COG7 CLs. It is possible that the amount of CS is higher than HS, but it is speculative, especially in the light of Figure 14. It is, however, clear that both HS and CS are present as significant fractions of the GAGs of cellular PGs.

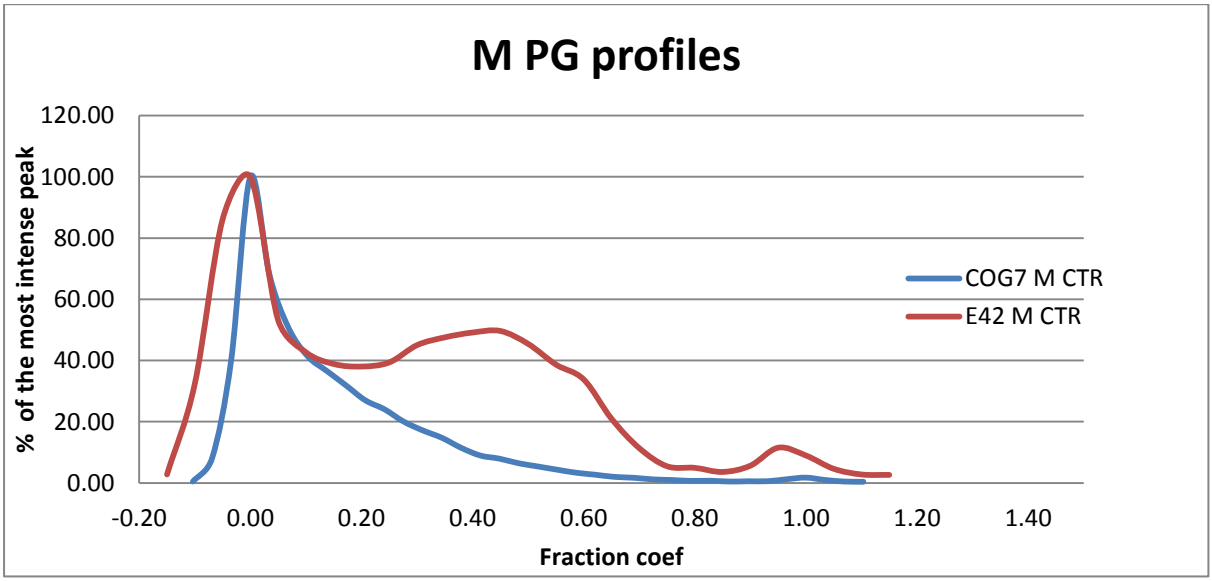

Figure 20. Overview of secreted PGs in COG7 and E42 cell lines. Radioactively labelled and harvested Ms were eluted through CL-6B column with blue dextran/potassium dichromate markers for Vt and V0 respectively. Samples loaded were equal to 30µl. Elution speed of 0.14 ml/min; collected fraction volume of 1 ml.

Figure 20 shows that secreted PGs from COG7 cells show immense, uniform destitution in weight, with the molecular mass of them averaging around 200 kDa which is the M_w of blue dextran. (Sigma Aldrich n.d.) On the other hand, the expression profile of the E42 cells shows three characteristic peaks at fraction coefficient of: 0, 0.4 and 1. The presence of peak at fraction coefficient of 1 suggests presence of small sulfated moieties in the M of E42. Those sulfated moieties are possibly sulfated disaccharides (GlcNAc/GalNAc-GlcA) either excreted from the cells or shed from the glycocalyx. There is no corresponding peak in COG7 M.

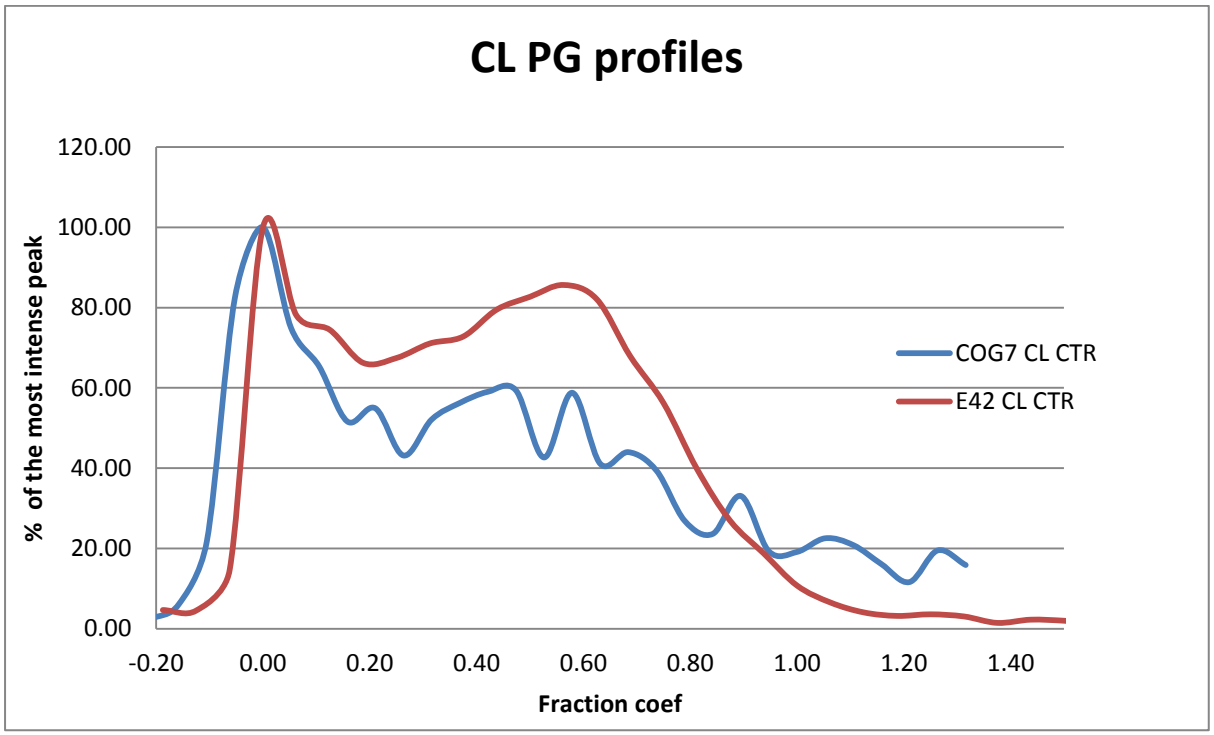

Figure 21. Overview of cellular PGs in COG7 and E42 cell lines. Radioactively labelled and harvested CLs were eluted through CL-6B column with blue dextran/potassium dichromate markers for V_t and V_0 respectively. Samples loaded were equal to 30µl. Elution speed of 0.14 ml/min; collected fraction volume of 1 ml.

Cellular PGs overview differs significantly from the M spectrum in both COG7 and E42 cell lines.

In the COG7 cell line, the cellular PGs show high heterogeneity in mass which is represented by the numerous peaks at different fraction coefficients (Figure 21, blue line). Peaks present after fraction coefficient of 1.0 are peculiar and those could either be an experimental contamination, background noise or non-incorporated ^{35}S-sulfate. Multiple different peaks suggest PGs with different M_ws. This corresponds to Figure 11 where second band showed similar weight distribution to the control cell line.

E42 cellular PGs show a pattern more similar to its secreted counterpart, but with some differences.

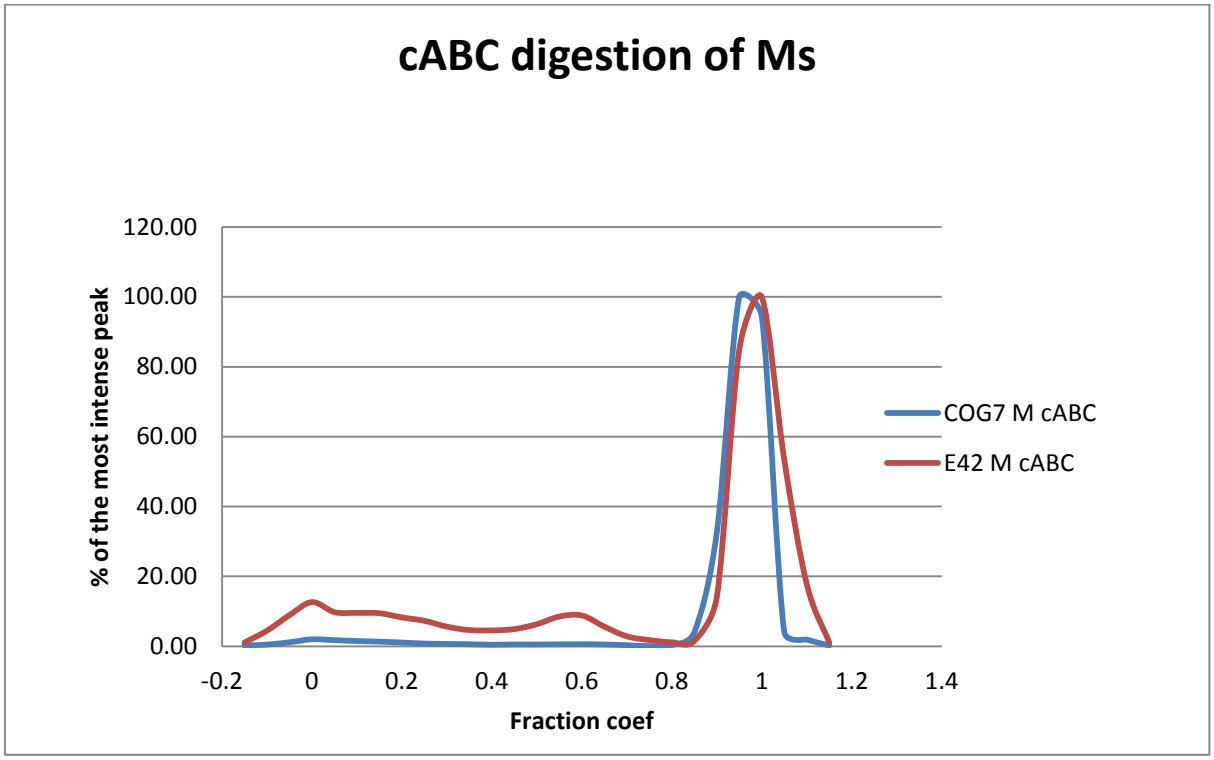

Figure 22. Gel filtration chromatograph of ^{35}S-labelled COG7 M and E42 M digestion with cABC. Radioactively labelled and harvested Ms were digested with cABC as per section 2.6.1. Sample was eluted in CL-6B column with blue dextran/potassium dichromate markers for V_o and V_t respectively Samples loaded were equal to 30µl. Elution speed of 0.14 ml/min; collected fraction volume of 1 ml.

It is clear that secreted PGs from healthy and COG7 cells show different modification patterns. Secreted COG7 PGs are almost entirely modified with CS. There are very little, if any, HS modifications. On the other hand, E42 produce significant amounts of HS, although the majority of modification comes from CS. This data follows Figure 15.

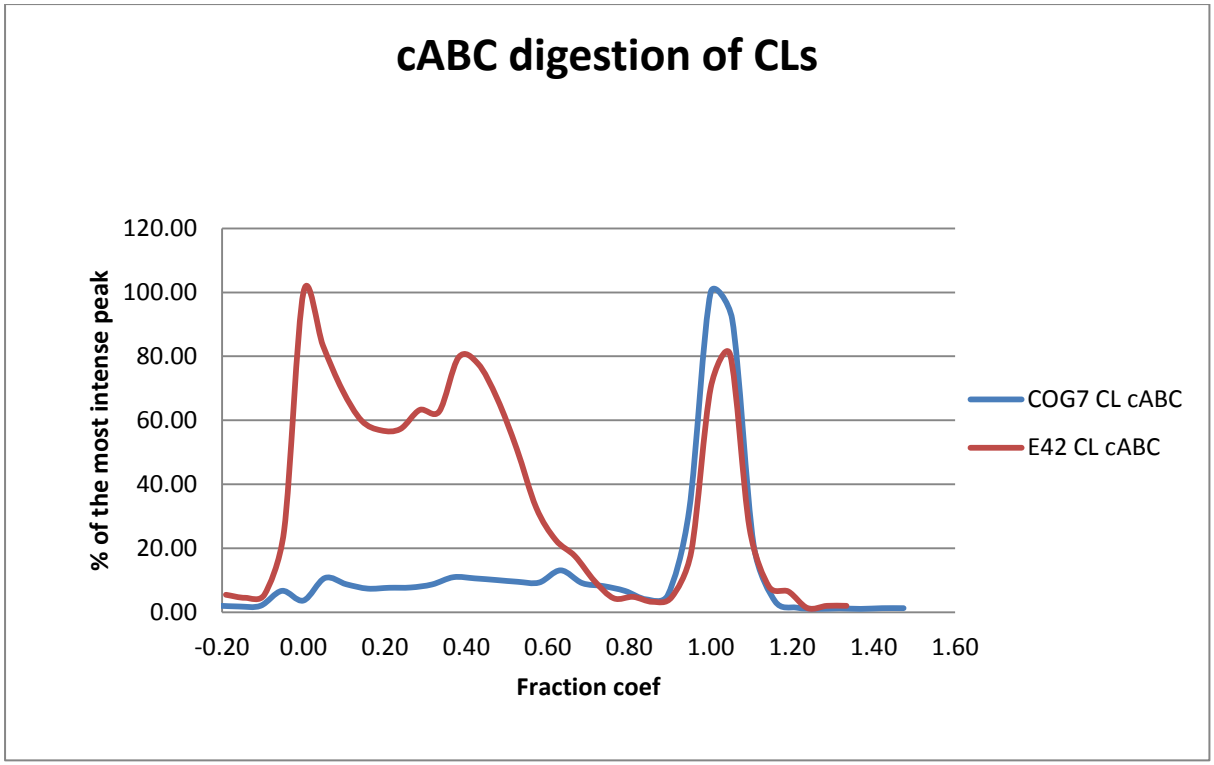

Figure 23. Gel filtration chromatograph of ^{35}S-labelled COG7 CL and E42 CL digestion with cABC. Radioactively labelled and harvested CLs were digested with cABC as per section 2.6.1. Sample was eluted in CL-6B column with blue dextran/potassium dichromate markers for V_o and V_t respectively Samples loaded were equal to 30µl. Elution speed of 0.14 ml/min; collected fraction volume of 1 ml.

It is clear that both E42 and COG7 cells have CS modification present on their cellular PGs. However, the extent of which CS modifies PGs in E42 CL is lower when compared to COG7 CL. This follows Figure 14. Cellular PGs show different cABC digestion profile, when compared to secreted PGs. However, the magnitude of the difference is greater among E42 cells. Secondly cellular PGs of healthy cells have significant HS modification on them. Compared to their secreted PGs, cellular PGs of COG7 show higher extent of modification with HS.

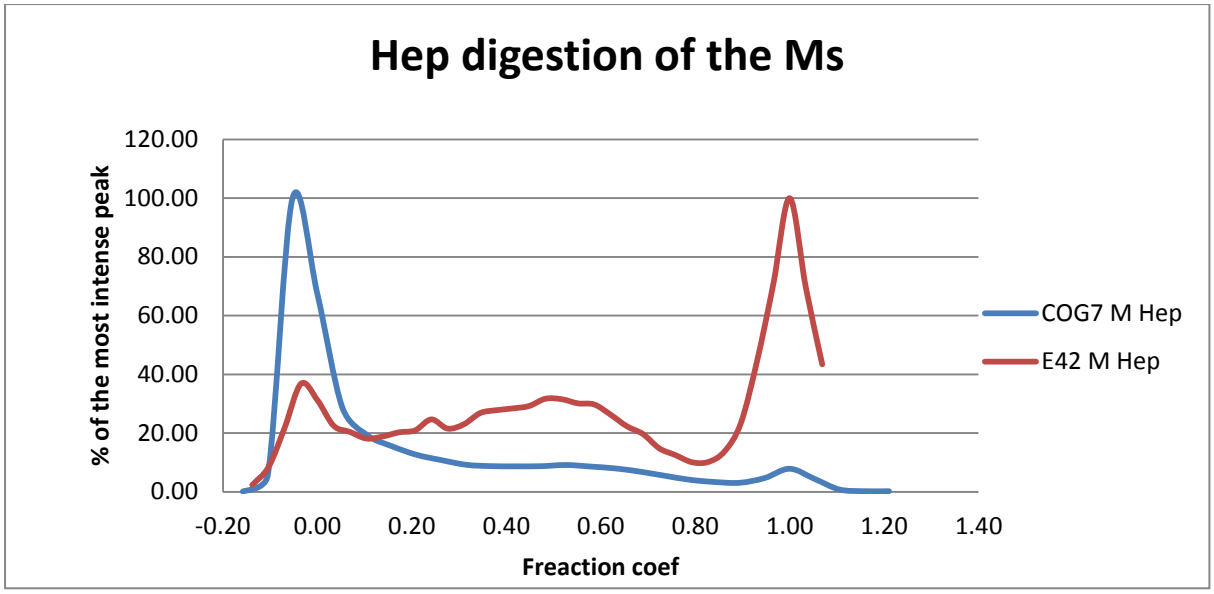

Figure 24. Gel filtration chromatograph of ^{35}S-labelled COG7 M and E42 M digestion with Hep. Radioactively labelled and harvested Ms were digested with Hep as per section 2.6.2. Sample was eluted in CL-6B column with blue dextran/potassium dichromate markers for V_o and V_t respectively Samples loaded were equal to 30µl. Elution speed of 0.14 ml/min; collected fraction volume of 1 ml.

Figure 24 corresponds to Figure 22 with respect to characterization of PG modification in Ms. It shows that there is very little HS on COG7 PGs and that the majority of secreted COG7 PGs are modified with CS.

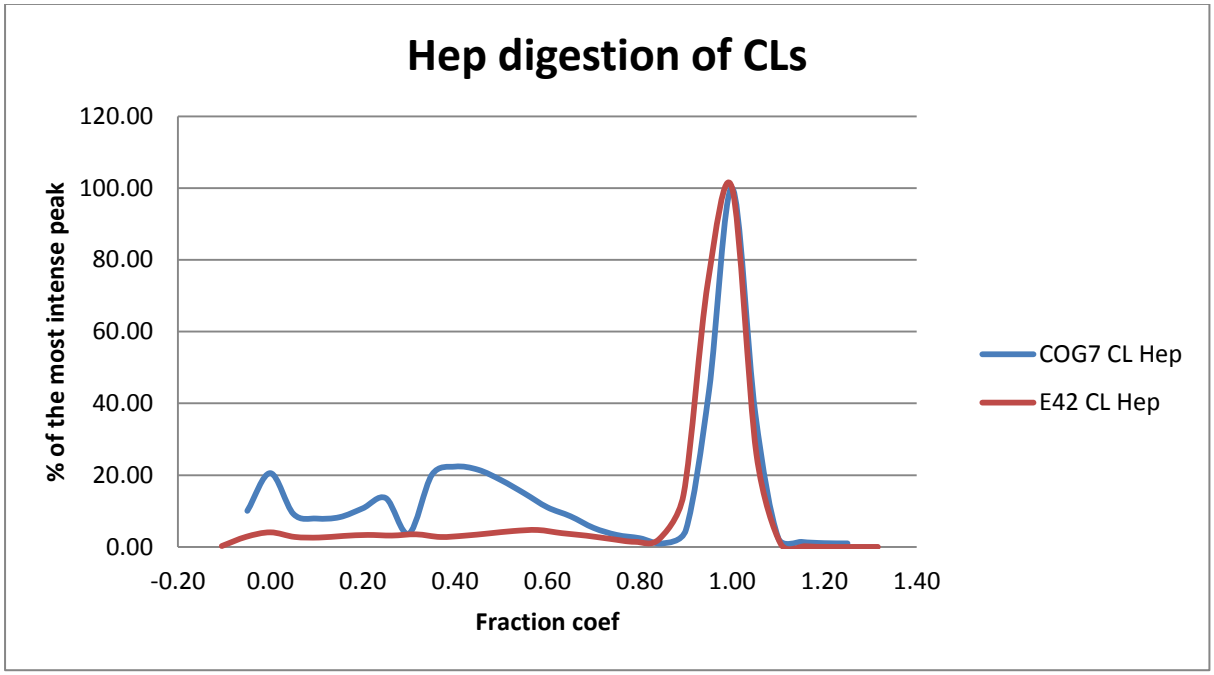

Figure 25. Gel filtration chromatograph of 35S-labelled COG7 CL and E42 CL digestion with Hep. Radioactively labelled and harvested Ms were digested with Hep as per section 2.6.2. Sample was eluted in CL-6B column with blue dextran/potassium dichromate markers for Vo and Vt respectively Samples loaded were equal to 30µl. Elution speed of 0.14 ml/min; collected fraction volume of 1 ml.

Figure 25 shows that cellular PGs in COG7 cells are different than those in E42 cells. This is consistent with the radioactive gel images (Figure 13) and chromatographic data (Figure 21). It also confirms the fact, that CS PGs constitute a minor fraction of the cellular PGs in healthy fibroblasts, where HS is the major part.

It is clear, that HS is present in COG7 cells, as well as CS is. Moreover, the CS is present on heavy and medium mass PGs (peaks at fraction coefficient 0 (heavy) and 0.40 (medium weight)).

3.4 Mass spectrometry

Mass spectrometry (MS) is a powerful tool used in biochemical and molecular biology research in many aspects. The most used quality of MS is the ability to identify peptides, and in turn proteins based on their molecular mass (Mw). In this project MS was used to identify potential differences between the above two cell types.

COG7 Medium Against Human Database										
Accession	Description	Score	Coverage	# Proteins	# Unique Pepti	# Peptides	# PSMs	# AAs	MW [kDa]	calc. pI
4502403	biglycan preproprotein	25.311669	21.47	3	5	5	6	368	41.62754	7.518066
4505047	lumican precursor	13.107829	11.24	1	3	3	3	338	38.4048	6.609863
45935371	serglycin precursor	11.164232	15.19	1	2	2	3	158	17.64064	4.95752
256017259	aggrecan core protein isoform 1 precursor	7.412071	0.86	2	1	1	2	2431	250.2196	4.081543
19743846	decorin isoform a preproprotein	7.0398788	3.06	1	1	1	2	359	39.72184	8.543457

E42 Medium Against Human Database										
Accession	Description	Score	Coverage	# Proteins	# Unique Pepti	# Peptides	# PSMs	# AAs	MW [kDa]	calc. pI
47419930	chondroitin sulfate proteoglycan 4 precursor	32.81	4.74	1	5	5	7	2322	250.4	5.47
19743846	decorin isoform a preproprotein	13.57943	7.24	2	2	2	4	359	39.72184	8.543457
4505047	lumican precursor	13.325198	9.47	1	2	2	3	338	38.4048	6.609863
4502403	biglycan preproprotein	9.9888964	5.43	1	1	1	2	368	41.62754	7.518066
167001141	glypican-1 precursor	9.5619388	5.56	1	1	1	2	558	61.64102	7.29834
D44_HUMAI	CD44 antigen	8.377944	3.64	1	2	2	3	742	81.5034	5.325684
DC1_HUMAI	Syndecan-1	6.4921951	5.48	1	1	1	2	310	32.44186	4.627441
RP1_HUMA	Neuropilin-1	3.9990795	2.49	1	1	1	1	923	103.0686	5.884277
38201675	syndecan-4 precursor	3.5995555	7.07	1	1	1	1	198	21.62803	4.500488

Table 1. Mass spectrometry analysis results for COG7 and E42 M samples against a human database. Table shows only PGs hits. Results arranged by score. M samples of 5.0 ml volumes were dialysed [section 2.9] and eluted through ion-exchange column [section 2.10] and collected in elute 1. Elute 1 was analysed via MS.

It seems that the control fibroblasts possess greater heterogeneity among its secreted PGs. E42 cells secrete at least nine PGs, compared with only five secreted by COG7 cells. Moreover, some PGs secreted by COG7, are not present in E42 M: aggrecan and serglycin. On the other hand, there are a number of PGs that are absent in COG7 cells: CD44 antigen, Syndecan-1, Neuropilin-1 and glypican.

MS data was an indicator for further research in order to establish more information about nature of PGs present in and secreted from COG7 cells. The differences observed so far are interesting.

There is no MS data concerning CL of COG7 due to technical limitation of obtaining sufficient amount of a viable sample.

3.5 Western Blotting

3.5.1 Introduction

Western blotting is an analytical method that uses antibodies to detect proteins of interest. In PG analysis there are many of available antibodies that could be used.

In theory, Western blotting is based on protein separation in SDS-PAGE gels, based on their size and a subsequent transfer to and detection in a membrane.. On that membrane, proteins are detected by incubation with antibodies that are specific against the target proteins.

There are essentially two types of Western blots: semi-dry and wet. The nomenclature of the types comes from the protein transfer method that is used in the transfer step. Semi-dry blots are used for analysis of membrane and hydrophobic proteins, while wet blots are used for more globular proteins.

In PG Western blot analysis, one can divide the used antibodies into two types: anti-protein core and anti-STUB. STUB antibodies bind to epitopes that appear after enzymatic digestion of GAG chains. Those antibodies can recognize sulfated sugars that have sulfate substitutes at different positions at sugar chain. C6S, C4S are sugars that have sulfate groups at 4^{th} and 6^{th} carbon in a saccharide, respectively. C0S-STUB defines an epitope without any sulfation. Antibody recognition of PG protein cores may sometimes require prior enzymatic removal of the GAG chains, while others are claimed to work also in the presence of GAG chains. Some antibodies have also been directed towards epitopes residing in GAG chains

.

3.5.2 Overview; anti-STUB & anti- aggrecan

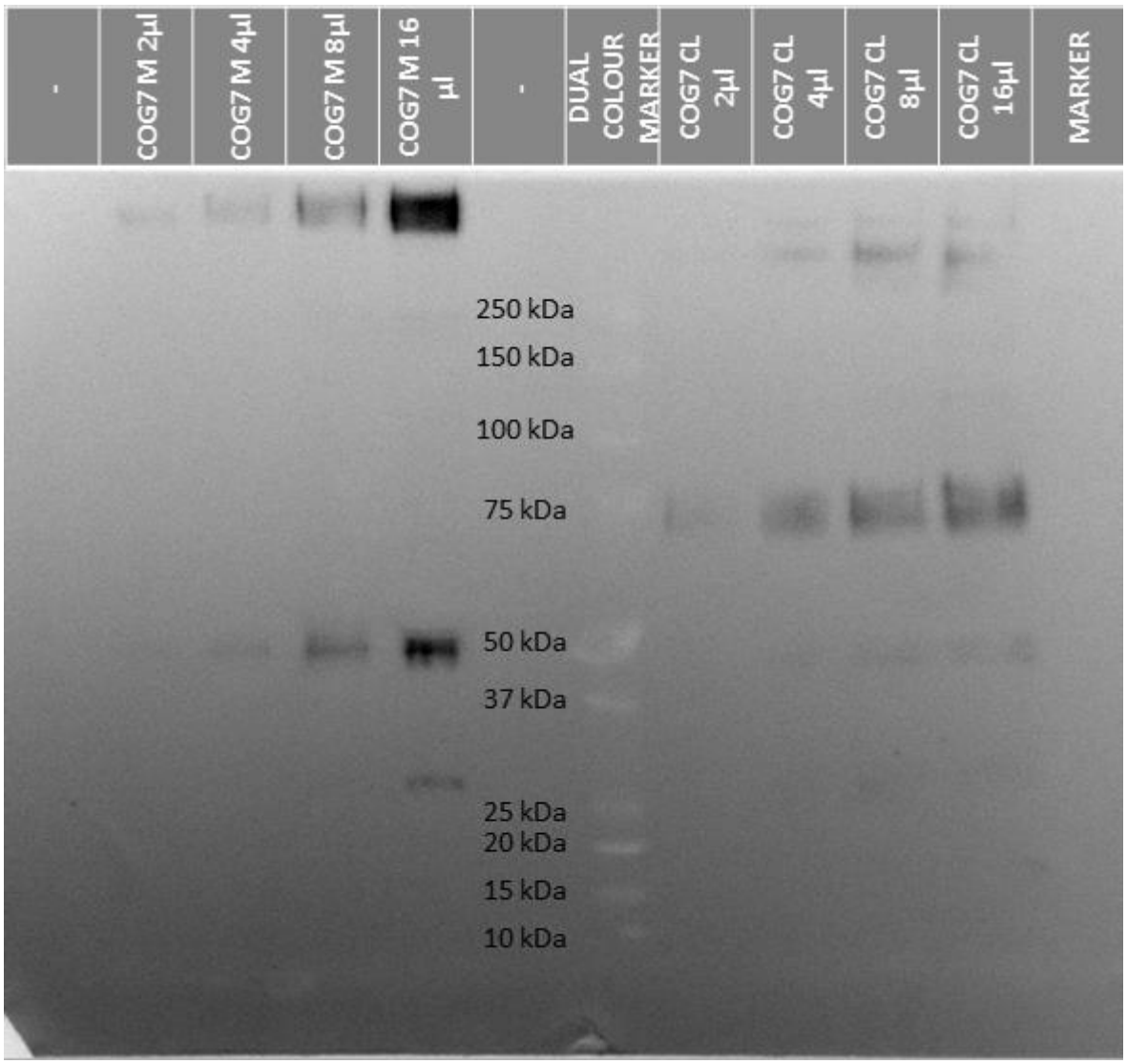

Figure 26. Western blot analysis of COG7M and COG7 CL with anti-C4S STUB antibodies. Consecutive wells have different sample volumes. Membrane developed with 1.0 ml of ECL Detection Reagent for 5 min. Membrane exposed for 5 min on CCD camera at luminescence setting; "-"control well.

This WB shows that there are different PGs present in CL and M fraction of COG7 cells. Differential sequence of sample volume was used in order to determine the suitable sample size. It is clear that the CL fraction has a lesser amount of PGs, which is shown by weaker signals of the bands at COG7 CL 16 µl when compared with COG7 M 16 µl. This difference in amount of PGs between CL and M depends on many factors, one of which is the time allowed for secretion. Moreover, the high molecular mass PGs are in majority for the secreted PGs- this is showed by the strong bands in the upper region of the blot. It is clear that COG 7CL PGs have C4S STUB epitopes at a M_w of 75 kDa, which is missing for the secreted PGs.

There are some similarities between the two fractions. At M_w of 50 kDa both fractions show bands, although the band is stronger in M.

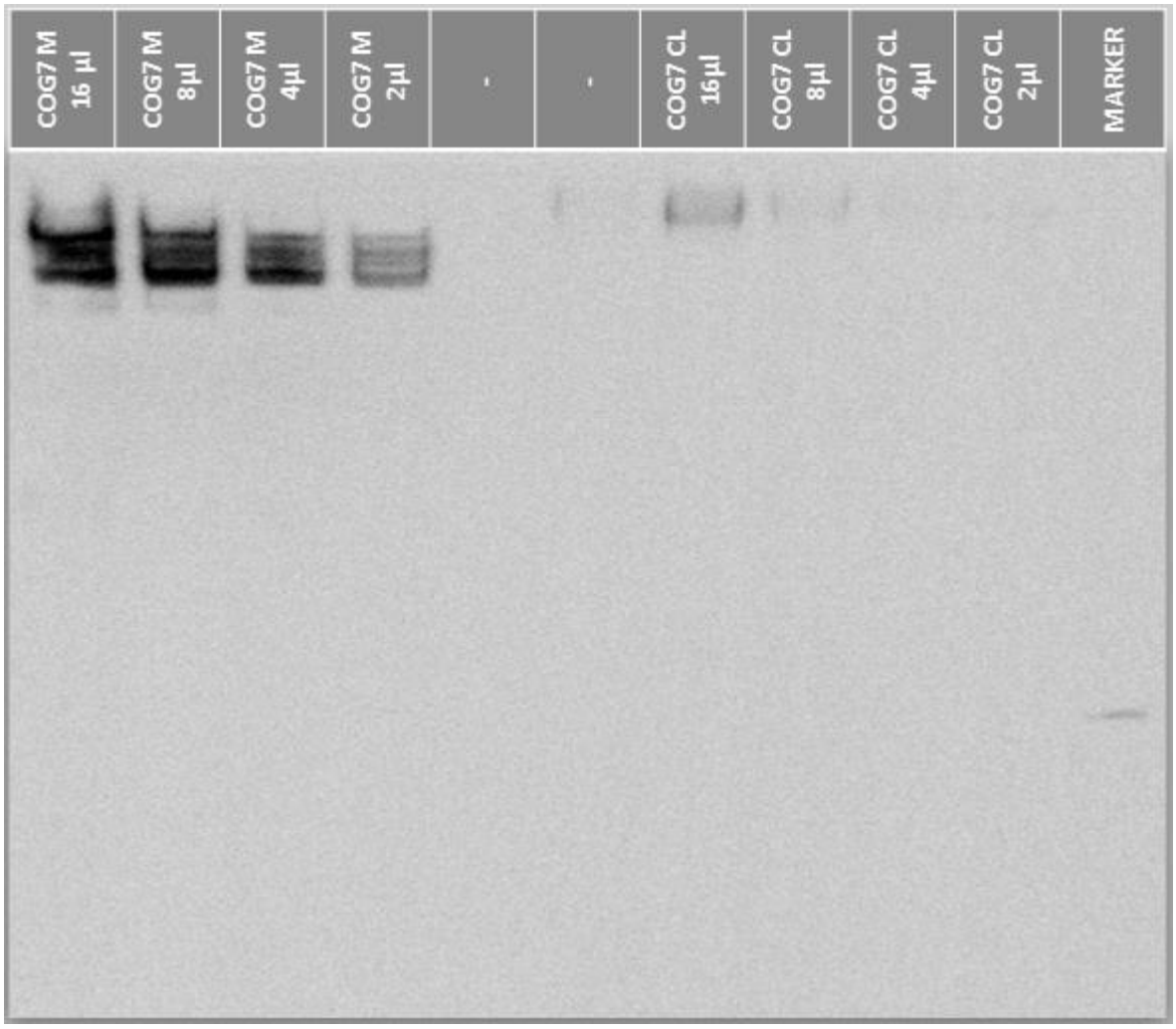

Figure 27. Western blot of COG7 M and CL fraction with an anti-aggrecan antibody. Membrane developed with 1.0 ml of ECL Detection Reagent for 5 min. Membrane exposed for 5 min on CCD camera at luminescence setting; "-"empty well.

It is clear that the M contains a significant amount of aggrecan. This is in contrast to the CL, which possesses significantly less aggrecan. It is clear that secreted aggrecan comes in three isoforms. It is a possible explanation for the presence of a ladder with different molecular masses. Isoforms 2 and 3 have reduced molecular mass with 246 and 239 kDa respectively; isoform 1 is reported as having a canonical "sequence" (Uniprot n.d.).

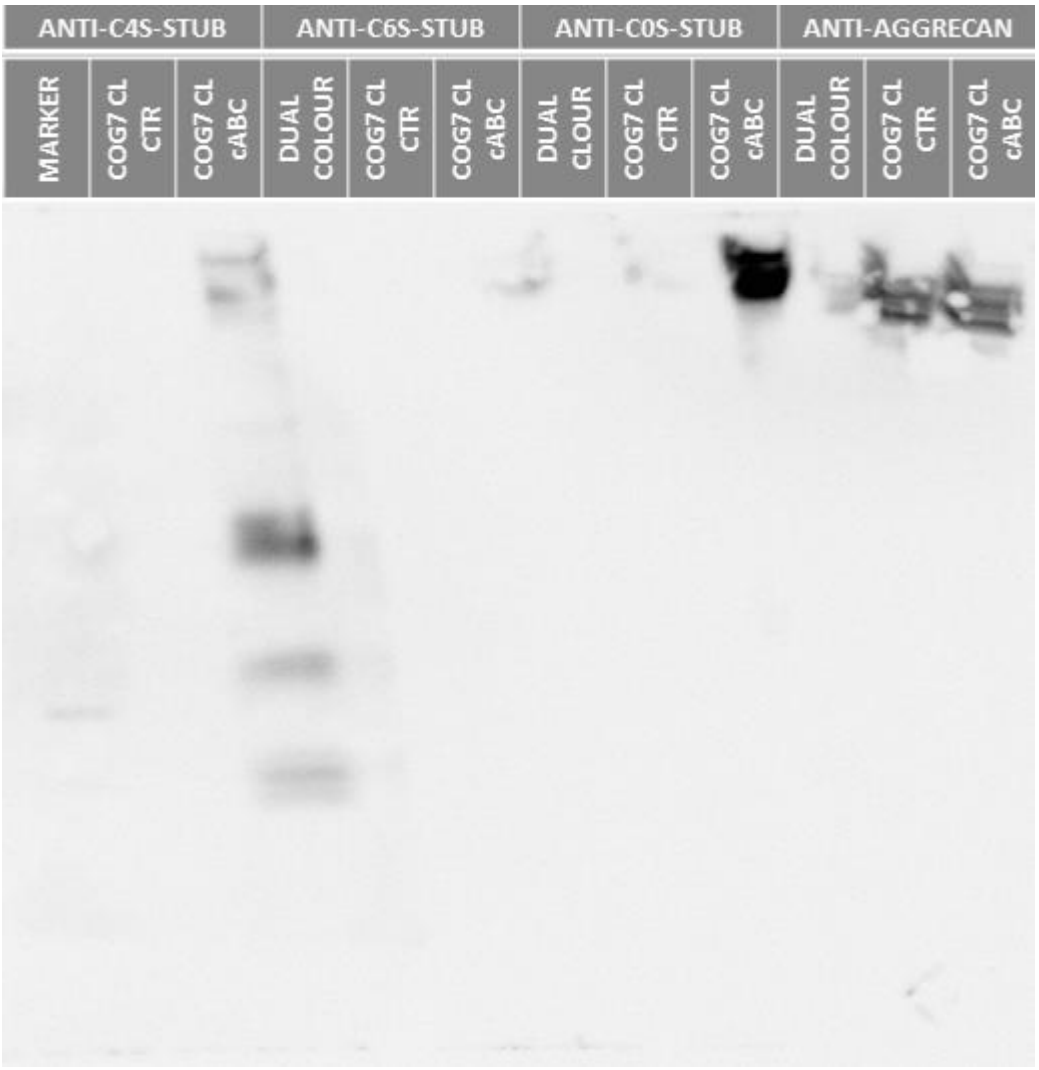

Figure 28. Western blot of COG7 CL with C6S-, C4S- and C0S- anti-STUB antibodies, and anti-aggrecan antibodies. Sample size 16 µl/well; Membrane developed with 1.0 ml of ECL Detection Reagent for 5 min. Membrane exposed for 5 min on CCD camera at luminescence setting; CTR- control

This blot shows the expression of STUB epitopes in the cellular PGs. It is clear, that the most prevalent STUB is C0S, where there is possibly none or little C6S sulfation of the STUB. Moreover C4S STUB shows great heterogeneity which is different from what is seen for the C0S STUB, which seems to be homogenous. Probably only one PG has this STUB epitope and it is most likely aggrecan. The presence of aggrecan is shown in Figure 28 and in Figure 27, but the prevalence of aggrecan in Figure 27 is low. The reason for this discrepancy could be that a strong signal that is coming from the M "consumes" all the substrate and/or all of the antibodies and leaves little signal for the CL fraction. In the Figure 28, the anti-aggrecan part of the blot was incubated separately and thus the prevalence of anti-aggrecan antibodies and the availability of substrate were greatly increased. This, possibly, increased the sensitivity of the detection and a low but significant abundance of aggrecan could be detected.

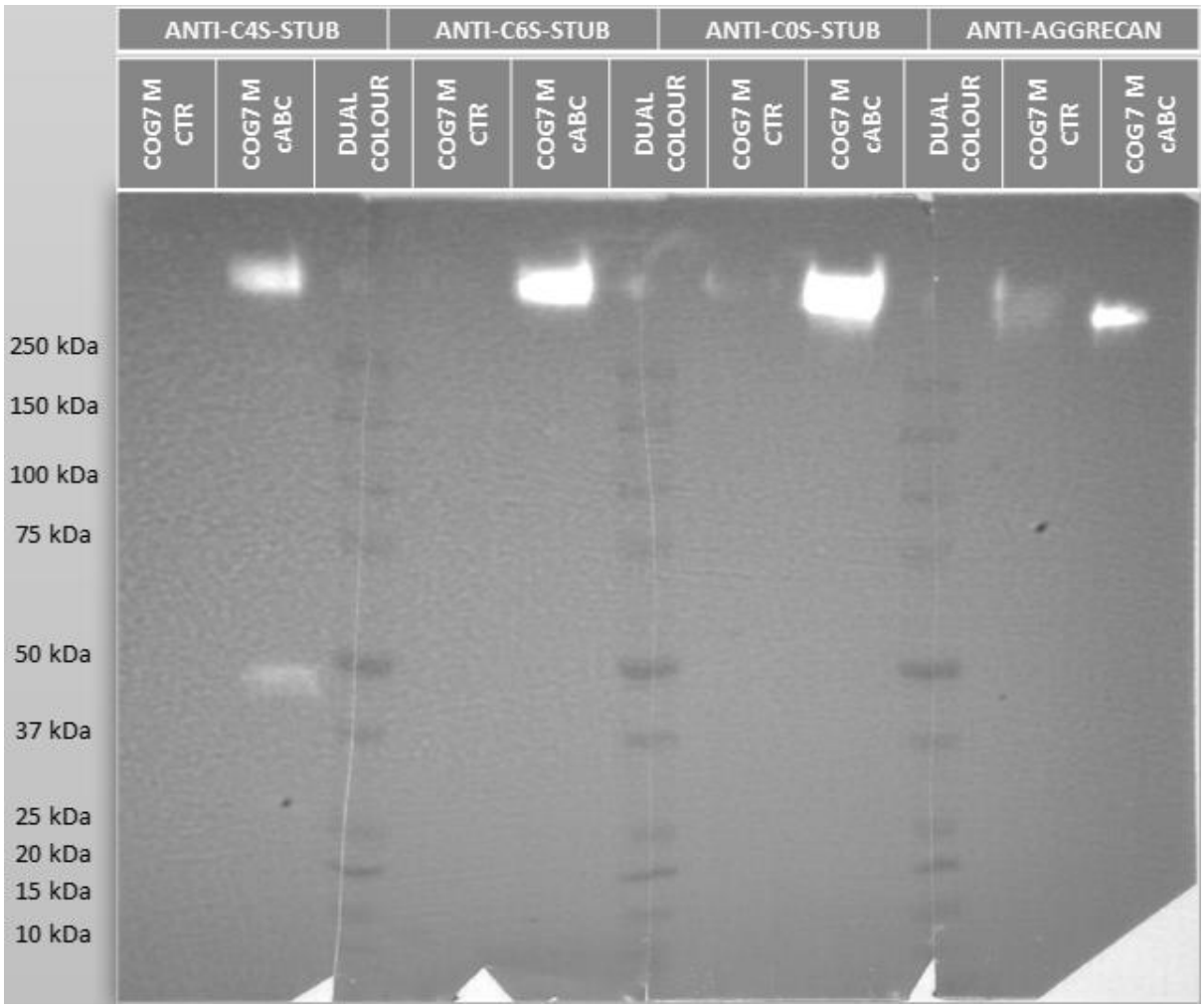

Figure 29. Western blot of COG7 M with anti-STUB antibodies and anti-aggrecan antibodies. Membrane developed with 1.0 ml of ECL Detection Reagent for 5 min. Membrane exposed for 5 min on CCD camera at luminescence setting; CTR- control.

Figure 29 demonstrates the presence of STUB epitopes on the PGs in the M of COG7 cells after cABC treatment and the presence of aggrecan in the same fraction. It is clear that secreted PGs possess epitopes for all the STUB antibodies tested. This is less certain for the cellular PGs, but still possible, but the C6S-STUB epitope gives at best only a very weak signal in the CL. However, the internal heterogeneity of C4S-STUB in the M is lower (two distinctive bands), when compared to the CL (possibly five bands, Figure 28).

The weaker signal in the anti-aggrecan COG7 M CTR lane could in fact be due an enhancement of the epitope accessibility after enzymatic removal of the GAG chains from the aggrecan protein core.

One can notice that the bands are shown in white against dark background. This deviation from standard was caused by corruption of the original file, which rendered it unreadable and

therefore a back-up image was used. Nonetheless, the conclusions from both pictures are similar.

3.5.3 Anti-serglycin & Anti-decorin

Serglycin and decorin are two PGs that were indicated to be present in COG7 cells by mass spectrometry.

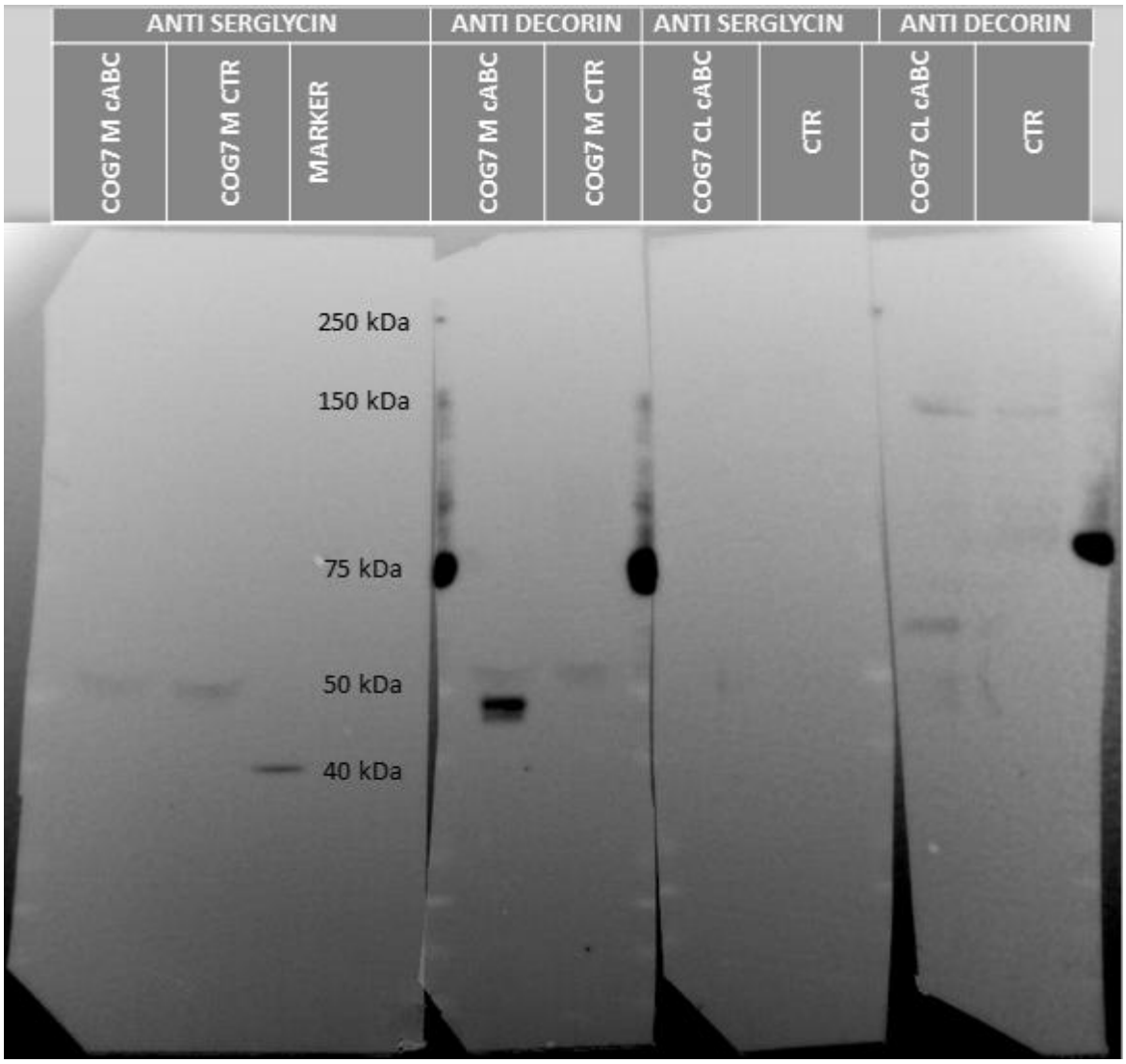

Figure 30. Western blot of COG7 M and CL with anti-serglycin and anti-decorin. 16 µl of sample /well. Membrane developed with 1.0 ml of ECL Detection Reagent for 5 min. Membrane exposed for 5 min on CCD camera at luminescence setting; CTR- control.

Figure 30 confirms observations by MS with respect to the Ms. However there is more information that could be drawn from the above figure:

1. Serglycin PG is modified in the COG7 M fraction by a modification other than CS chains. I is possible that band at 50 kDa in the anti-serglycin lane for COG7 M is either a serglycin bound to other molecule (Malla et al. 2013) or a non-specific band.
2. This modification is extensive, raising the M_w from 17.5 kDa (protein core) to approximately 50 kDa; difference of 32.5 kDa.
3. Decorin PG is modified with CS chains. This modification contributes approximately 2 kDa.
4. There is no serglycin in the CL of COG7 cells.
5. There are two decorin bands in the CL at 150 kDa and 60 kDa. Such high M_w of decorin protein is puzzling and presence of two bands in the cABC lane, compared to one of 150 kDa in the control lane indicates that 60 kDa band is modified with CS. The 150 kDa band could be an unmodified trimer of decorin, or decorin modified with something else than CS.

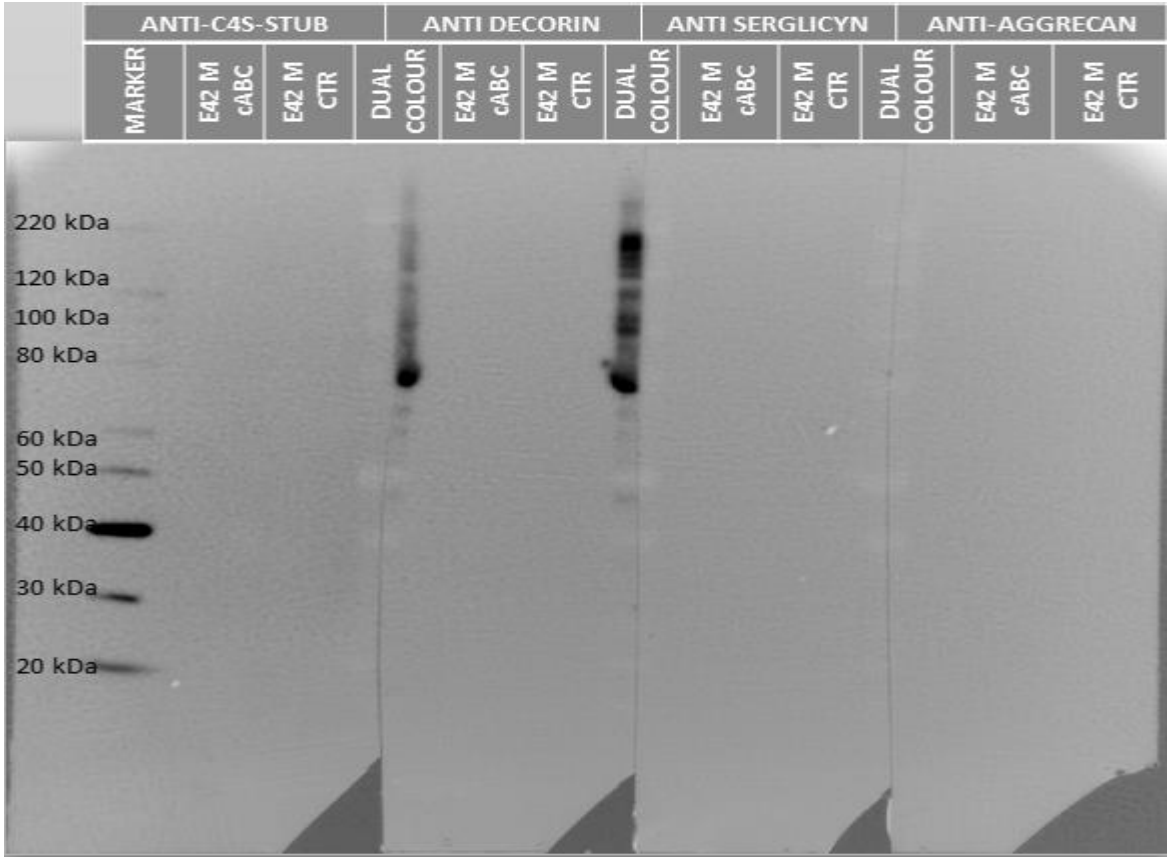

Figure 31. Western blot of E42 M fraction against anti-C4S-STUB, decorin, serglycin and aggrecan. 16 µl of sample/well. Membrane developed with 1.0 ml of ECL Detection Reagent for 5 min. Membrane exposed for 5 min on CCD camera at luminescence setting; CTR- control.

The blot indicates that decorin, serglycin and aggrecan PGs are not present in the M of E42 cells. Moreover, there is no evidence for C4S-STUB epitopes on the secreted PGs after cABC treatment. However, decorin is present in the MS data (Table 1) in the E42 M sample, which implies that the procedure could be repeated with more samples.

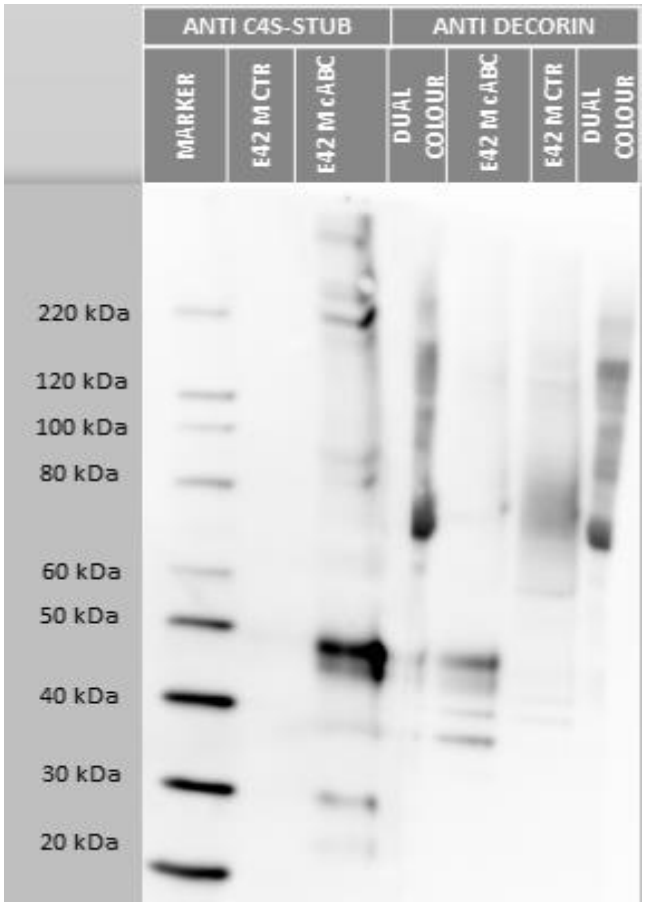

Figure 32. Western blot of E42 M against anti-C4S-STUB and decorin. 8 µl of sample/well; Membrane stripped prior to 1st Ab incubation. Membrane developed with 1.0 ml of ECL Detection Reagent for 5 min. Membrane exposed for 5 min on CCD camera at luminescence setting; CTR- control.

This blot was carried out to confirm presence of decorin in the E42 M fraction. It is clear that decorin is present and that some of its modification is CS. The fully glycosylated form has a M_w of approximately 70 kDa and is shown as a smear. However, this indicates that there are multiple different variants which follow the current literature (3 possible N-glycosylation sites; 1 possible O-glycosylation site)(Uniprot n.d.). However, the presence of the C4S-STUB epitope on this blot is contradictory to previous observations. This is the only time, where C4S-STUB epitope was visualized on E42 M fraction. It could be that since the membrane was stripped before re-probing that there is a residual signal from a previous blotting procedure or there is in fact C4S-STUB epitope which was only visualized on this membrane.

This issue needs to be resolved in the future. However, looking at this blot alone, the alignment of the band at 49 kDa between E42 M C4S-STUB and anti-decorin (cABC) suggest that decorin has C4S-STUB epitope in E42 M.

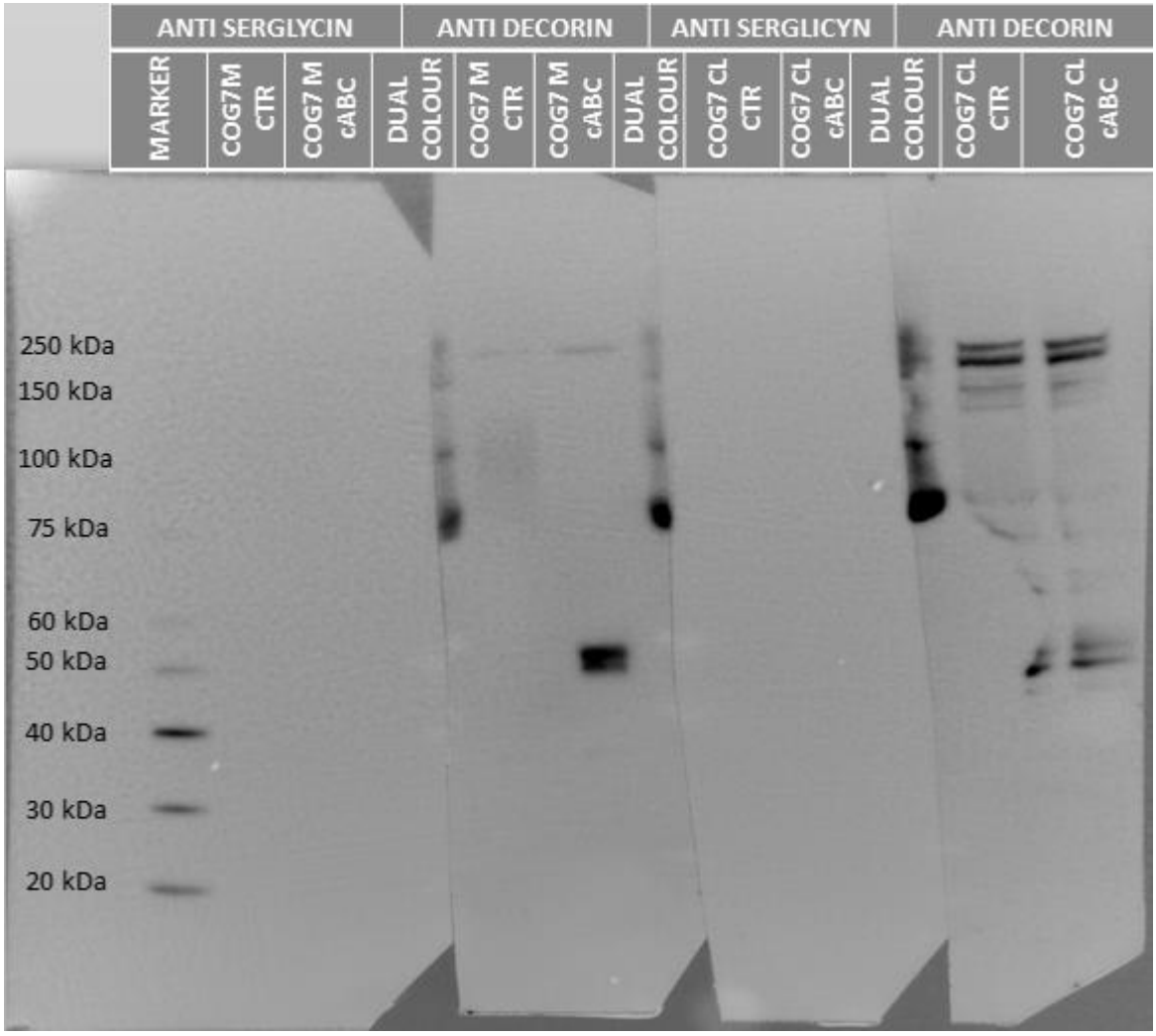

Figure 33. Western blot of COG7 M and CL with anti-serglycin and anti-decorin antibodies. 16 µl of sample/well. Membrane developed with 1.0 ml of ECL Detection Reagent for 5 min. Membrane exposed for 5 min on CCD camera at luminescence setting; CTR- control

This Western blot shows that decorin is not only present in M, but also in the CL of COG7 cells. However, the nature of decorin present in the CL is somewhat different from the secreted variant. It is clear that decorin from CL is not modified by CS and that it forms some kind of complexes (or oligomers) of high molecular mass (approx. 250 kDa). This possible multimerization is also seen in the M, but to a lesser extent (shown by the band at 250 kDa).

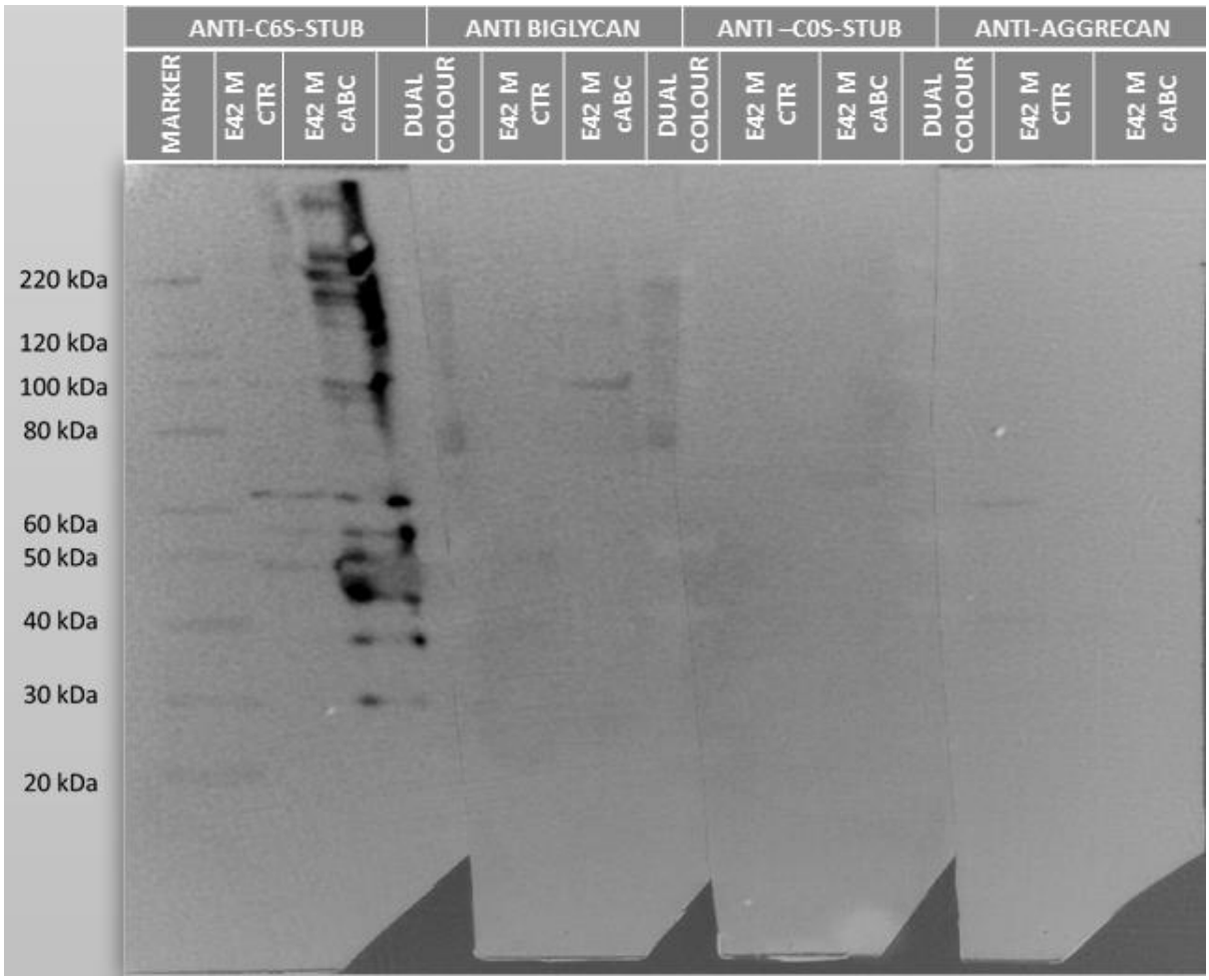

Figure 34. Western blot of E42 M against anti-C6S-, C0S-STUB, biglycan and aggrecan; 8 µl of sample/well. Membrane developed with 1.0 ml of ECL Detection Reagent for 5 min. Membrane exposed for 5 min on CCD camera at luminescence setting; CTR- control

This Western blot shows that there is no detectable C0S-STUB epitope in E42 M fraction. Moreover, it shows that there is also no detectable aggrecan in E42 M, which supports the previous findings: MS data (Table 1, Figure 31). The novel information coming from this experiment is the presence of biglycan (weak band at 100 kDa), even though it was shown in MS data (Table 1), this gives more evidence to its presence. The most prominent mark on this blot is the strong signal originating from anti-C6S-STUB antibody. Lack of signals from other STUBs (C40S- no signal (Figure 31) and C4S-only one membrane (Figure 32)), proves that one of the STUBs epitopes present in secreted glycans from E42 is C6S, whereas C0S is absent and C4S is doubtful.

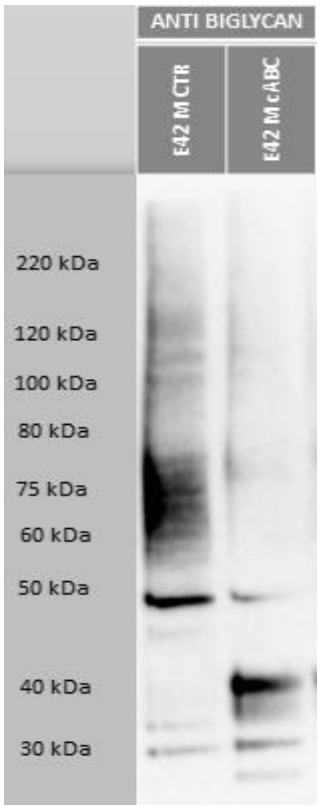

Figure 35. Western blot of E42 M against anti-biglycan; 8 µl of sample per well. Membrane developed with 1.0 ml of ECL Detection Reagent for 5 min. Membrane exposed for 1 minute on CCD camera at luminescence setting; CTR- control.

This blot is another experiment that supports the MS data. There is biglycan present in E42 M with CS modification. There are no known biglycan isoforms (Uniprot n.d.). This possesses the question about the 30 kDa band and its nature. Possibly this band is a result of an unspecific binding of the anti-biglycan antibodies.

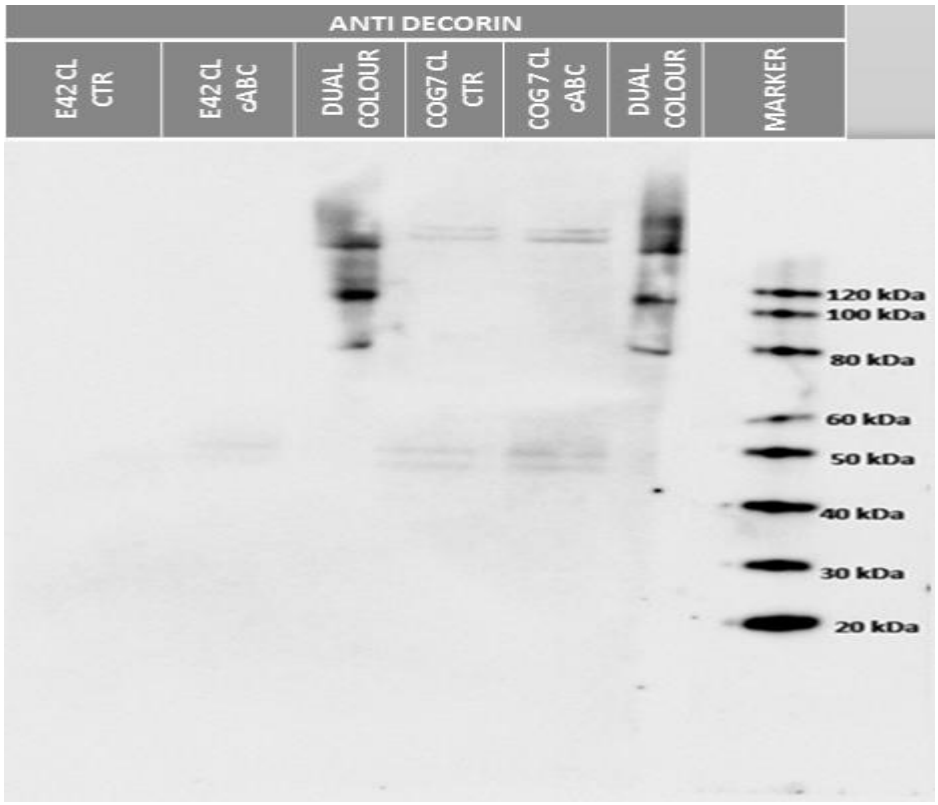

Figure 36. Western blot of CL from COG7 and E42; 8 µl of sample/well. Membrane developed with 1.0 ml of ECL Detection Reagent for 5 min. Membrane exposed for 5 min on CCD camera at luminescence setting; CTR-control

There is an indication of the presence of decorin in CLs of COG7 cells, but no signal from E42 CLs. However, the M_w of decorin indicated on the gel does not correspond to the theoretical value (39 kDa). It is possible that decorin in COG7 CL is modified with something else than CS.

The presence of four, distinctive bands shows that decorin can form oligomers. The "heavy" bands (top of the gel, approximately 250 kDa) could be such oligomers. Similar band patterns could be observed in Figure 33.

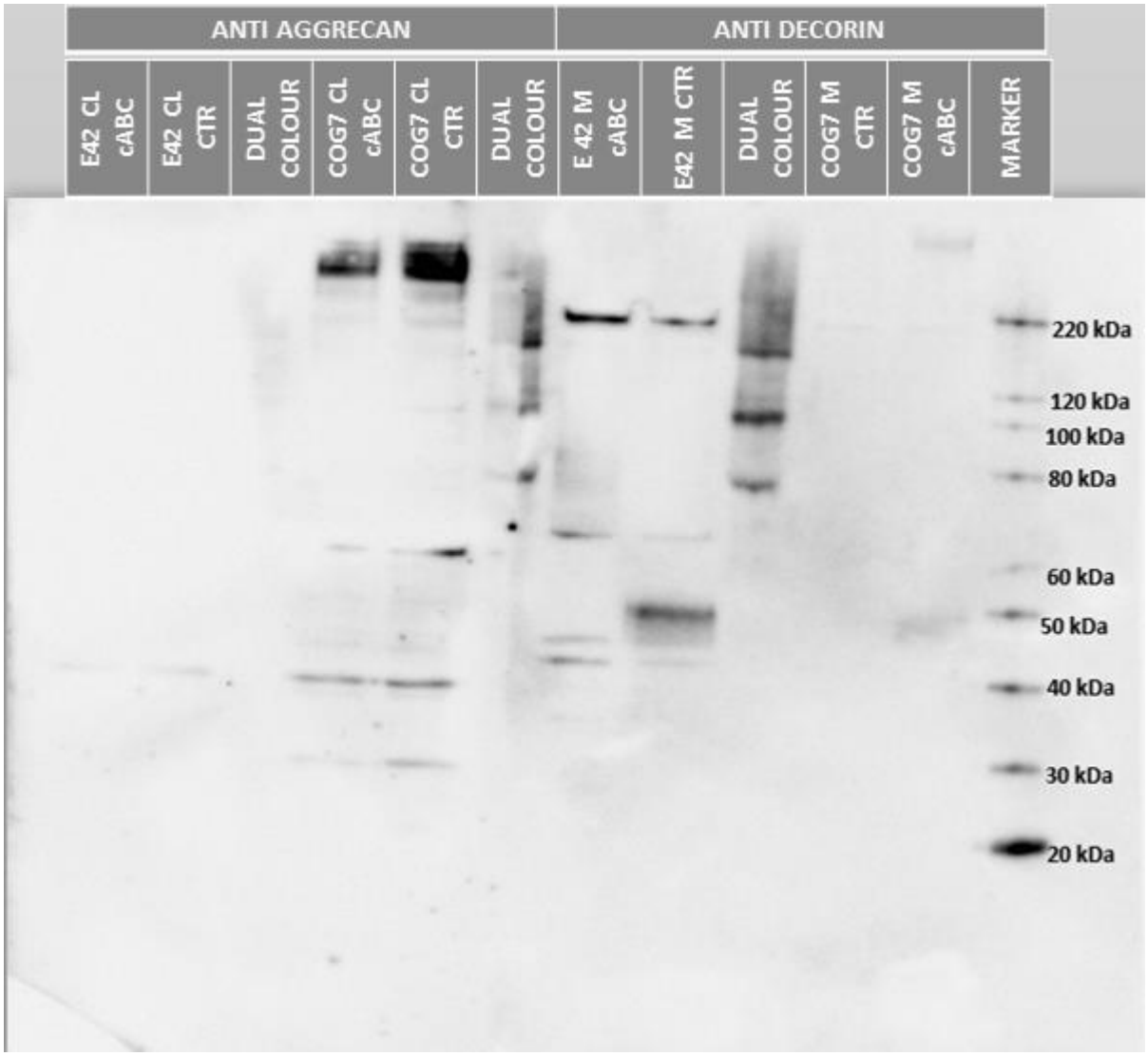

Figure 37. Western blot of COG7 &E42 M samples against decorin and aggrecan; 8 µl of sample/well. Membrane developed with 1.0 ml of ECL Detection Reagent for 5 min. Membrane exposed for 5 min on CCD camera at luminescence setting; CTR- control.

This blot clearly shows the potential abundance difference in decorin levels in between COG7 M and E42 M, which is supported by the MS data (Table 1). It also shows that there is no

aggrecan present in the CL of E42, in contrast to COG7, where aggrecan is abundant. There is small difference upon cABC digestion in the cellular aggrecan (reduction of peak intensity at 250 kDa), but no shift in molecular mass- which corresponds to fact that aggrecan protein core is 250 kDa itself. However the mass change of aggrecan is difficult to observe at the upper region due to the fact that neither aggrecan with CS nor without CS could have entered the SDS-PAGE gel properly. Perhaps the binding of anti-aggrecan antibodies is dependent on CS level and the amount of GAGs attached to the core. The increased signal level of the upper band area (>150 kDa) in cABC treated decorin could indicate that the presence or absence of CS is influential on the formation of heavy weight aggregates.

3.6 Protein biochemical analysis

3.6.1 Protein synthesis level- BCA™ Protein Assay

From the Western blot analysis, it was clear that COG7 and E42 possess different characteristics with respect to protein core synthesis. In order to establish whether the COG7 cells secrete or produce different amounts of proteins when compared to control fibroblasts, a protein quantification experiment was carried out using BCA™ Protein Assay.

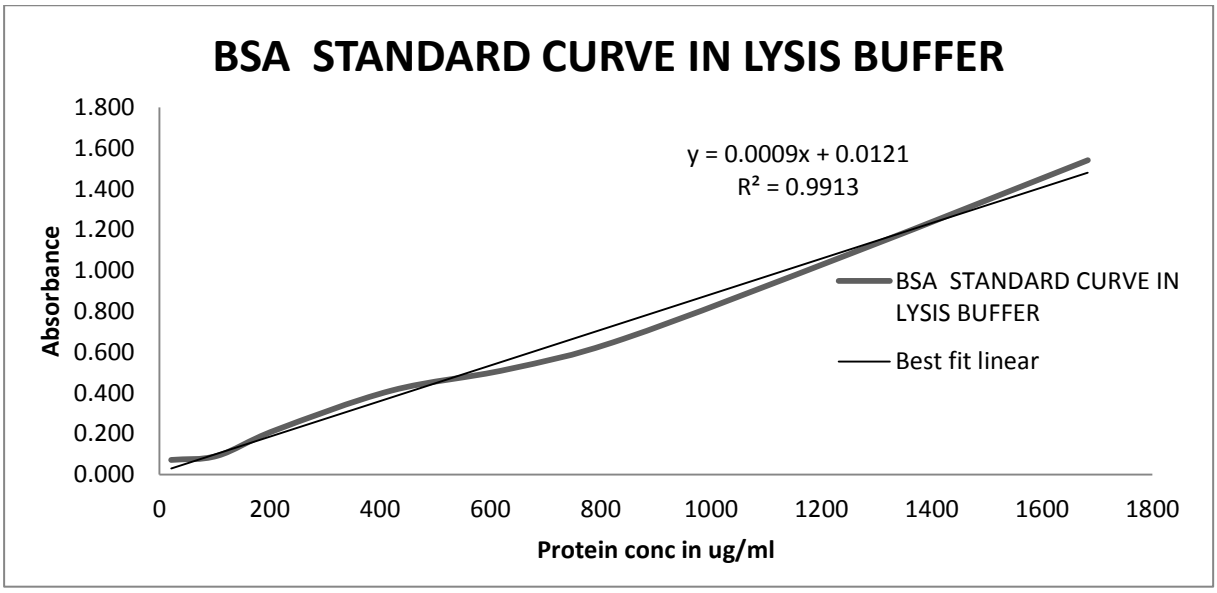

Figure 38. BSA standard curve with the lysis buffer used as a solvent. Absorbance values taken at 562 nm wavelength.

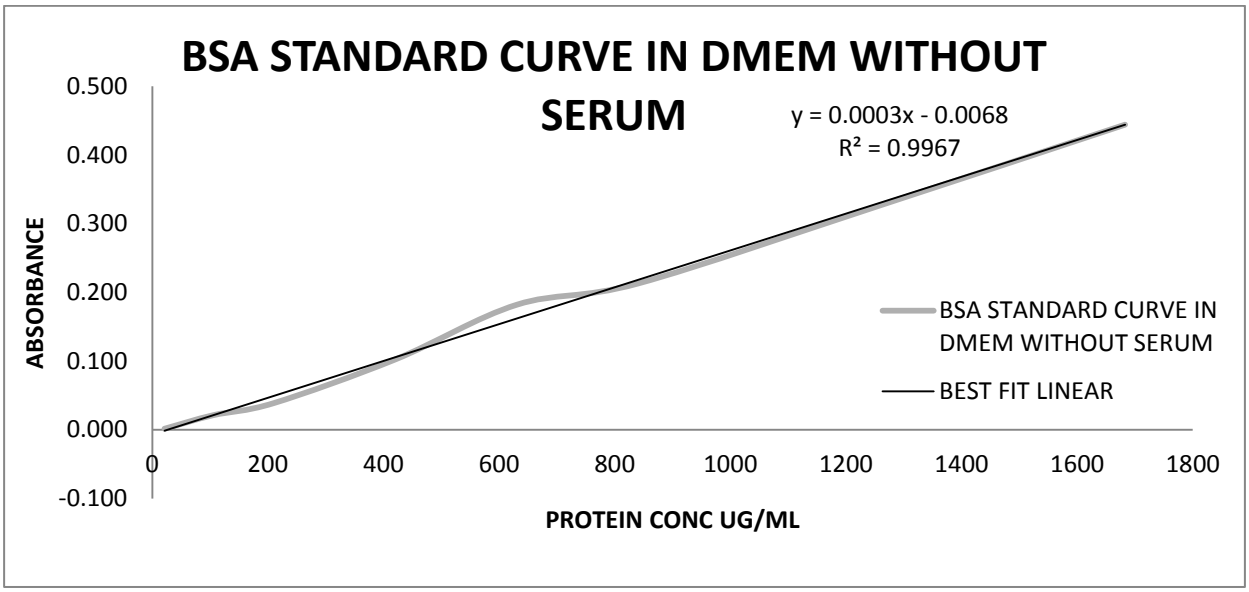

Figure 39. BSA standard curve. DMEM without bovine serum used as a solvent. Absorbance values taken at 562 nm wavelength.

Standard curves created for known concentration of bovine serum albumin (BSA) were used to establish the unknown concentrations in the samples. Figure 38 was used when analysing the CLs samples, whereas Figure 39 was used for analysis of M samples.

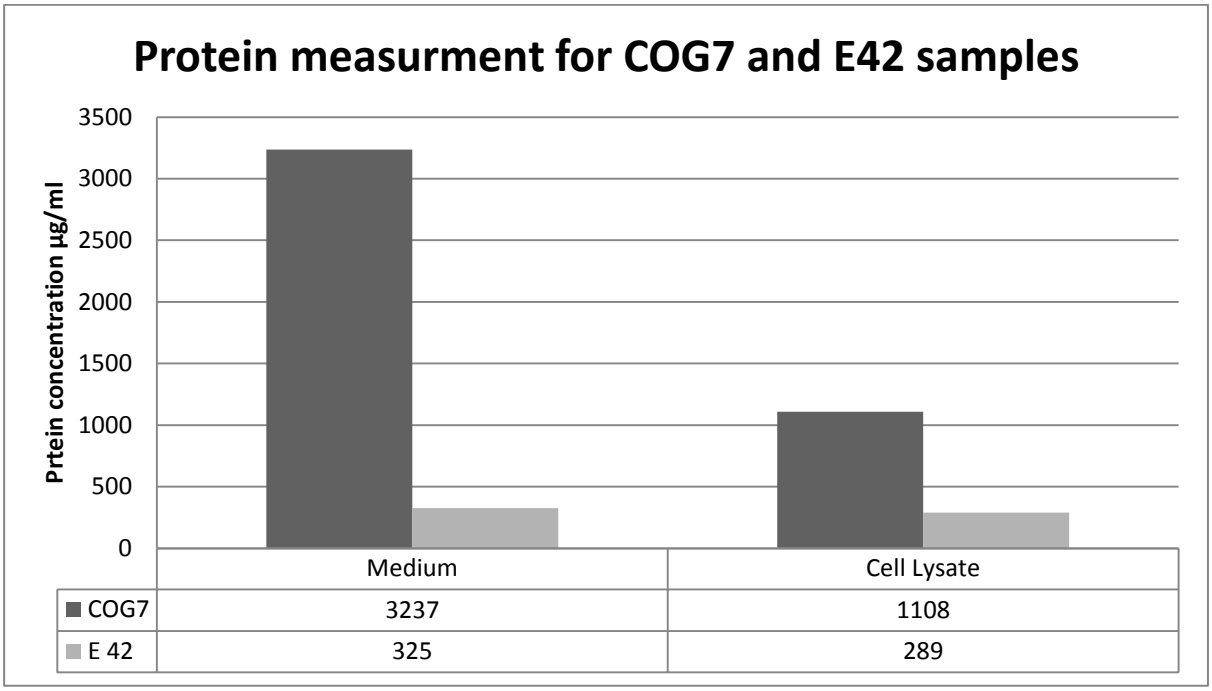

Figure 40. Protein measurement using BCA™ Protein Assay in COG7 and E42 samples from M and CL. Values given in µg/ml of analyte.

The COG7 samples contained much more protein than the E42 samples, both for the media and cell fractions.

This significant difference, especially in M sample, has given some experimental challenges when it comes to loading gels with equal amounts of proteins and during detection of high-levels signals in Western blots.

3.6.2 The protein patterns of Ms and CLs- silver staining

Silver staining was performed in order to further characterize the proteins present in the COG7 M & CL.

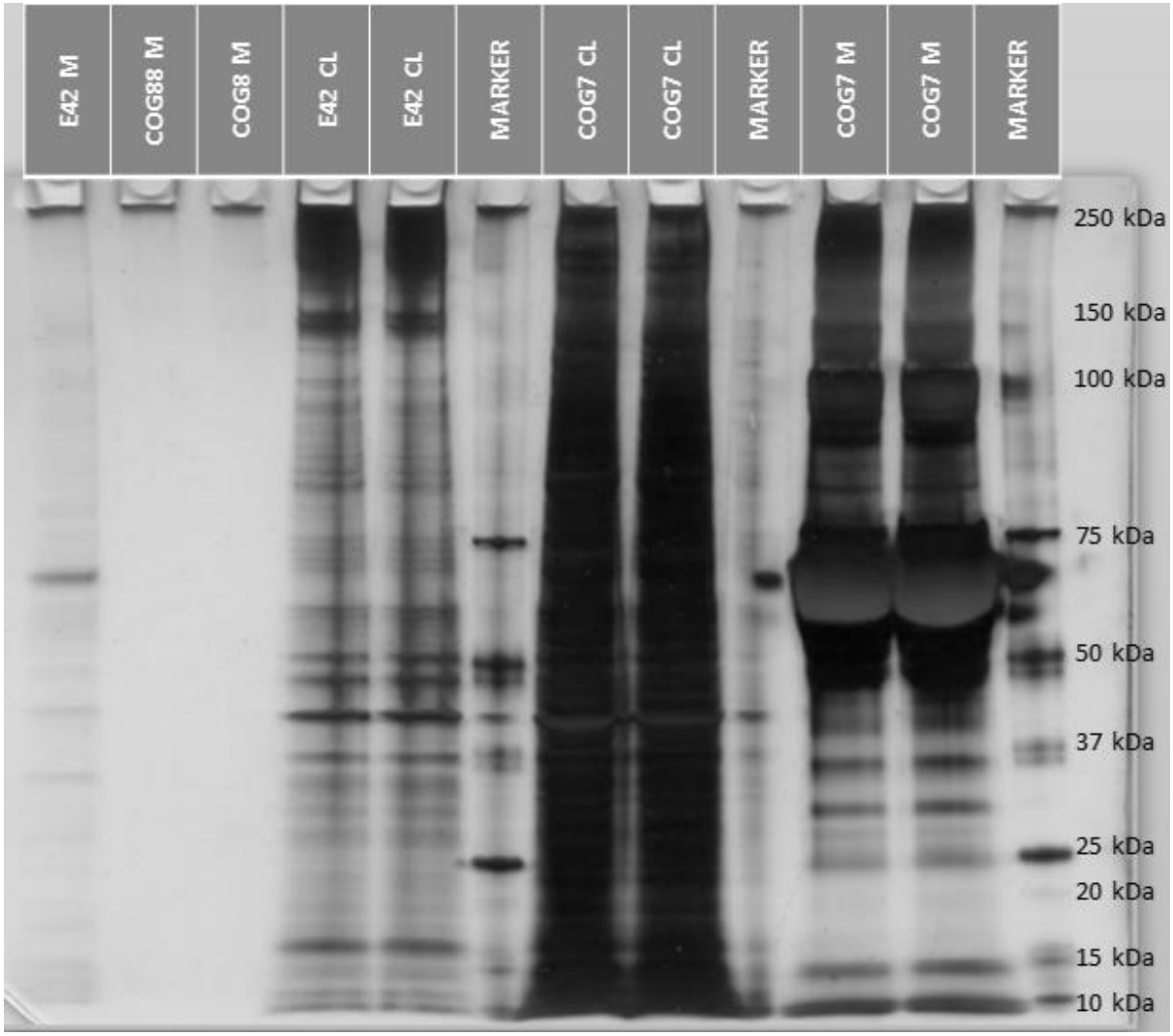

Figure 41. Silver staining of COG7 CL & M, E42 CL & M and COG8 M. Sample size of 8 µl/well. M and CL samples were loaded directly onto the gel from harvested Ms, without any dilution or prior ion-exchange step. The silver stain was developed as per section 2.13 with development time of 4.5 min.

Silver staining has shown clearly that there is a large difference in the protein concentration between COG7 and E42 cell types in both CL and the Ms. There is a very strong band at 60 kDa in COG7 M which corresponds to serum albumin (unpublished data, personal

correspondence with Anders Moen). Presence of significant amounts of bovine serum proteins was confirmed by MS for the COG7 samples, but not for the E42 M samples. The source of bovine albumin was traced to serum additive from complete medium. The difference between the two cell lines in this respect, that both were subjected to a procedure that is designed to remove serum proteins before collection of secreted macromolecules in serum-free medium, indicates a prolonged residence time of endocytosed serum proteins in COG7 cells. This could be a result of a delayed recycling of endocytosed material, which occurs efficiently within 15 min in normal mammalian cells. This finding is interesting and requires further investigation.

3.7 Ion-exchange chromatography

3.7.1 Introduction

Ion-exchange chromatography allows for separation of molecules based on their affinity to the ion moiety on the column. It is a method used for separation of different molecules, including proteins and PGs.

In analysing PGs, ion-exchange is used to separate these highly negatively charged molecules from other proteins. Glycans (PGs also) carry negatively charged groups (sialic acid for glycans, and sulfate modifications and glucuronic acid for PGs). PGs, however, are the most negatively charged macromolecules, which allows for separation of most PGs from other proteins. PGs bind strongly to positively charged DEAE columns and are retained until the salt gradient reaches a concentration allowing for displacement of PGs from the column. In this experiment, where stepwise elution was performed, most PGs should elute in elute 2.

3.7.2 COG7 M ion-exchange profile on Silver stained gel

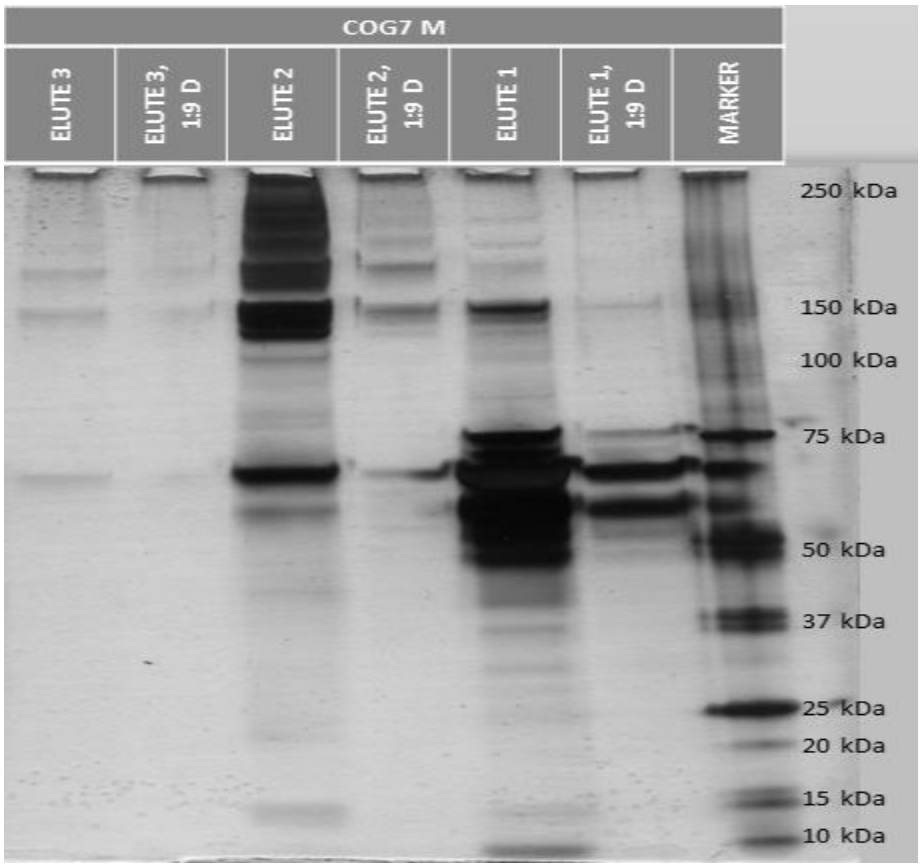

Figure 42. Silver stained gel after ion-exchange chromatography of COG7 M fraction. "1:9 D" represents 1 in 9 dilution of the sample in water. Elute 1- proteins eluted in low salt buffer (0.1 M NaCl). Elute 2- protein eluted in high salt buffer (1.0 M NaCl). Elute 3 – proteins eluted at high salt buffet (1.0 M NaCl) immediately after elute 2.

It is clear that some PGs from the M fraction have been retained on the column and were eluted in the elute 2. Most of the PGs have high M_w (>100 kDa), although there is one strong band at approximately 60 kDa. Unusually, this band is persistent in elute 1 as well and it shows as very strong peak in Figure 41 (COG7 M lane). This could be due to high levels of this protein, that it shows in elute 2. It is simply retained in column due to high abundance or it could be simply different PG or a protein.

1:9 dilutions were performed in order to achieve better band separation and, therefore, identification.

Top bands (>150 kDa) and the strong bands at approx. 60 kDa from Elute 2 were cut out from the gel and analysed by MS in order to detect possible PGs, but no new candidates were found. However, strong presence of bovine serum albumin was confirmed.

4 Discussion

The aim of this project was to investigate PG synthesis and modification in COG7 cells. PG synthesis in COG8 deficient cells were at the same time investigated by another student. Since it is established that cells with dysfunctional COG-complex have distorted N-glycosylation and O-glycosylation (Freeze & Aebi 2005; Ng et al. 2007), it is logical to assume that PGs could be affected as well. Mutations in COG complex were discovered in the six of its eight sub-units :COG1,COG2, COG4, COG5, COG6 , COG7 and COG8 (Foulquier et al. 2006; Reynders et al. 2009; Paesold-Burda et al. 2009; Lübbehusen et al. 2010; Wu et al. 2004; Foulquier et al. 2007; Zeevaert et al. 2008), with COG2 mutation being the most recent discovery (Kodera et al. 2014).

COG1, COG4, COG7 and COG8 showed lack or decrease in sialyation on the N-glycans with COG1 having least amount of sialyation and COG4 showing the highest amount of sialyation. 11% of N-glycans in COG1 have agalactosylated N-glycan structures(Reynders et al. 2009). In COG7 cells the level ST-antigen was reduced but T-antigen O-glycan remained unchanged. The ratio between T and ST antigens was higher (0.11) than control (0-0.056) (Xia et al. 2013).

N-glycosylation and O-glycosylation defects in COG7 patients are described in details. The prevailing defects in N-glycosylation are decrease in sialyation and the high (40%) percentage of agalactosylated glycan structures. Membrane bound surface O-glycans have reduced level of sialyation and reduction of activity of CMP-sialic acid and UDP-galactose transporters as well as reduction in activity of several galactosyltransferases have been reported. (Reynders et al. 2009; Ng et al. 2007; Shestakova et al. 2006; Zeevaert et al. 2008). However, as of May 2014 there is no literature regarding COG7 deficiency and PG synthesis. Judging by the presence of N- and O-glycosylation defects in COG7 patients, it is safe to assume that PG synthesis would be affected too. To investigate PG synthesis in COG7 cells, radioactive metabolic labelling followed by size-exclusion gel chromatography, Western blotting, and mass spectrometry techniques were applied. Regretfully, COG7 cells begun to demise in viability sometime after procurement and during the remaining course of the project no more new samples were available to perform more experiments.

It is clear that the PGs synthesized in COG7 cells differ drastically from healthy cells (E42). The evidence for that comes from metabolic labelling experiments and analysis of both CLs and molecules secreted to the M and their visualization on SDS-PAGE gel. The PGs synthesized by COG7 cells show a higher molecular mass than the corresponding for control cells (Figure 10, Figure 11) These differences in molecular mass might be a result of extended GAG chain length and/or differences in the sulfation level, but could also be a result of differences of protein core masses or complex formation of modified protein cores (however, secreted decorin by E42 and COG7 cells has similar mass, that follows the predicted value (Figure 30, Figure 32) of decorin). The molecular mass of the modified PGs in COG7 cells differs also from those produced by COG8 and COG4 mutants, which suggests that COG mutations have sub-unit specific consequences in PG biosynthesis (Figure 10, Figure 11).The striking is also the difference in expression diversity between healthy cells and COG7 cells. COG7 cells display only two bands of PGs in the secreted fraction (M) whereas E42 show a greater heterogeneity (Figure 10, Figure 11).

One of the possible reasons for reduced diversity in the secreted PGs in COG7 cells could be unavailability of substrates or enzymes needed for proper modification. This hypothesis would fall into the idea of the COG complex functioning as a retrograde transport facilitator (Shestakova et al. 2006; Bruinsma et al. 2004; Ungar et al. 2006) in both the vesicular and maturation protein transport model of the Golgi apparatus. Simply COG is unable to take part in the retrograde transport of the Golgi resident enzymes that are inevitably moved from *cis* to *medial* to *trans -cisternae* along with cargo molecules while the *cisternae* progress (mature) through the Golgi. In the vesicular transport model only some resident Golgi enzymes are transported along with cargo molecules, thus a little retrieval is needed for the lost enzymes. The resident Golgi enzymes cannot follow the default return route to newly formed *cisternae* at *cis* site.

While HSPG synthesis is reported to take place in the *medial* Golgi region, CSPG synthesis has been shown to occur very late in the Golgi apparatus in most cell lines studied. There are several examples that enzymes involved in HSPG synthesis return to the ER upon Brefeldin A treatment, while enzymes involved in CSPG synthesis do not, indicating a localization in the *trans* Golgi network (reviewed in Prydz & Dalen 2000). Thus, if HSPG synthesis fails early in the *medial* Golgi region, more sites could become available for CS GAG polymerization. This might not, however, explain a 4-fold increase in the secretion of CSPGs. This increase

could also be related to the cellular homeostasis of CSPGs, where under normal circumstances, a significant fraction of the CSPGs synthesized are routed towards degradation in a microtubule-dependent manner (Fagereng et al. unpublished observation). While the existence of GAGosomes, an assembly of enzymes involved in GAG synthesis, has been proposed for both HS and CS synthesis, the organization and turnover of the enzymes involved is not fully known. Thus, why CSPG synthesis is not inhibited, while HSPG synthesis is, requires more experiments to find out.

Secondly the reason for reduced diversity in secreted PG in COG7 cells could be induced by an impaired signalling pathway. PGs are involved in cell signalling (Bartus et al. 2012; Schaefer & Schaefer 2010; Hildebrand et al. 1994) and therefore altered PG secretion will in turn affect PG expression in a type of negative feedback loop. This might be the case in COG7 cells where due to improper glycosylation of PGs, those molecules cannot function properly and thus would affect signalling (Büttner et al. 2013).

The striking characteristics of secreted COG7 PGs are that these are almost exclusively modified by CS (Figure 12, Figure 17). One could understand this modification as over-polymerization with CS, but it also could be viewed as under-polymerization of HS. The current understanding of HS PGs (HSPG) is that they are involved in modulation of signalling (Hufnagel et al. 2006) and mediation of the formation of efficient ligand-receptor complexes (Eswarakumar et al. 2005). HSPGs are needed for binding of fibroblast growth factors (FGFs) to their cell surface receptors (Yayon et al. 1991; Eswarakumar et al. 2005). The HSPGs do not transmit the signal, but act as accessory molecules that potentiate the signal. Thus, under-HS modification on a PG could lead to reduced FGF binding effectiveness on the COG7 cell surface. Even though it is not clear whether the PGs in the M only are secreted molecules, PGs that eventually are shedded from the cell membrane would also be present in the M. The most frequently shed PGs are members of the syndecan PG family, mostly carrying HS chains. The shedding has been reported to be influenced by the extent of GAG modification. Compiling the fact that the amount of HS in COG7 CLs is lower than in E42 CLs (Figure 14) and that HS modification relatively speaking is marginal on PGs found in the M of COG7 cells (Figure 15), it is possible to suggest that COG7 cells would have a distorted FGF signalling.

Since the sulfate incorporation, as a single analysis, is only semi-quantitative, it is difficult to draw conclusions regarding the number of GAG chains and the level of sulfation of individual chains.

While considering HS modification, it is clear that PGs synthesized in COG7 cells are less modified with HS. This is observed bot for cellular PGs (CL fraction) and in the M (Figure 14, Figure 15). Control fibroblasts extensively modify secreted PGs with HS, while COG7 cells do this to a much lesser extent. It is clear that secreted PGs from E42 have substantial HS modification (40 % HS). When compared this value to that for PGs secreted from COG7 cells (5 % HS), it is clear that reduction is significant.

Shestakova et al in 2006 showed that in COG7 knock-down (KD) cells, GlcNAc T1 enzyme is severely mislocalized from evenly distributed across the Golgi stacks (Röttger et al. 1998)to dispersed vesicles throughout cytoplasm with glycosylation defects occurring earlier in the glycosylation pathway (Shestakova et al. 2006). Even though GlcNAcT1 is not directly involved in HS polymerization, it is clear that mislocalization of Golgi resident enzymes in COG7 cells could occur. EXT1 and EXT2 were shown to localize in the *cis*-Golgi in (Multhaupt & Couchman 2012) and EXT1 and EXT 2 are enzymes involved in polymerization of HS chains (Kreuger & Kjellén 2012b). Moreover, knock down studies of EXT1 showed that EXT1-deficient embryonic bodies showed increased biosynthesis of CS (doubled production), while HS synthesis was absent (Le Jan et al. 2012). In theory, hypothesized by Kreuger & Kjellén, reduced synthesis of HS leaves "open" linkage regions for CS synthesis that otherwise would be occupied by HS. Moreover, lack of HS biosynthesis would increase the amount of PAPS and UDP-sugars available for CS synthesis (Kreuger & Kjellén 2012b). However, the radioactive sulfate incorporation in the fraction of macromolecules secreted from COG7 cells was several times higher than for control fibroblasts (Fig 1). This indicates increased CS synthesis, since this sulfate was mostly removed by chondroitinase treatment. The possible contribution of an increase in PG protein core synthesis or increased GAG chain lengths was not addressed. Regrettably, ^{3}H-glucosamine and ^{35}S Met labelling was not performed in this thesis, so the contributions from changes in GAG chains and PG core protein synthesis was not addressed by metabolic labelling.

Non-radioactive M and CL samples were prepared for mass spectrometry. In an ion-exchange chromatography step, the PGs were isolated from the bulk of proteins in the samples. From

the metabolic labelling studies, secreted PGs showed greater heterogeneity in E42 control fibroblasts, than in COG7 cells. In fact, COG7 secreted PGs show only two fractions of sulfated PGs and those are of high M_w (Figure 12, Figure 20). The MS data provided insight into the M composition and it supports the compositional diversity. In COG7 M the most abundant PG was biglycan followed by lumican whereas in E42 M the most abundant PG was chondroitin sulfate proteoglycan 4 followed by decorin, although decorin and lumican abundance in E42 M was nearly equal The reason for this expressional diversity is not clear. It is possible that MS intrinsic limitation lead to skewed results for the analysis of M samples from COG7 cells. COG7 M samples showed a high protein concentration. This could correspond to a general increase in protein secretion, as observed for PGs, but the samples had especially high levels of serum bovine albumin also when compared to control cells. This high level of protein could reduce the sensitivity of mass spectrometry where in M samples from control cells, the protein level was at an appropriate level for MS analysis (Anders Moen, personal correspondence). On the other hand, after ion-exchange chromatography followed by silver staining, MS analysed samples from elute 2 did not show any previously undetected PGs.

PGs may also be analysed by Western blotting when the appropriate antibodies are available. In many cases, removal of the GAG chains is required for the antibody to recognise the protein core in question. The PG decorin was present in M from both control fibroblasts and COG deficient cells (i.e. COG7 M and E42 M). The secreted variant does not differ extensively between the normal and COG7 cells. The only significant difference is the level of CS modification. COG7 M expresses decorin that is modified not only with CS, but does also possess another type of modification. This is in contrast to E42 M, where the fraction of secreted decorin is fully glycosylated with only chondroitin (showed in Figure 32, where the 39 kDa band is present). It is possible that the differently glycosylated decorin is needed for proper tissue functionality. It is possible that GAG synthesized on COG7 decorin is a hybrid chain or that there are more than one chain, but the latter option is less likely since there is only one known O-glycosylation site on decorin protein core (Uniprot.).However, there are 3 N-glycosylation sites present on decorin. It is possible that there is altered use of those sites due to mislocalized transferases.

The CL of COG7 cells showed unusual results with the anti-decorin antibody (Figure 33). Where there is, possibly, no decorin present in E42 CL, the COG7 CL demonstrated a ladder-

like pattern. It seems that the decorin remaining in the CL of COG7 cells is not modified by CS. It is possible that decorin, in the cell fraction, has not yet reached the chondroitin polymerization enzymes, which are located at the *trans*-side of the Golgi apparatus. This would imply rapid cellular release upon CS modification. Secondly, if we assume that decorin is modified with a hybrid chain, it is possible that elongation of the chondroitin chain cannot proceed without initial polymerization of HS on the same protein. However, there is no evidence indicating a presence of a hybrid HS/CS chain(s) on COG7 CL decorin. It is much more probable that N- and O-glycosylation sites are occupied by keratan sulfate since keratan sulfate can originate from both N- and O-glycan sites. Yet, there is secretion of CS –modified decorin in the COG7 cells (Figure 30). It is entirely possible that there is some HS polymerization activity, but its rate of polymerization does not connect with the ongoing protein synthesis. This reduction in polymerization of heparan could be due to a slow rate of retrograde transport of heparan polymerizing enzymes from *trans*- and *medial*- to *cis*-*cisternae* in the Golgi apparatus. Therefore, since only 20 % of the nominal COG complex level is present in the COG7 patient (Wu et al. 2004), this overall retrograde transport rate could be significantly slower This transport retardation could, in turn, influence the overall polymerization rate of HS.

The presence of the "decorin ladder" in COG7 CL could be explained twofold. Firstly, the small differences in molecular mass between bands (approximately 2-4 kDa) are, most probable, due to the number of N-glycosylations. Decorin has three potential N-glycosylation sites and using combinations of all three sites or none can lead to significant variation in mass (Uniprot). Secondly, the presence of heavy bands at 150 kDa could be explained by either the presence of decorin clusters (multiple decorin molecules aggregating together) or that decorin is coupled to some other protein complex. It is most probable that band showed at high molecular level is decorin bound to collagen type I or type II (Uniprot). Collagen is the prevailing protein in the fibroblasts and its binding to decorin is well known. The heavy M_w decorin is present as a secreted variant in E42 M (Figure 37) and to some extent in COG7 M. It is unclear what characteristics this variant shows, but it is clear that it is CS modified to some degree. This modification could influence its aggregation properties.

When analysing the protein content and composition of media and cell fractions from control fibroblasts and COG7 cells, these were first washed and incubated in serum-free M, following a procedure designed to avoid such external proteins in the samples. The initial image after

silver staining indicated dramatic increase in the protein levels for the samples from the COG7 cells, but MS revealed that there was a dramatically higher content of bovine serum proteins in these samples, when compared to the control samples. This is most easily explained by a prolonged retention of serum proteins in the COG7 cells. The same phenomenon was observed also for COG8 cells (Anders Moen, personal communication), Since the washing procedure designed to remove serum proteins includes a 30 min incubation where internalized proteins would normally be released by recycling, does the fact that these proteins appear in the M in a subsequent incubation period for cells deficient in COG7 and COG8 indicate that recycling to the cell surface is delayed in these cells. However, further experiments are required to establish this possibility.

4.1 Future studies

The duration of master studies program is limited. Therefore some of the analysis shows incomplete or conflicting data. Thus, with no doubt, there is a strong need for repeat of experiments to validate the results obtained.

Due to failure to thrive of COG7 cells during a period of time, it would be beneficial to establish a system that would provide a researcher with new samples swiftly. A knock-down protocol could be used.

It is of paramount importance to carry out ^{3}H-glucosamine and ^{35}S-Met labelling on COG7 cells to establish the exact characteristics of the GAGs on the PGs and address the issue of increased sulfate labelling. $^{35}S\text{-}SO_4^{2-}$ labelling is powerful method, but to establish a full experimental picture, ^{3}H-glucosamine and ^{35}S-Met labelling is also needed. More work should be carried out in CL fraction studies with respect to MS and Western blotting. Regretfully, E42 CL fractions did not produce sufficient amounts of protein, thus a functioning protocol should be established in order to achieve the desired protein concentration both for the CL and the M.

Fluorescent labelling and confocal visualization of the Golgi resident enzymes should be performed. It would be interesting to carry out localization studies on two HS polymerizing enzymes: EXT1 and EXT2 in COG7 cells. It is possible that EXT1 and EXT2 co-localize with CS polymerizing enzymes in the *trans*-Golgi region. Such localization would explain the reduced levels of HSPGs produced in COG7 cells.

Recycling studies should be carried out on COG7 cells to investigate the recycling phenomenon indicated in this thesis. Following the idea that the COG complex is involved in intra-Golgi retrograde recycling of protein, it could also be involved in a number of other retrograde transport processes. It would be interesting to assess how COG7 cells recycle proteins endocytosed from the extracellular environment.

5 References

Aebi, M., 2013. N-linked protein glycosylation in the ER. *Biochimica et Biophysica Acta - Molecular Cell Research*, 1833(11), pp.2430–2437.

Amsbio, S., *Chondrotinase ABC Data sheet.*,

Bartus, K. et al., 2012. Chondroitin sulphate proteoglycans: Key modulators of spinal cord and brain plasticity. *Experimental Neurology*, 235(1), pp.5–17.

Bonfanti, L. et al., 1998. Procollagen traverses the Golgi stack without leaving the lumen of cisternae: evidence for cisternal maturation. *Cell*, 95(7), pp.993–1003.

Bruce Alberts, Alexander Johnson, Julian Lewis, Martin Raff, Keith Roberts, and P.W., 2002. *Molecular Biology of the Cell, 4th edition*, Garland Science.

Bruinsma, P., Spelbrink, R.G. & Nothwehr, S.F., 2004. Retrograde transport of the mannosyltransferase Och1p to the early Golgi requires a component of the COG transport complex. *The Journal of biological chemistry*, 279(38), pp.39814–39823.

Büttner, M. et al., 2013. Over-sulfated chondroitin sulfate Derivatives induce osteogenic differentiation of hMSC independent of BMP-2 and TGF-β1 signalling. *Journal of Cellular Physiology*, 228(2), pp.330–340.

Caffaro, C.E. & Hirschberg, C.B., 2006. Nucleotide Sugar Transporters of the Golgi Apparatus: From Basic Science to Diseases. *Accounts of Chemical Research*, 39(11), pp.805–812.

Dick, G. et al., 2012. Proteoglycan synthesis and Golgi organization in polarized epithelial cells. *The journal of histochemistry and cytochemistry : official journal of the Histochemistry Society*, 60(12), pp.926–35.

Emr, S. et al., 2009. Journeys through the Golgi--taking stock in a new era. *The Journal of cell biology*, 187(4), pp.449–453.

Esko, J.D., Kimata, K. & Lindahl, U., 2014. Proteoglycans and Sulfated Glycosaminoglycans. In *Essentials of Glycobiology. 2nd edition*. Cold Spring Harbor Laboratory Press, pp. 1–28.

Eswarakumar, V.P., Lax, I. & Schlessinger, J., 2005. Cellular signaling by fibroblast growth factor receptors. *Cytokine & growth factor reviews*, 16(2), pp.139–49.

Foulquier, F. et al., 2007. A new inborn error of glycosylation due to a Cog8 deficiency reveals a critical role for the Cog1-Cog8 interaction in COG complex formation. *Human molecular genetics*, 16(7), pp.717–30.

Foulquier, F. et al., 2006. Conserved oligomeric Golgi complex subunit 1 deficiency reveals a previously uncharacterized congenital disorder of glycosylation type II. *Proceedings of*

the National Academy of Sciences of the United States of America , 103 (10), pp.3764–3769.

Freeze, H.H. & Aebi, M., 2005. Altered glycan structures: the molecular basis of congenital disorders of glycosylation. *Current opinion in structural biology*, 15(5), pp.490–8.

Hildebrand, A. et al., 1994. Interaction of the small interstitial proteoglycans biglycan, decorin and fibromodulin with transforming growth factor beta. *The Biochemical journal*, 302 (Pt 2, pp.527–34.

Hufnagel, L. et al., 2006. On the role of glypicans in the process of morphogen gradient formation. *Developmental biology*, 300(2), pp.512–22.

IBEX Pharmaceuticals, 2011. *Heparinase III*,

Jaeken, J., 2013. *Congenital disorders of glycosylation.* 1st ed., Elsevier B.V.

Le Jan, S. et al., 2012. Functional overlap between chondroitin and heparan sulfate proteoglycans during VEGF-induced sprouting angiogenesis. *Arteriosclerosis, thrombosis, and vascular biology*, 32(5), pp.1255–63.

Kjellen, L. & Lindahl, U., 1991. Proteoglycans: Structures and interactions. *Annual review of biochemistry*, 60, pp.443–75.

Kodera, H. et al., 2014. Mutations in COG2 encoding a subunit of the conserved oligomeric golgi complex cause a congenital disorder of glycosylation. *Clinical genetics*, (3), pp.1–6.

Kolset, S.O. & Tveit, H., 2008. Serglycin--structure and biology. *Cellular and molecular life sciences : CMLS*, 65(7-8), pp.1073–85.

Kreuger, J. & Kjellén, L., 2012a. Heparan sulfate biosynthesis: regulation and variability. *The journal of histochemistry and cytochemistry : official journal of the Histochemistry Society*, 60(12), pp.898–907.

Kreuger, J. & Kjellén, L., 2012b. Heparan sulfate biosynthesis: regulation and variability. *The journal of histochemistry and cytochemistry : official journal of the Histochemistry Society*, 60(12), pp.898–907.

Lee, M.C.S. et al., 2004. Bi-directional protein transport between the ER and Golgi. *Annual review of cell and developmental biology*, 20, pp.87–123.

Lübbehusen, J. et al., 2010. Fatal outcome due to deficiency of subunit 6 of the conserved oligomeric Golgi complex leading to a new type of congenital disorders of glycosylation. *Human molecular genetics*, 19(18), pp.3623–33.

Malla, N. et al., 2013. In vitro reconstitution of complexes between pro-matrix metalloproteinase-9 and the proteoglycans serglycin and versican. *The FEBS journal*, 280(12), pp.2870–87.

Mikami, T. & Kitagawa, H., 2013. Biosynthesis and function of chondroitin sulfate. *Biochimica et Biophysica Acta - General Subjects*, 1830(10), pp.4719–4733.

Mowbrey, K. & Dacks, J.B., 2009. Evolution and diversity of the Golgi body. *FEBS Letters*, 583(23), pp.3738–3745.

Multhaupt, H. a B. & Couchman, J.R., 2012. Heparan sulfate biosynthesis: methods for investigation of the heparanosome. *The journal of histochemistry and cytochemistry : official journal of the Histochemistry Society*, 60(12), pp.908–15.

Ng, B.G. et al., 2007. Molecular and clinical characterization of a Moroccan Cog7 deficient patient. *Molecular genetics and metabolism*, 91(2), pp.201–4.

Oka, T. et al., 2004. The COG and COPI Complexes Interact to Control the Abundance of GEARs , a Subset of Golgi Integral Membrane Proteins □. *Molecular biology of the cell*, 15(May), pp.2423–2435.

Paesold-Burda, P. et al., 2009. Deficiency in COG5 causes a moderate form of congenital disorders of glycosylation. *Human molecular genetics*, 18(22), pp.4350–6.

Patterson, G.H. et al., 2008. Transport through the Golgi Apparatus by Rapid Partitioning within a Two-Phase Membrane System. *Cell*, 133(6), pp.1055–1067.

Prydz, K. & Dalen, K.T., 2000. Synthesis and sorting of proteoglycans. *Journal of cell science*, 113 Pt 2, pp.193–205.

Reynders, E. et al., 2009. Golgi function and dysfunction in the first COG4-deficient CDG type II patient. *Human molecular genetics*, 18(17), pp.3244–56.

Reynders, E. et al., 2011. How Golgi glycosylation meets and needs trafficking: the case of the COG complex. *Glycobiology*, 21(7), pp.853–863.

Rothman, J.E. & Wieland, F.T., 1996. Protein sorting by transport vesicles. *Science (New York, N.Y.)*, 272(5259), pp.227–234.

Röttger, S. et al., 1998. Localization of three human polypeptide GalNAc-transferases in HeLa cells suggests initiation of O-linked glycosylation throughout the Golgi apparatus. *Journal of cell science*, 111 (Pt 1), pp.45–60.

Schaefer, L. & Schaefer, R.M., 2010. Proteoglycans: from structural compounds to signaling molecules. *Cell and tissue research*, 339(1), pp.237–246.

Shestakova, A., Zolov, S. & Lupashin, V., 2006. COG complex-mediated recycling of Golgi glycosyltransferases is essential for normal protein glycosylation. *Traffic (Copenhagen, Denmark)*, 7(2), pp.191–204.

Sigma Aldrich, *Blue Dextran Info Sheet*,

Stamnes, M., 2004. Golgi Complex. *University of Iowa*, 2, pp.312–315.

Sugahara, K. & Kitagawa, H., 2000. Recent advances in the study of the biosynthesis and functions of sulfated glycosaminoglycans. *Current Opinion in Structural Biology*, 10(5), pp.518–527.

Suvorova, E.S., Duden, R. & Lupashin, V. V, 2002. The Sec34/Sec35p complex, a Ypt1p effector required for retrograde intra-Golgi trafficking, interacts with Golgi SNAREs and COPI vesicle coat proteins. *The Journal of cell biology*, 157(4), pp.631–643.

Ungar, D. et al., 2002. Characterization of a mammalian Golgi-localized protein complex, COG, that is required for normal Golgi morphology and function. *The Journal of cell biology*, 157(3), pp.405–415.

Ungar, D. et al., 2006. Retrograde transport on the COG railway. *Trends in Cell Biology*, 16(2), pp.113–120.

Uniprot, Biglycan. Available at: http://www.uniprot.org/uniprot/P21810.

Uniprot, Biglycan precursor. Available at: http://www.uniprot.org/uniprot/P21810.

Uniprot, P07585- Decorin. Available at: http://www.uniprot.org/uniprot/P07585.

Uniprot, P10124-Serglycin. Available at: http://www.uniprot.org/uniprot/P10124.

Uniprot, PGCA_HUMAN- Aggrecan. Available at: http://www.uniprot.org/uniprot/P16112.

Willett, R., Ungar, D. & Lupashin, V., 2013. The Golgi puppet master: COG complex at center stage of membrane trafficking interactions. *Histochemistry and cell biology*, 140(3), pp.271–83.

Wilson, C. et al., 2011. The Golgi apparatus: an organelle with multiple complex functions. *The Biochemical journal*, 433(1), pp.1–9.

Wu, X. et al., 2004. Mutation of the COG complex subunit gene COG7 causes a lethal congenital disorder. *Nature medicine*, 10(5), pp.518–523.

Xia, B. et al., 2013. Serum N-glycan and O-glycan analysis by mass spectrometry for diagnosis of congenital disorders of glycosylation. *Analytical biochemistry*, 442(2), pp.178–85.

Yayon, a et al., 1991. Cell surface, heparin-like molecules are required for binding of basic fibroblast growth factor to its high affinity receptor. *Cell*, 64(4), pp.841–8.

Zeevaert, R. et al., 2008. Deficiencies in subunits of the Conserved Oligomeric Golgi (COG) complex define a novel group of Congenital Disorders of Glycosylation. *Molecular Genetics and Metabolism*, 93(1), pp.15–21.

Zolov, S.N. & Lupashin, V. V, 2005. Cog3p depletion blocks vesicle-mediated Golgi retrograde trafficking in HeLa cells. *The Journal of cell biology*, 168(5), pp.747–759.

6Appendices

6.1 G-50 Fine columns creation

The columns used in metabolic labelling were created in-house, following the procedure:

1. Old 10 ml plastic pipettes were cut at the 7 ml volume level mark. Bottom part that contained nozzle was kept and rest of the pipette was discarded

2. Small portion of glass wool was placed and compacted at the inside part of the nozzle. The amount of glass wool used should be enough to keep gel material from leaking through nozzle

3. 4.0 ml of G-50 fine gel material was placed. G-50 fine was pre-soaked in dH_2O following the manufacturers manual

4. Column then was let to stand in order to settle the gel material

6.2 List of used equipment throughout the project

Name	Model	Manufacturer
Air incubator	DH Autoflow	NuAire
Balance	BP2215	Satorius
Balance	1212MSCS	Precis
Rubber Policeman	Cell lifter 3008	Costar
Cell culture flasks	75 cm2	Nunc
Centrifuge	GS-15 R	Beckman

Centrifuge	Allegra X-22	Beckman-Coulter
Dialysis Cassette	Slide-A-lyser	Pierce
Eppendorf Centrifuge	Mini-spin	Eppendorf
Exposure Cassette	Storage phosphor cassette	GE Healthcare
Freeze-dryer	Maxi dry lyo	FD1.0
Gel cell	XCell sure lock	Novex
Gel cell	Criterion Cell	BioRad
Heating block	DRI-Block DB20	Techne
Hotplate magnetic stirrer	345PR	Snijders
Image Eraser	Image Eraser #810-UMW	Amersham Biosciences
Light Microscope	DMIL	Leica
Light Microscope Lens	10/0.25	Leitz-Weltzar
Orbital Shaker	Gerhardt	Abshake
pH meter	420A+	Thermo Orion
Power supply	Bromma 2301	LKB
Scintillation counter	1900TR	Packard
Scintillation vials	Mini-vial 6 ml	Sarstedt
Slab gel dryer	SGD4050	Savant
PhosphoImager	Typhoon 9400	Amersham Biosciences
Ultra-deep freezer (-80°C)	MDF	Panasonic

Vertical shaker	USR-50 Pro	Labplus
Vortex mixer	Whirlimixer	Fisons
Water bath	Tempette Junior TE-8J	Techne

6.3 List of chemicals and expendables

Name	Catalogue # / Lot/ Name	Producer
20 x WB Transfer buffer	NP0006-1	Novex
20 x MOPS-SDS Running buffer (BioRad)	XT-MOPS #161-0788	BioRad
20 x MOPS-SDS Running buffer (Novex)	NP0001	Novex
20 x Reducing Agent	XT Reducing agent 20 x #161-0792	BioRad
^{35}S-SO_4^{2-} Sulfate	Lot# 177911	Perkin-Elmer
4x Sample buffer	XT Sample Buffer #161-0791	BioRad
6 well plate	6 well culture cluster, # 3516	Costar
Acetic Acid	Lot# 33209	Sigma
Amplify Solution	NAMP100V	Amersham Biosciences
Anti –Mouse IgG Antibody conjugated with horseradish peroxidase	NXA93-1ML1, lot # 9489919	GE Healthcare

Anti –Rabbit IgG Antibody conjugated with horseradish peroxidase	NA934, lot # 9499122	GE Healthcare
Blocking Agent	ECL Advanced Blocking Agent	GE Healthcare
Blue dextran	Lot# 283873	Amersham Biosciences
Bovine Serum Albumin	Lot#038K0704	Sigma Aldrich
Calcium Chloride ($CaCl_2$)	Lot# 100K0216	Sigma Aldrich
CL-6B Gel material	Sepharose CL-6B # 17-0160-01	GE Healthcare
DEAE gel material	DEAE Sephacel™ # 17-0500-01	GE Healthcare
DMEM	Lot# 3MB049	Lonza
DMSO-Dimethylsulfoxide	Lot#007165.02	Duchefa Biochemicals
EDTA	Lot#7640065	Sigma Aldrich
Ethanol	-	Arcus
Foetal Bovine Serum (FBS)	Lot#A64304-0133	PAA
G-50 Fine gel material	Sephadex G-50 Fine # 17-0042-02	GE Healthcare
HEPES	CAS# 7365-45-9	Sigma Aldrich
Hydrochloric Acid	20.252.290	VVR
L-Glutamine	Lot#0MB122	Lonza
Methanol	3221BN-2.5L	Sigma Aldrich
Molecular Marker	Magic Marker ™ # LC5602/23	Novex
Molecular Marker	Precision Plus Protein™ Unstained Standard #161-0363	BioRad
Molecular Marker	Precision Plus Dual Colour Standards # 161-0374	BioRad

Molecular Marker	Protein Molecular Weight Markers [methyl-^{14}C] methylated #NEC811001UC, lot # 1638419	Perkin Elmer
Penicillin /Streptomycin (P/S)	Lot#0MB129	Lonza
pH buffers , 4.01, 7.01 , 10.01	#910110	Thermo Orion
Proteo Silver Plus™	Lot# 080M6259	Sigma Aldrich
PVDF membrane	LC2005	Novex
RPMI 1640 Medium	Lot# 90988M	Lonza
Scintillation Count Liquid	Ultima Gold XR	Perkin Elmer
SDS-PAGE Gel	Criterion XT 4-12 % Bis-Tris #345-0123	BioRad
SDS-PAGE Gel	NuPAGE 4-12 % Bis-Tris #NP0322BOX	Novex
Sodium Acetate	Lot # 93170	Riedel-deHaen
Sodium Chloride	Lot # K36719833	BDH
Sodium deoxycholate	Lot#61H0536	Sigma Aldrich
Sodium hydroxide	1040517	SDS
Sodium Phosphate (dibasic)	Lot# 120K0126	Sigma Aldrich
Sodium Phosphate (monobasic)	Lot# 20K0227	Sigma Aldrich
TRIS	33621.26	VVR
Triton X-100	789704	Boerhinger Manheim
Tween 20	-	Sigma Aldrich

Ultra-centrifuge device, 10 k	UFC901024	Amicon
WB detection reagent	Amersham™ ECL Select™ WB detection reagent # RPM 2235	GE Healthcare

6.4 List of buffers and solutions

Name	Composition
1 x TTBS (Tris-Tween buffer saline)	20 mM Tris, 137 mM NaCl, 0.1 % Tween 20, Adjust to pH of 7.6 with HCl
1 x WB Transfer buffer	50 ml 20x WB transfer buffer, 100 ml Methanol, 850 ml dH_2O
10 x PBS, pH 6.8	18mM Sodium phosphate (monobasic), 84mM Sodium phosphate (dibasic), 150 mM NaCl. 1 x PBS (diluted with dH_2O) would give pH of 7.4.
2% ECL Advanced Blocking Solution	2 % of ECL Advanced Blocking agent in 1 x TTBS
^{35}S-SO_4^{2-}Medium	RPMI 1640 Medium (without sulfate), 1% P/S, 1 % L-Glutamine, 0.2 mCi/ml of ^{35}S-SO_4^{2-} sulfate
Anti aggrecan antibody 1:2000 dilution	2.5 µl of Anti aggrecan antibody in 5 ml of 2% ECL Advanced blocking solution
Anti biglycan antibody 1:2000 dilution	2.5 µl of Anti biglycan antibody in 5 ml of 2% ECL Advanced blocking solution
Anti C0S-STUB antibody 1:2000 dilution	2.5 µl of Anti C0S-STUB antibody in 5 ml of 2% ECL Advanced blocking solution
Anti C4S-STUB antibody 1:2000 dilution	2.5 µl of Anti C4S-STUB antibody in 5 ml of 2% ECL Advanced blocking solution
Anti C6S-STUB antibody 1:2000 dilution	2.5 µl of Anti C6S-STUB antibody in 5 ml of 2% ECL Advanced blocking solution
Anti decorin antibody 1:2000 dilution	2.5 µl of Anti decorin antibody in 5 ml of 2% ECL Advanced blocking solution
Anti serglycin antibody 1:2000 dilution	2.5 µl of Anti serglycin antibody in 5 ml of 2% ECL Advanced blocking solution

Blue dextran/ potassium dichromate mix	3 mg/ml Blue dextran, 2 mg/ml potassium dichromate
Buffer A (ion exchange)	0.1 M NaCl, 20 mM Sodium Phosphate (monobasic /dibasic), Adjust pH to 6.8 with changing sodium phosphate monobasic to dibasic ratio in solution
Buffer B (ion exchange)	1.0 M NaCl, 20 mM Sodium Phosphate (monobasic/dibasic), Adjust pH to 6.8 with changing sodium phosphate monobasic to dibasic ratio in solution
cABC buffer (10x)	0.05 M Sodium Acetate, 0.05 M Tris, 0.1 % BSA Adjust pH to 8.0 with HCl.
CL-6B Size exclusion chromatography running buffer	0.15 M NaCl, 0.05 M Tris, 0.2& Triton X-100
Incomplete medium	500 ml of DMEM, 1%P/S
Complete Medium	500 ml of DMEM, 10% FBS, 1% P/S, 1 % L-Glutamine
Fix solution for SDS-PAGE and Silver staining	5:1:4 solution of: Ethanol, Acetic acid and dH_2O
Freezing solution	DMEM, 10 % FBS, 1 % P/S, 1 % L-Glutamine, 10% DMSO
Hep buffer (10x)	0.05 M HEPES, 0.5 M NaCl, 10mM Calcium Chloride, 0.1 % BSA, Adjust pH to 7.0 with HCl
Lysing buffer	50 mM Tris-HCl, 150 mM NaCl, 0.05% Triton X-100, 1 mM EDTA, 0.05 % Sodium Deoxcholate, Adjust to 7.4 pH with HCl

6.5 List of primary antibodies

Epitope	Ig Type	Lot#	Manufacturer
Aggrecan	Rabbit	2000382	Millipore
C6S-STUB	Mouse IgM	A80120	Seikagaku
C4S-STUB	Mouse IgG1	2062302	Millipore
C0S-STUB	Mouse IgG	A70120	Seikagaku
Decorin	Mouse IgG1	ECI0212111	R&D Systems
Biglycan	Mouse IgG1	WLL02	R&D Systems
Serglycin	Rabbit	-	Obtained from Achilleas D. Theocharis

6.6 Protein Standards

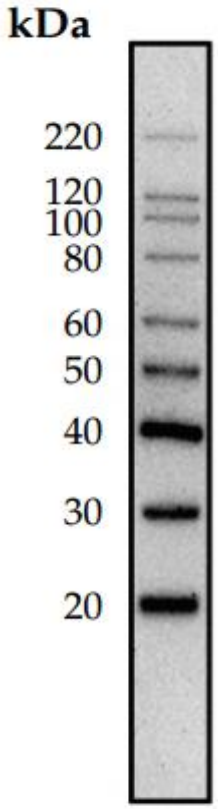

Magic Mark™ XP Western Protein Standard

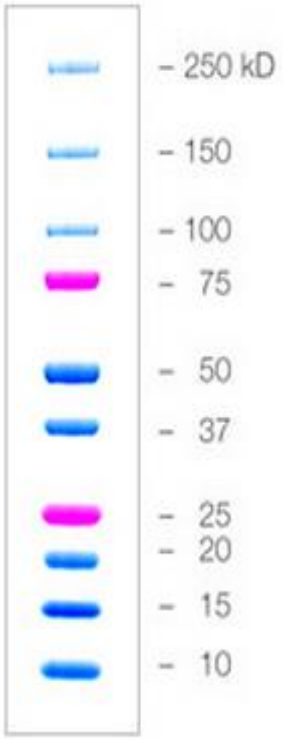

Precision Plus Protein™ Dual Colour Standard

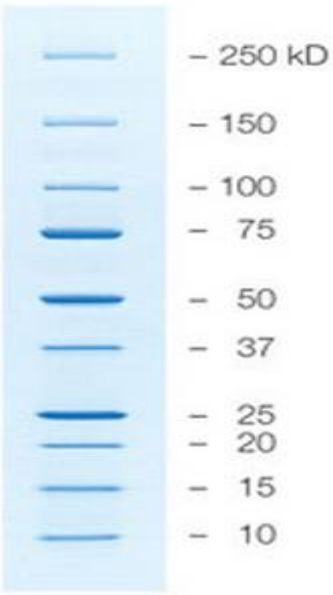

Precision Plus Protein™ Unstained Standard